

Integrated Science Assessment for Lead

Appendix 1: Lead Source to Concentration

January 2024

Center for Public Health and Environmental Assessment
Office of Research and Development
U.S. Environmental Protection Agency

DISCLAIMER

This document has been reviewed in accordance with the U.S. Environmental Protection Agency policy and approved for publication. Mention of trade names or commercial products does not constitute endorsement or recommendation for use.

DOCUMENT GUIDE

This Document Guide is intended to orient readers to the organization of the Lead (Pb) Integrated Science Assessment (ISA) in its entirety and to the sub-section of the ISA at hand (indicated in bold). The ISA consists of the Front Matter (list of authors, contributors, reviewers, and acronyms), Executive Summary, Integrated Synthesis, and 12 appendices, which can all be found at <https://assessments.epa.gov/isa/document/&deid=359536>.

Front Matter

Executive Summary

Integrated Synthesis

Appendix 1. Lead Source to Concentration

Appendix 2. Exposure, Toxicokinetics, and Biomarkers

Appendix 3. Nervous System Effects

Appendix 4. Cardiovascular Effects

Appendix 5. Renal Effects

Appendix 6. Immune System Effects

Appendix 7. Hematological Effects

Appendix 8. Reproductive and Developmental Effects

Appendix 9. Effects on Other Organ Systems and Mortality

Appendix 10. Cancer

Appendix 11. Effects of Lead in Terrestrial and Aquatic Ecosystems

Appendix 12. Process for Developing the Pb Integrated Science Assessment

CONTENTS

DOCUMENT GUIDE	1-iii
LIST OF TABLES	1-v
LIST OF FIGURES	1-vi
ACRONYMS AND ABBREVIATIONS	1-vii
APPENDIX 1 LEAD SOURCE TO CONCENTRATION	1-1
1.1 Introduction	1-1
1.2 Sources of Atmospheric Pb	1-2
1.2.1. Aviation Gasoline and Aircraft Emissions	1-7
1.2.2. Industrial Sources	1-9
1.2.3. Fuel Combustion	1-11
1.2.4. Fires	1-12
1.2.5. Traffic and Roads	1-15
1.2.6. Volcanoes	1-17
1.2.7. Legacy Sources	1-18
1.2.8. Other Sources	1-20
1.3 Fate and Transport of Pb Emitted into Air	1-21
1.3.1. Fate and Transport in Air	1-21
1.3.2. Fate and Transport in Soil	1-24
1.3.3. Fate and Transport in Water and Sediments	1-30
1.3.4. Fate and Transport in Urban Media	1-48
1.4 Monitoring of Pb in Ambient Air	1-53
1.4.1. Network Monitoring	1-53
1.4.2. Federal Reference Methods	1-56
1.4.3. Sampling Considerations	1-58
1.4.4. Recent Advances in Sampling and Analysis	1-59
1.5 Ambient Air Pb Concentration Trends	1-61
1.5.1. National Scale Ambient Air Concentrations and Long-Term Trends	1-62
1.5.2. Seasonal and Diurnal Trends	1-70
1.5.3. Particle Size Characteristics	1-72
1.5.4. Background Concentrations	1-74
1.6 Summary and Conclusions	1-74
1.7 References	1-75

LIST OF TABLES

Table 1-1	Annual lead emissions (tons) from aircraft operating modes _____	1-9
Table 1-2	Parameters related to fires and associated Pb measurements discussed herein _____	1-15
Table 1-3	Distribution of regulatory Pb-total suspended particle concentrations in $\mu\text{g}/\text{m}^3$ for 2020–2022 _____	1-64
Table 1-4	Distribution of Pb concentrations for various types of measurements and monitoring site locations in $\mu\text{g}/\text{m}^3$ for 2020–2022 _____	1-64
Table 1-5	Seasonal variations in Pb concentration in ambient air _____	1-70

LIST OF FIGURES

Figure 1-1	U.S. Pb emissions by sector. _____	1-3
Figure 1-2	U.S. county-level Pb emissions density estimates in lbs/year/mile ² . _____	1-4
Figure 1-3	U.S. anthropogenic Pb emissions trend 1990–2020. _____	1-5
Figure 1-4	The biogeochemical cycle of tetramethyl/tetraethyl Pb. _____	1-22
Figure 1-5	Ambient air Pb and air soil concentrations and median splines in $\mu\text{g}/\text{m}^3$ from Detroit, Michigan. _____	1-51
Figure 1-6	Map of U.S. ambient air monitoring sites reporting regulatory Pb data to U.S. EPA during the 2020–2022 period. _____	1-55
Figure 1-7	Map of U.S. ambient air monitoring sites reporting non-regulatory Pb data to U.S. EPA during the 2020–2022 period. _____	1-56
Figure 1-8	Pb maximum rolling 3-month average in $\mu\text{g}/\text{m}^3$ for the 2020–2022 period. _____	1-63
Figure 1-9	Site-level trends in maximum rolling 3-month average Pb concentrations for 2010–2022. _____	1-65
Figure 1-10	National trend in Pb annual maximum 3-month average concentrations in $\mu\text{g}/\text{m}^3$, 2010 to 2022. _____	1-66
Figure 1-11	Distribution of annual maximum 3-month concentrations measured at regulatory Pb monitoring sites, 1980 to 2022. _____	1-67

ACRONYMS AND ABBREVIATIONS

As	arsenic	K	potassium
AQCD	Air Quality Criteria Document	Me-L	metal ligand
AQS	Air Quality System	Mg	magnesium
Ca	calcium	Mn	manganese
CEC	cation exchange capacity	NAAQS	National Ambient Air Quality Standards
CFR	Code of Federal Regulations	NATTS	National Air Toxics Trends Stations
CSN	Chemical Speciation Network	NCore	National Core multipollutant monitoring network
DI	deionized	NEI	National Emissions Inventory
DO	dissolved oxygen	OM	organic matter
DOC	dissolved organic carbon	OX	oxide-bound
DOM	dissolved organic matter	PM	particulate matter
ED-XRF	energy-dispersive X-ray fluorescence spectrometry	PTFE	polytetrafluoroethylene
EF	enrichment factor	SLAMS	state and local air monitoring stations
FAAS	flame atomic absorption spectroscopy	SPM	suspended particulate matter
Fe	iron	SS/CAR	specifically sorbed/carbonate-bound
FEM	Federal Equivalent Method	STR	soil temperature regimes
FRM	Federal Reference Method	Ti	titanium
FTC	freeze thaw cycle	TRI	Toxic Release Inventory
HA	humic acid	TSS	total suspended solids
HAP	hazardous air pollutant	TSP	total suspended particulate
ICP-MS	inductively coupled plasma mass spectrometry	UFP	ultrafine particle
IMPROVE	Interagency Monitoring of Protected Visual Environments	U.S EPA	United States Environmental Protection Agency
		Zn	zinc

APPENDIX 1 LEAD SOURCE TO CONCENTRATION

1.1 Introduction

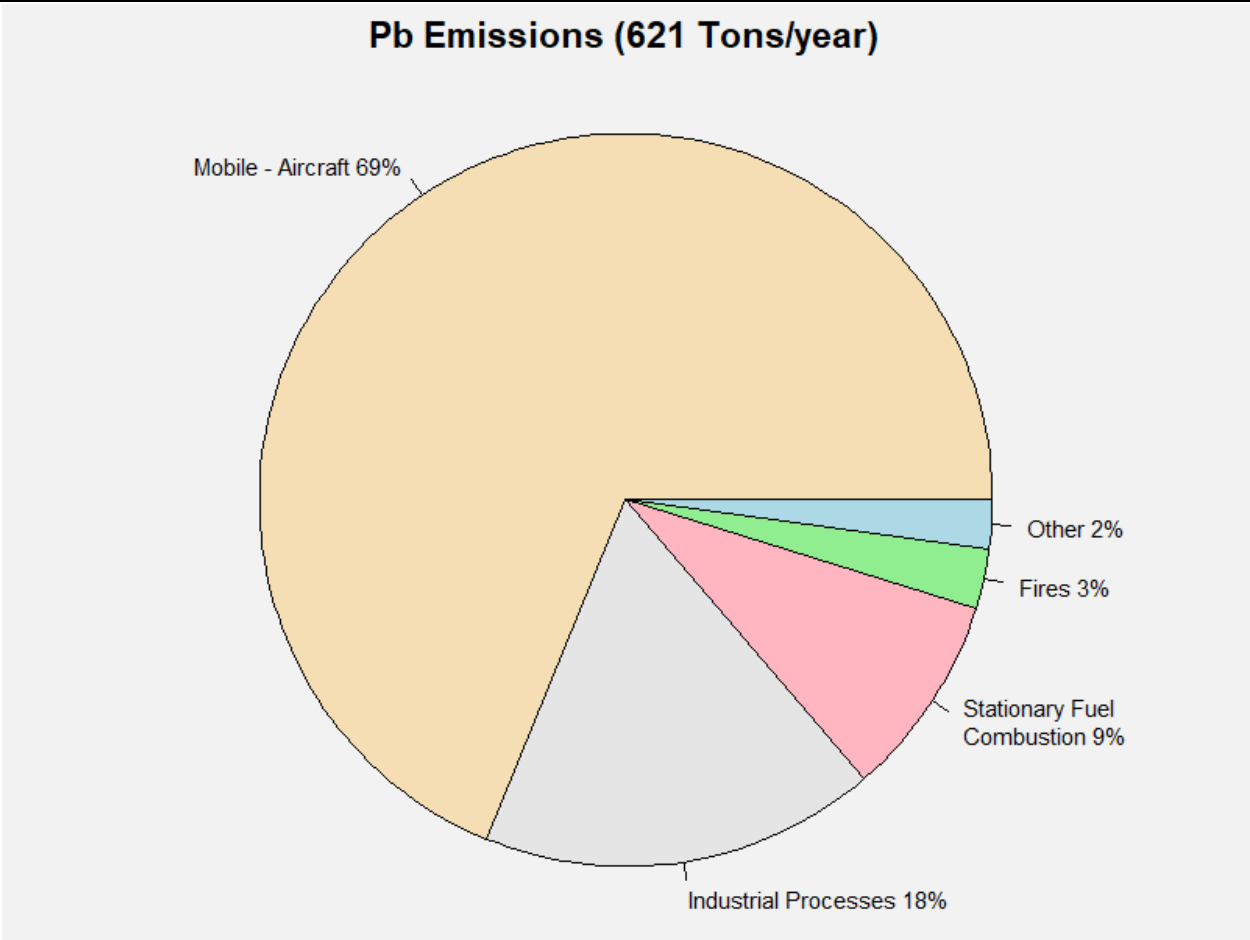
This appendix characterizes the current state of atmospheric and environmental science relevant to understanding lead (Pb) exposure and Pb-related health and ecological effects described in subsequent appendices. It builds on previous research reviewed in the 2013 Integrated Science Assessment for Lead (hereinafter referred to as the 2013 Pb ISA) ([U.S. EPA, 2013](#)) and previous Pb Air Quality Criteria Documents (AQCDs) ([U.S. EPA, 2006, 1986, 1977](#)) and emphasizes relevant advances in sources and emissions, fate and transport, sampling and analysis methods, and concentration trends. Because of the large body of literature on the subject, this appendix focuses primarily on new studies from the United States and Canada, with a few exceptions for highly relevant international publications. The scope is not limited to airborne Pb from contemporary emission sources because non-atmospheric processes, as well as legacy sources, are also relevant for understanding the effects of airborne Pb. For example, transport and transformation processes in soil and water after deposition are also relevant. Therefore, current research in other media is also included to promote understanding of airborne Pb in the context of non-atmospheric sources and media.

In previous ISAs, an up-to-date review of air emissions, monitoring, and concentration trends has been accomplished through a combination of analysis of United States Environmental Protection Agency (U.S. EPA) ambient air monitoring network data and a synthesis of observations reported in the peer-reviewed literature. Reference data such as total emissions, coverage of network monitors, average concentrations, and concentration trends can become out of date before the document is published because these data are so frequently updated. To facilitate provision of the most current emissions and concentration data from the Pb monitoring network, a set of relevant maps and graphics that have been routinely included in the atmospheric appendix or chapter in previous ISAs are now drawn from a separate document “Overview of Lead (Pb) Air Quality in the United States.” Many of the figures and tables in this appendix are from the 2022 Overview ([U.S. EPA, 2022a](#)). These will be updated annually and made available at <https://www.epa.gov/air-quality-analysis/lead-naaqs-review-analyses-and-data-sets>. This appendix complements the Overview by providing a literature-based synthesis of recent research on Pb sources, fate and transport, measurement, and concentration trends. Section 1.2 provides an overview of sources and emissions of Pb in ambient air and other environmental media. Section 1.3 gives descriptions of the fate and transport of Pb in air, soil, and aqueous media. Section 1.4 describes advances in Pb measurement methods, and Section 1.5 describes ambient air Pb concentrations, including spatial and temporal variability on national and local scales and the size distributions of Pb-bearing particulate matter (PM).

1.2 Sources of Atmospheric Pb

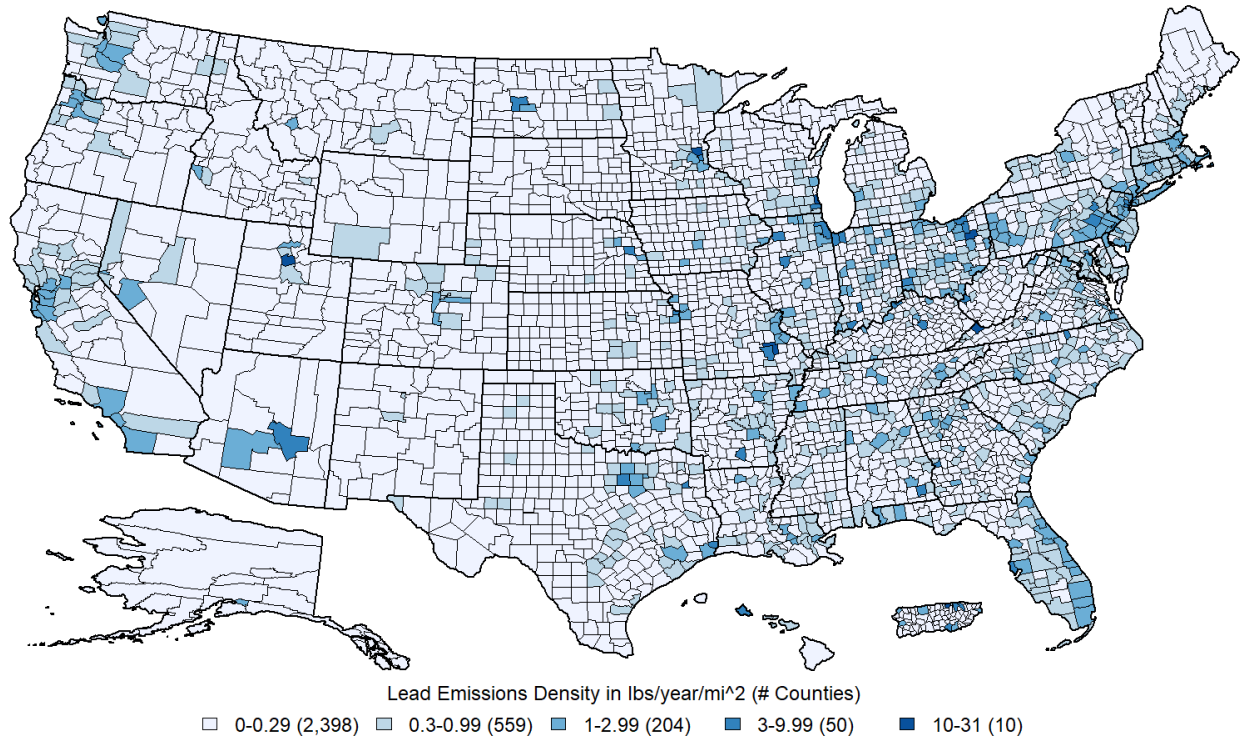
Figure 1-1 summarizes the major sources of U.S. Pb emissions based on the 2020 National Emissions Inventory (NEI) ([U.S. EPA, 2023a](#)), which is divided into mobile and stationary sources. Total estimated national Pb emissions for 2020 were 621 tons, with 69% accounted for by aircraft, 18% from industrial processes, 9% from stationary fuel combustion, and 3% from fires. All other sources combined were estimated to account for about 2% of total U.S. Pb emissions. The sum of emissions from all industrial sources of 218,000 lbs agreed well with total national stack emissions from the Toxic Release Inventory (TRI) of 210,000 lbs for 2020 ([U.S. EPA, 2023d](#)). Not shown in Figure 1-1 are emissions from resuspended soil. Resuspension of Pb from historical sources has not been quantified in this way on a national scale but has been demonstrated to be a dominant source in urban areas where it has been studied and estimates of Pb resuspension near roads and industrial sources have been reported in a number of studies described in previous assessments ([U.S. EPA, 2013, 2006](#)) and in Section 1.3.4.

Figure 1-2 shows the geographic distribution of Pb emissions from the 2020 NEI. High county emissions often correspond to counties that also experienced the highest ambient concentrations described in Section 1.5.1. Total Pb emissions have steadily decreased for decades, largely due to the elimination of leaded gasoline use in automobiles before 1996 and in later years because of reductions in emissions from metals processing sources ([U.S. EPA, 2013, 2006](#)). As shown in Figure 1-3, from 1990 to 2020, there has been a steep decline in total U.S. Pb emissions from about 5 kton/year to less than 1 kton/year and a replacement of industrial sources with non-road mobile sources as the dominant category of emissions, which reflects the prominence of aircraft using leaded aviation fuel as the largest emissions source ([U.S. EPA, 2023c](#)). Up-to-date graphics of total U.S. Pb emissions estimates by source, geographic distribution of Pb emissions estimates, and the 30-year total U.S. emissions estimates trends are available in “Overview of Lead (Pb) Air Quality in the United States” ([U.S. EPA, 2022a](#)), and updated annually at <https://www.epa.gov/air-quality-analysis/lead-naaqs-review-analyses-and-data-sets>.



Source: [\(U.S. EPA, 2023c\)](#).

Figure 1-1 U.S. Pb emissions by sector.



Source: ([U.S. EPA, 2023c](#)).

Figure 1-2 U.S. county-level Pb emissions density estimates in lbs/year/mile².



Source: ([U.S. EPA, 2023c](#)).

Figure 1-3 U.S. anthropogenic Pb emissions trend 1990–2020.

The NEI is a national compilation of emissions information provided by state, local, and tribal air agencies, as well as source sector emission estimates developed by the U.S. EPA. Uncertainties are not reported here because the inventory database does not include sector emissions uncertainty estimates. The intent is to create the most complete inventory for use in air quality modeling, national rule assessments, international reporting, and other reports. It focuses largely on anthropogenic sources, with information about natural sources where available. The NEI program develops data sets, blends data from multiple sources, and performs quality assurance steps that further enhance and augment the compiled data. The accuracy of individual emission estimates may vary from facility to facility or county to county, and for some sources, data may be incomplete or lacking. For example, there are no soil resuspension data in the NEI. Sources of error may include the measurements used for developing source-specific emissions factors, biases related to modeled activity levels, or sources missing from the inventory. While uncertainties are difficult to predict, the NEI undergoes continuous improvement by the U.S. EPA with the assistance of state, local, and tribal agencies by their reporting emissions information for facilities, other stationary sources, and mobile sources. Each 3-year cycle of NEI development incorporates improvements based on lessons learned from the previous cycles, and estimation procedures for emissions sectors typically evolve over time in response to identified deficiencies as the data are used. As a result, in

spite of inexact and potentially unknown uncertainties, the NEI largely meets the needs for general emissions assessments and national trends reporting. Quality assurance procedures and acceptance criteria for the NEI are detailed in the NEI technical support document ([U.S. EPA, 2023a](#)).

While emissions inventory data are essential for understanding emissions, there are potential limitations and uncertainties. Uncertainty estimates for major emission sources or comparison of uncertainties between different types of sources were not found in the recent literature, and this was also the case in previous Pb air quality criteria documents and the 2013 Pb ISA. [Harris et al. \(2006\)](#) pointed out it is generally not clear how facilities calculate emissions reported to the NEI or TRI and that they do not attempt to quantify uncertainties. A comparison across several inventories covering the same area found the inventories sometimes did not include all emission sources, contained data that were not current, and reported emissions that varied considerably within the same year, leading to a recommendation that emissions data would benefit from data sharing, greater uncertainty analysis, and standardization of emissions estimation methods ([Harris et al., 2006](#)).

Source attribution studies have been carried out to investigate the extent to which different sources contribute to environmental concentrations either in remote areas to distinguish between major source types or at or near industrial sites to distinguish between component industrial processes for a given source. The basic approach was described in detail in the 2013 Pb ISA ([U.S. EPA, 2013](#)). Isotopes of Pb are measured in source samples to obtain a library of source signatures that can then be compared to ambient samples to estimate source contributions when an ambient sample is analyzed. As examples, isotope ratios vary between gasoline, coal, smelter, and municipal waste emissions, and specific ratios can ultimately be traced back to geologic conditions under which the Pb associated with each source was formed. As described in the 2013 Pb ISA, isotope ratios were first applied to PM in the mid-1960s to identify the impact of motor vehicle exhaust on urban Pb deposition. Several Pb isotope source attribution studies were reviewed in the 2013 Pb ISA, including both general source attribution studies and studies targeting quantification of specific source contributions, including coal and waste incineration. In more recent years, there has been little research activity on ambient air, but a continued focus on quantifying specific source contributions, especially smelting (Section 1.2.2), wildfires (Section 1.2.4), and legacy Pb from leaded gasoline (Section 1.2.7). Recent source attribution studies using a Pb isotope ratio approach have also been applied to Pb deposition (Section 1.3.1.2), soil (Section 1.3.2.1), and sediments (Section 1.3.3.4).

For context, much of the Pb in the United States is neither emitted into air nor transported into air from other media. Non-air Pb sources include plumbing ([Santucci and Scully, 2020](#); [Frank et al., 2019](#); [USGS, 2018](#); [Rosen et al., 2017](#); [Stillo and Macdonald Gibson, 2017](#); [Hanna-Attisha et al., 2016](#); [Pieper et al., 2015](#); [Brown et al., 2011](#)), mine waste ([Duval et al., 2020](#); [Gutiérrez et al., 2020](#); [Pavlowsky et al., 2017](#)), and food ([FDA, 2022](#); [Martín-Domingo et al., 2017](#); [Ritchie and Gerstenberger, 2013](#); [Guney and Zagury, 2012](#)). Even airborne Pb is only partly produced by contemporary Pb emissions into the atmosphere. Contemporary sources are discussed in this section, including aviation gasoline and aircraft

emissions (Section 1.2.1), industrial emissions (Section 1.2.2), fuel combustion from stationary sources (Section 1.2.3), wildland fires (Section 1.2.4), traffic-related emissions (Section 1.2.5), and volcanoes (Section 1.2.6). Substantial contributions to airborne Pb can also be attributed to historical sources of airborne Pb (Section 1.2.7) and non-atmospheric Pb sources, the Pb from which can in some cases become airborne through the processes of suspension and resuspension (Section 1.3.4). The resulting airborne Pb concentrations observed in ambient air (Section 1.5) can thus potentially be the result of a combination of contemporary atmospheric sources, resuspension of historical atmospheric sources and non-atmospheric sources.

1.2.1. Aviation Gasoline and Aircraft Emissions

Leaded aviation gasoline, or avgas, used by piston engine aircraft, is the largest national source of Pb emitted into the atmosphere identified by the NEI and is responsible for 69% of atmospheric Pb emissions in the United States. Pb additives, usually in the form of tetraethyl Pb, prevent engine knocking that could result in sudden engine failure ([U.S. EPA, 2013](#)). Most avgas is considered “100 Low Lead”, which contains 2.12 g Pb/gallon ([ASTM, 2021](#); [U.S. EPA, 2013](#)). In 2017, 208M gallons of avgas were consumed in the U.S. ([FAA, 2020](#)), leading to ~470 tons of total Pb emissions ([U.S. EPA, 2022a](#)). In 2020, the COVID-19 pandemic caused a 60% reduction in air traffic ([Sher et al., 2021](#)).

At the time of the last review, it was reported that Pb emissions from aircraft come in gaseous or particulate forms ([U.S. EPA, 2013](#)). In aviation exhaust PM, Pb is largely composed of lead bromide (PbBr₂) crystals coated with hydrocarbons ([Griffith, 2020](#); [U.S. EPA, 2013](#)). These particles are typically under 100 nm in diameter, although they can form larger agglomerates ([Turgut et al., 2020](#)). Pb particles emitted from piston engine aircraft exhaust have been observed as small as 13 nm diameter, which are significantly smaller than the mode of particles emitted from vehicle exhaust (35 nm) ([Griffith, 2020](#)). Pb had the highest concentration of any element measured by inductively coupled plasma mass spectrometry (ICP-MS) in PM₁₀ collected directly from aircraft engine exhaust ducts (median Pb value of 4.6×10^6 ng/m³) and was 40 times more concentrated than the next most abundant element (Na) ([Turgut et al., 2020](#)). Avgas constituents, including tetraethyl Pb, can evaporate into the headspace of storage and fuel tanks or be exhausted from the engine in the gas phase ([NASEM, 2021](#); [U.S. EPA, 2013](#)). Annual evaporative emissions of Pb from refueling are estimated at 75 kg ([NASEM, 2021](#)).

Around a single airport at which leaded fuel is used, Pb in air is highest around the runways ([Rahim et al., 2019](#); [Turgut et al., 2019](#); [Feinberg et al., 2016](#); [Feinberg and Turner, 2013](#)). The U.S. EPA used an estimate of 7.34 g of Pb emissions during a single take-off and landing cycle to estimate airport Pb emissions in the NEI ([U.S. EPA, 2013](#)). Touch-and-go operations are commonly practiced during pilot training and account for up to 23% of flights, depending on the airport ([U.S. EPA, 2020b](#)). Touch-and-go operations generally remain in air near the airport and can involve the aircraft circling overhead for hours, potentially contributing Pb to the local environment near airports used for training ([U.S. EPA, 2020b](#)).

Aircraft run-up, the series of checks performed by pilots immediately prior to take-off, contributed up to 82% of the 3-month average Pb concentration at one airport modeled by the U.S. EPA ([U.S. EPA, 2020b](#)). Aircraft engine run-up has been identified as one of the most important emission sources for ground-level Pb concentrations and was estimated at one airport to burn approximately 15.3 g/second of fuel and 50 g/second of fuel for a single- and multiple-engine aircraft, respectively ([U.S. EPA, 2013](#); [Carr et al., 2011](#)). Median run-up times measured at one airport were 40 and 63 seconds for single- and multiple-engine aircraft, respectively ([U.S. EPA, 2020b](#)). These times correspond to a three-month average Pb concentration of 0.092 $\mu\text{g}/\text{m}^3$, though this measurement was only conducted for one three-month period at one airport ([U.S. EPA, 2020b](#)). Model-extrapolation analyses for airports using leaded avgas estimated 3-month average Pb concentration at the site of maximum impact for some airports with high landing and take-off activity, to be <1–475 ng/m^3 at one airport ([U.S. EPA, 2020b](#)) and 10–20 ng/m^3 at another airport ([Feinberg and Turner, 2013](#)). Fuel consumption estimated at one airport during taxi ranged from 1.6 g/second to 5.1 g/second for single- and multiple-engine aircraft, respectively ([U.S. EPA, 2013](#); [Carr et al., 2011](#)). The time an aircraft spends in taxi can have a significant influence on Pb concentrations, as taxi time can vary greatly ([Feinberg et al., 2016](#)). Taxiing was responsible for 12% of total Pb emissions reported in one study, with about half of those emissions occurring when the aircraft was idle and awaiting clearance for take-off ([Feinberg et al., 2016](#)). These studies indicate runways to be the primary hot spot for Pb emissions at airports that use avgas. Annual aircraft Pb emissions from each flight phase are reported in Table 1-1.

There are 13,117 airports and over 5,000 heliports in operation in the United States ([NASEM, 2021](#)). Remote states, such as Montana and Alaska, rely heavily on air transportation. Alaska contains nearly 10% of the total amount of airports in the United States ([NASEM, 2021](#)). Several studies have observed lower Pb emissions when air traffic is lower ([Rahim et al., 2019](#); [Zahran et al., 2017](#)). There have also been observations of significantly decreased Pb concentrations near airports during periods of precipitation compared to when it is dry ([Rahim et al., 2019](#)).

Soil and air Pb concentrations decrease with distance from an airport. Model-extrapolated airborne Pb concentrations decrease with increasing distance from runway, from $\sim 0.6 \mu\text{g}/\text{m}^3$ at the maximum impact site to 0.01 $\mu\text{g}/\text{m}^3$ 500 m from the runway ([U.S. EPA, 2020b](#)). Soil samples collected from an Oklahoma airport were analyzed for Pb, for which elevated soil Pb concentrations were generally observed within 500 m from an airport ([McCumber and Strevett, 2017](#)). However, a few sites demonstrated higher soil Pb concentrations more than 500 m from an airport, suggesting influence from other sources such as industrial, historical, or non-air sources. This study also identified hot spots (10–170 mg Pb/kg) near fueling centers, suggesting avgas as the primary source ([McCumber and Strevett, 2017](#)). Twenty-four-hour average air Pb concentrations ranging from 17–70.6 ng/m^3 were reported and remained above background levels (10 ng/m^3) up to 900 m from a Santa Monica airport ([Carr et al., 2011](#)), illustrating the possible dispersion of Pb emissions from aircraft. At the same airport, $\text{PM}_{2.5}$ Pb concentrations dropped from 24 ng/m^3 to $\sim 6 \text{ng}/\text{m}^3$ after shortening the runway by 450 m ([Hudda et al., 2022](#)). This 75% reduction in airborne Pb concentration was attributed to a 50% decrease in aviation

operations following the shrinking of airport size ([Hudda et al., 2022](#)). Ambient air Pb was measured in a U.S. EPA one-year monitoring study at 17 U.S. airports for a full year ending in December of 2013 ([U.S. EPA, 2015](#)). Monitoring was required for a set of airports with estimated Pb emissions between 0.50 and 1.0 tons Pb per year that also met additional criteria including the dominant use of one runway and the level of piston-engine aircraft activity. Airport Pb concentrations monitored depend on level of piston-engine aircraft activity, the patterns of runway use, meteorology, and the placement of the monitor relative to the run-up area, and other factors. Maximum 3-month average Pb concentrations ranged from 0.1 to 0.33 $\mu\text{g}/\text{m}^3$ and exceeded 0.15 $\mu\text{g}/\text{m}^3$ at 2 of the 17 airports ([U.S. EPA, 2015](#)). In general, blood lead levels have been shown to increase with proximity to airports, volume of piston-engine aircraft traffic, and avgas consumption at airports ([Zahran et al., 2023](#)). These results are discussed further in Section 2.4.1.

Unleaded gasoline for motor vehicles became available following government-sponsored programs like the Federal Motor Vehicle Control program ([U.S. EPA, 2022b](#)). To reduce Pb emissions from aviation, unleaded avgas has recently been developed for most piston engine aircraft ([Swift Fuels, 2023](#); [Bertorelli, 2021](#); [AVweb, 2013](#)).

Table 1-1 Annual lead emissions (tons) from aircraft operating modes

Aircraft type	Taxi-Out	Run-Up	Take-off	Climb	Approach	Landing	Taxi-in	Total
Multiple engine	1.31×10^{-3}	6.27×10^{-4}	3.78×10^{-4}	4.07×10^{-4}	1.86×10^{-4}	8.51×10^{-5}	2.20×10^{-4}	3.21×10^{-3}
Single engine	9.94×10^{-3}	4.37×10^{-3}	3.74×10^{-3}	4.43×10^{-3}	3.69×10^{-3}	8.00×10^{-4}	2.72×10^{-3}	2.97×10^{-3}

Source: ([U.S. EPA, 2020b](#))

1.2.2. Industrial Sources

The 2013 Pb ISA summarized emissions inventory data and source apportionment results that attributed substantial amounts of airborne Pb to the metals industry ([U.S. EPA, 2013](#)). Studies identifying primary smelting mainly of other metals from various ores, secondary smelting—mainly of Pb batteries, and steel manufacturing as important contributors to Pb emissions were reviewed. Observations from several publications of downwind airborne Pb concentrations and Pb-PM content from the last remaining primary Pb smelter in the United States were summarized, as well as emissions from smelters for other metals that continue to operate. Other industrial emissions contributed less than the metals industry at the time of the 2013 Pb ISA, and there were few publications and little discussion of their emissions and contribution.

According to the 2020 NEI, industrial sources now account for 18% of U.S. emissions, making them the second largest category of sources after aviation fuel ([U.S. EPA, 2023a](#)). Roughly half of industrial emissions are from metal industries, both ferrous and non-ferrous in approximately equal amounts, and emissions sources include smelters, steel mills, foundries, and metal fabrication operations. The other half of industrial emissions is not related to metals processing and includes industries such as glass and cement manufacturing. Recent research on industrial Pb sources and emissions is largely limited to a few high-profile areas. Since publication of the 2013 Pb ISA, there have been several studies published on various aspects of Pb emissions from smelters, but there are few recent studies on other industrial Pb emissions, whether metals related or otherwise.

The highest ambient air Pb concentrations in the United States in Figure 1-2 are observed near metal industry sources. Historically, some large Pb smelters have been among the largest single sources of U.S. Pb emissions. Together they dominated local Pb emissions and accounted for a large fraction of national Pb emissions after the removal of Pb from gasoline ([U.S. EPA, 2013](#)). Recent studies have also continued to identify specific smelters as major urban Pb sources ([Wang et al., 2011](#)). Numerous previous field studies have documented Pb emissions from smelters as well as elevated ambient air Pb concentrations in the vicinity of primary smelters and soil Pb concentrations decreasing with distance from smelters ([Bowers et al., 2014](#); [U.S. EPA, 2013](#)). Recent research generally confirms these earlier observations by also showing that soil Pb concentrations decreased with distance from North American smelters and that isotope ratios consistent with smelter emissions could be identified in soil some distance from the smelter ([Widory et al., 2018](#); [Félix et al., 2015](#)).

One major focus of recent research has been Pb size distributions of smelter emissions. A bimodal particle size distribution with maxima at 0.18 μm and 9.9 μm was consistently observed over several years of sampling in the vicinity of a large copper (Cu) smelter in Hayden AZ ([U.S. EPA, 2013](#); [Csavina et al., 2011](#)). [Csavina et al. \(2014\)](#) confirmed that airborne Pb followed a bimodal particle size distribution in the vicinity of industrial operations that had both mining and smelting operations in both Arizona and Australia and suggested that the finer particles (<1 μm) were produced from smelters and the coarser particles were from windblown dust sources like mine tailings, crushing and grinding operations, and regional or nearby urban sources. Pb isotope ratios were used to show that fine particles smaller than 1 μm aerodynamic diameter in the vicinity of large smelters were mainly due to emissions from the smelter, while the isotope signature of coarse particles near the smelter were more similar to PM from a regional background aerosol or nearby urban environments ([Félix et al., 2015](#); [Csavina et al., 2014](#)). For similar mining operations in the absence of a smelter, only a coarse mode was observed ([Csavina et al., 2014](#)). Fugitive emissions of airborne dust studied using a Bayesian framework also reinforced that substantial Pb emissions are associated with coarse PM. Pb associated with airborne dust from loading and storage areas were estimated from time-dependent airborne Pb concentration measurements in multiple locations in the vicinity of a Pb-zinc (Zn) smelter in Trail, British Columbia, and found to make significant contributions to Pb emissions ([Hosseini and Stockie, 2016](#)). As substantiated by results from multiple smelters, large smelting operations can be a large local source of airborne Pb in both fine and

coarse PM, and Pb emissions from smelters can also have a broad area of impact because of their concentration in the fine particle size range ([Csavina et al., 2014](#)).

There have also been advances in describing the physical and chemical properties of Pb in smelter emissions. Previous speciation data from smelter emissions reviewed by [U.S. EPA \(2006\)](#) and [Skeaff et al. \(2011\)](#) are qualitative or semi-quantitative in nature ([Skeaff et al., 2011](#)). [Skeaff et al. \(2011\)](#) set as their objective the development of a quantitative chemical speciation of stack particulates from three Cu smelters with a mass balance as close to 100% as possible using X-ray diffraction, scanning electron microscopy, and electron probe microanalysis. Acceptable mass balances were achieved, and Pb accounted for 7.5% to 14% of PM by weight across the three smelters. Although insoluble PbSO₄ was consistently the dominant form of Pb ([Skeaff et al., 2011](#)), another study found that in the vicinity of a smelter in Hayden AZ, the PM size range most enriched in Pb overlapped with the most hygroscopic PM mode ([Youn et al., 2016](#); [Sorooshian et al., 2012](#)).

1.2.3. Fuel Combustion

Fuel combustion contributes ~55 tons of Pb/year to the atmosphere (9% of total emissions) with the greatest contributions from coal and oil fired boilers (20 tons) and coal-fired electric power generation (15 tons) ([U.S. EPA, 2023a](#)). Previous reports have provided extensive background on the role of Pb in coal combustion. Pb is found in coal in varying amounts (5–35 mg Pb/kg) ([U.S. EPA, 2013, 2006](#)). Fly ash, a byproduct of coal combustion, is composed primarily of silicon and oxygen ([Zierold and Odoh, 2020](#); [U.S. EPA, 2006](#)). Pb in fly ash is enriched 2–10 times compared with that in parent coal ([Zierold and Odoh, 2020](#); [Wang et al., 2019](#)) for concentrations in fly ash samples ranging from 25.3–308 mg Pb/kg ([Wang et al., 2019](#)) or 1.4–2120 mg Pb/kg depending on the source ([Zierold and Odoh, 2020](#)). In a study performed in Colorado and the Appalachian Basin, 54% of Pb from parent coal was found in fly ash particles at concentrations of 41.8 mg Pb/kg ([Swanson et al., 2013](#)).

Pb emissions from coal-fired power plants have decreased by 36% since 1993 due to pollution control measures and plant closures, though power plants can still dominate local Pb emissions ([U.S. EPA, 2020a](#); [Zierold and Odoh, 2020](#); [Gingerich et al., 2019](#)). In New Mexico, average Pb concentrations in PM_{2.5} samples were 0.65 ng/m³ (range 0.20–1.04 ng/m³), with approximately 0.44 ng/m³ attributed to the two nearby coal-fired power plants ([Gonzalez-Maddux et al., 2014](#)). Another study identified elevated Pb concentrations on rock samples taken near power plant sites, with Pb the most enriched of the 15 elements analyzed by X-ray fluorescence (XRF) spectroscopy ([Nowinski et al., 2012](#)). Pb concentrations were higher for the skyward facing side of the rock compared with the interior, suggestive of atmospheric Pb deposition ([Nowinski et al., 2012](#)). In general, Pb concentrations are not correlated with the amount of electricity generated at an individual plant ([Bray et al., 2017](#)), complicating predictions of Pb emissions from coal-fired power plants.

Petroleum-fueled power plants emit ~6.4 g Pb/1000 L of fuel oil burned ([U.S. EPA, 2006](#)). Though there are uncertainties surrounding the concentration of Pb in crude oil ([U.S. EPA, 2013](#); [Murphy et al., 2007](#)), New York City had average Pb concentrations of 3.40 ng/m³ (range 1.22–10.98 ng/m³) in 2009 which land use regression models associated with residual oil burning ([Ito et al., 2016](#)). Used motor oil, which may be burned in personal space heaters, contains some Pb ([Murphy et al., 2007](#)). Fuel extraction also contributes to elevated ambient air Pb concentrations. Several studies near the Athabasca Oil Sands in Alberta, Canada report ambient air Pb concentrations ~0.35 ng/m³, though some of this Pb may come from long-range or regional transport ([Graney et al., 2019](#); [Landis et al., 2019](#)), and oil fields of this size are not present in the United States. Biomass fuel consumption has average Pb emissions of 0.56 mg Pb/kg fuel ([U.S. EPA, 2006](#)). Residential wood burning releases airborne Pb at concentrations of 3.3–12.2 mg Pb/kg wood and 2.89–30.3 mg Pb/kg wood for woodstoves and fireplaces, respectively ([U.S. EPA, 2013](#)). Pb-containing particles are ubiquitous in urban areas, indicating widespread emissions from combustion sources ([Murphy et al., 2007](#)). A mode for Pb urban aerosol was identified at 200 nm, though Pb was also observed in 50 nm particles, the smallest particle size detected by single particle mass spectrometry ([Murphy et al., 2007](#)).

1.2.4. Fires

Pb deposited historically in forests is remobilized during wildfires, and Pb in anthropogenic structures and vehicles can also contribute when wildfires burn infrastructure. Fire emissions account for 18 tons Pb per year according to the 2020 NEI, making wildfires the fourth largest source of Pb emissions in the United States, behind piston engine aircraft, industrial processes, and fuel combustion, accounting for ~3% of total Pb U.S. Pb emissions ([U.S. EPA, 2023a](#)). PM from fires is mostly carbonaceous, but also contains other elements in low concentrations, including Pb. Preliminary emissions testing results indicate that more Pb is emitted from smoldering emissions than flaming emissions, and that current emission factors are substantially lower than previous literature observations, probably because of lower Pb levels in the environment due to the phase-out of leaded gasoline. Because fires are the largest source of primary PM in the United States ([U.S. EPA, 2021a, 2019](#)), even trace level emissions make fires a potentially important source of airborne Pb. Limited studies have observed Pb concentrations attributed directly to smoke from wildfires. Without reliable emissions data before its inclusion in the 2020 NEI, previous studies focused on air, ash, and soil concentrations to evaluate Pb from fires. This section is therefore organized as follows: air concentration studies from the previous 2013 Pb ISA, followed by new air concentration studies, and ending with ash and soil measurement studies. Studies are summarized in Table 1-2.

The 2013 Pb ISA noted a handful of air concentration studies that have found elevated Pb concentrations in PM₁₀ and PM_{2.5} during biomass burning episodes ([U.S. EPA, 2013](#)). [Qureshi et al. \(2006\)](#) observed a spike in Pb-PM_{2.5} at 42 ng/m³ in Queens, NY during a fire event in Quebec. This 24-hour spike was considerably larger than the 3-month average (July to September) of 5.1 ng/m³. Another

study quantified the increase of Pb-PM₁₀ measured in Finland at 1.7–3.0 times higher during forest fire emissions from a fire in Russia compared to the reference concentration of 3.5 ng Pb /m³ ([Anttila et al., 2008](#)). Similarly, [Golobokova et al. \(2020\)](#) observed air above Lake Baikal in Siberia before and during large wildfires. They found levels of Pb were double the base level during the wildfires, with base level concentrations averaging 0.16 ng/m³ and fire concentrations averaging 0.33 ng/m³. [Isley and Taylor \(2020\)](#) evaluated trace element and Pb isotope compositions in aerosols from four wildfires near Sydney, Australia. They found Pb concentrations pre-fire up to ~120 ng/m³ and concentrations during and post-fire up to ~210 ng/m³. They attributed 94% of the Pb mass to anthropogenic pollutants, namely historical Pb from previous emissions. These four studies found elevated Pb measurements, up to 8 times higher, during days with fire emissions present. The concentrations varied depending on location, with more isolated locations, such as shipboard on Lake Baikal and rural Finland, measuring lower concentrations compared with locations with legacy Pb, such as Sydney, Australia and New York City, NY. Despite these differences, the relative increase is similar across studies.

Also examining Pb attributed to PM_{2.5}, [Boaggio et al. \(2022\)](#) analyzed Pb air concentrations on smoke-affected days across 13 years. They found Pb to be insignificantly different on smoke days compared with non-smoke days apart from during wildfires that burned substantial infrastructure. The median percent change for Pb comparing smoke to non-smoke days was found to be 2-3% lower, but the maximum was more than 40 times higher at the station that received smoke from the 2018 Camp Fire which destroyed ~18,000 structures. Another study detected Pb-bearing particles in the coarse mode (PM_{10-2.5}) during the Camp Fire ([Sparks and Wagner, 2021](#)). After the burning of the Notre Dame Cathedral in Paris which contained approximately 460 tons of Pb, an increase in particulate Pb concentrations from 0.050 to 0.105 µg/m³ was observed 50 km downwind of the fire ([van Geen et al., 2020](#)). These results emphasize the importance of accounting for Pb mobilized from burning infrastructure and vehicles during more destructive wildfires, typically occurring in the wildland-urban interface.

Pb found from burning of anthropogenic structures was also seen in ash studies. [Burton et al. \(2016\)](#) looked at ash following a fire in California in 2009 and found Pb was higher in ash samples collected from burned residences and buildings compared with soil and sediment Pb concentrations. Similarly, [Alexakis \(2020\)](#) found the median values of Pb in residential ash (78 mg Pb/kg) were 1.5 times higher than those found in wildland ash (53.5 mg Pb/kg) after a fire in western Attica. The residential ash sample concentrations of Pb ranged up to 205 mg Pb/kg. Additionally, [Campos et al. \(2016\)](#) studied Pb levels in burnt soils after a wildfire in Portugal and found unburnt soil concentrations ranging from approximately 40–50 mg Pb/kg with burnt soil concentrations ranging from approximately 55–150 mg Pb/kg. These two studies find ash concentrations of Pb similar to those found by [Alexakis \(2020\)](#), who noted elevated concentrations in residential ash. Soil Pb concentrations ranged from 30–9,000 mg Pb/kg within 1 km of the Notre Dame Cathedral fire in Paris, whose roof and spire were composed of 460 tons of Pb ([van Geen et al., 2020](#)). This study also observed elevated concentrations in the direction of prevailing winds during the fire ([van Geen et al., 2020](#)). The 2013 Pb ISA also cites a study focusing on

wildfire ash by [Odigie and Flegal \(2011\)](#) that found measurements of Pb in ash following the Jesusita Fire in 2009 ranging from 4.3 to 51 mg Pb/kg. Another study from the same group measured Pb and other trace metals remobilized by the Williams Fire in 2012 and found Pb concentration in ash ranging from 7 to 42 mg Pb/kg ([Odigie and Flegal, 2014](#)). Both studies concluded the Pb was primarily of anthropogenic origin remobilized by the fires.

Table 1-2 Parameters related to fires and associated Pb measurements discussed herein

Reference	Fire Location	Fire Duration and Size	Measurement location	Pb concentration
Qureshi et al. (2006)	Quebec, Canada	July 5–9, 2002 250,000 hectares	Queens, New York	42 ng/m ³ in PM _{2.5}
Anttila et al. (2008)	St. Petersburg, Russia	April–August 2006, unspecified size	Virolahti, Finland	3.5 ng/m ³ in PM ₁₀
Golobokova et al. (2020)	Lake Baikal, Russia	July 23–August 1, 2019 Unspecified size	Lake Baikal, Russia	0.33 ng/m ³ in presence of fire, 0.16 ng/m ³ without fire
Isley and Taylor (2020)	Sydney, Australia	1994, 1997, 2001–2002, 2004 >1,300,000 hectares	Sydney, Australia	Up to ~210 ng/m ³ during fire, up to ~120 ng/m ³ pre-fire
Boaggio et al. (2022)	Paradise, California – Camp Fire	November 8–25, 2018 153,336 acres	Point Reyes, California	13 ng/m ³ in PM _{2.5}
Sparks and Wagner, (2021)	Paradise, California – Camp Fire	November 8–25, 2018 153,336 acres	San Francisco, California	0.26 ng/m ³ in PM ₁₀
van Geen et al., (2020)	Paris, France – Notre Dame Cathedral	15 hr on April 15, 2019 6240 m ²	50 km downwind in Paris, France	Up to 0.105 µg/m ³ in PM ₁₀ , 30–9,000 mg/kg in soil
Burton et al. (2016)	Los Angeles, California – Station Fire	August 26–October 16, 2009 680 km ²	Angeles National Forest	1.1–16.4 µg/L in water
Alexakis (2020)	Attica, Greece – Attica Wildfire	July 23–26, 2018 1,431 hectares	Attica, Greece	53.5–205 mg/kg in ash
Campos et al. (2016)	Ermida, Portugal	July 26, 2010 295 hectares	Ermida, Portugal	40–50 mg/kg in unburned soil, 55–150 mg/kg in burned soil
Odigie and Flegal (2011)	Santa Barbara, California – Jesusita Fire	May 5–18, 2009 8,733 acres	Santa Barbara, California	4.3–51 mg/kg in ash
Odigie and Flegal (2011)	Los Angeles, California – Williams Fire	September 2–4, 2012 4,192 acres	Los Angeles, California	7–42 mg/kg in ash

1.2.5. Traffic and Roads

In 2006, the major sources of Pb emissions from on-road mobile sources were fuel combustion and vehicle wear ([U.S. EPA, 2006](#)). After the phase-out of Pb as an anti-knock agent in gasoline for on-

road automobiles in the 1990s, Pb emissions from tailpipes declined rapidly. As a result, the relative contribution of non-tailpipe emissions, such as resuspension of Pb in soil and road dust into air as well as brake, tire, and road wear, has increased. The 2013 Pb ISA found a significant source of Pb in non-tailpipe emissions from wheel weights. [Aucott and Caldarelli \(2012\)](#) estimated that $13.8 \pm 5.0\%$ of the deposited mass of wheel weights are dispersed each year through abrasion and grinding by traffic ([U.S. EPA, 2013](#)). However, since 2013, wheel weights containing Pb have been banned in many states. In addition to wheel weights, tire abrasion (mean of two tire samples in Korea = 13 mg Pb/kg tire) and brake wear (30.5 mg Pb/kg brake dust from light duty vehicles in Korea) also contribute to Pb emissions ([Jeong et al., 2022](#); [U.S. EPA, 2013](#)). When comparing non-exhaust emission sources, asphalt had the highest Pb concentration (738 mg Pb/kg) followed by road paint (88 mg Pb/kg) ([Jeong et al., 2022](#)). A study that used material metal concentrations, traffic volume, emissions factors, and sales data to estimate the quantity of Pb emitted from brake wear and tires in Stockholm, Sweden in 2005 estimated that 24 kg (0.026 ton) of Pb were emitted from brake wear each year, compared with 2.6 kg (0.0029 ton) of Pb from tire tread wear; an estimated 549 kg (0.61 ton) was emitted from brake wear in 1998 ([U.S. EPA, 2013](#); [Hjortenkrans et al., 2007](#)).

Road dust is loose material that can be collected by sweeping and vacuuming the traveled portion of a road. Also called road sediment or street sediment, it is inclusive of particles associated with non-tailpipe Pb emissions from traffic ([Dietrich et al., 2022](#)). Road dust also contains PM deposited from other sources onto or near roads, and is geochemically related to urban soil ([Alshetty and Shiva Nagendra, 2022](#); [Dietrich et al., 2022](#); [Jeong et al., 2022](#)). Road dust emissions are a function of dust load and vehicle traffic (frequency of vehicle passing and average weight of vehicles) ([Alshetty and Shiva Nagendra, 2022](#)), with average road sediment concentration of Pb in Busan South Korea in 2014 reported as 210 mg Pb/kg road dust ([Jeong et al., 2020](#)). Road dust in Philadelphia had mean and median Pb concentrations of 516 mg Pb/kg and 202 mg Pb/kg, respectively, with higher values reported for industrial sites and lower for mixed use sites ([O'Shea et al., 2020](#)), while road dust in Toronto had a median Pb concentration of 63 mg Pb/kg (range 21–220 mg Pb/kg) ([Wiseman et al., 2021](#)). [Deocampo et al. \(2012\)](#) observed high spatial variability for Pb concentrations in Atlanta road dust, describing a median road dust Pb concentration of 63 mg Pb/kg in a downtown Atlanta area, but a median of 93 mg Pb/kg and a maximum concentration of 972 mg Pb/kg in a residential area (also in the urban core). They reported significant variation on a scale of tens to hundreds of meters. Most road dust particles are large, with sizes ranging from 10–60 μm ([O'Shea et al., 2021](#)). On average, 13%–18% of road dust analyzed in two areas in India was $<10 \mu\text{m}$, 6%–9% was $<2.5 \mu\text{m}$, and 4%–6% was $<1 \mu\text{m}$ ([Alshetty and Shiva Nagendra, 2022](#)). Road dust and soils can serve as both sources and sinks to one another ([Dietrich et al., 2022](#)).

Resuspension of Pb in road dust and soils back to the atmosphere is covered in Section 1.3.4. The relationship between Pb air concentrations and distance to the road is an emerging area of research. [Cahill et al. \(2016\)](#) looked at this question for three size fractions of PM in Detroit in 2010. They found that for coarse PM, Pb concentrations were $\sim 4 \text{ ng/m}^3$ at 10 meters from the highway, $\sim 1 \text{ ng/m}^3$ at 100 meters north or south of the highway, and $\sim 1.5 \text{ ng/m}^3$ 300 meters north of the highway. They deduced that the

increase at 300 meters could be attributed to a heavily trafficked road around 380 meters north of the highway. For PM_{2.5} (0.09 to 2.5 μm), they found Pb concentrations were ~4 ng/m³ 10 meters north, ~3 ng/m³ 100 meters north, and ~2.5 ng/m³ 300 meters north of the highway. For very fine PM (0.09 to 0.26 μm), Pb concentrations were ~0.75 ng/m³ 100 meters south, ~0.25 ng/m³ 10 meters north, ~0.95 ng/m³ 100 meters north, and ~0.4 ng/m³ 300 meters north. Another study found similar near-road concentrations for fine Pb with a mean of 5.23 ng/m³ and slightly lower concentrations of coarse Pb with a mean of 1.14 ng/m³ (Silva et al., 2021). Contrary to the previous study, they found Pb to be significantly related to distance to nearest road in coarse concentrations only (Silva et al., 2021). A third study also did not find a relationship with distance to road in median PM_{2.5} water soluble Pb (Oakes et al., 2016), with a slight decline with distance for acid soluble PM_{2.5} Pb and PM_{10-2.5} Pb. These studies found Pb associated with PM generally decreases with distance to road. However, the size of this gradient depends on the particle size distribution of Pb and even with consistent size, there could be subtle differences when breaking Pb down into water and acid soluble fractions. For a monitoring site in central Los Angeles located near a major interstate freeway, trends in ambient air Pb concentrations were related to traffic volume. Pb concentrations decreased slightly from 2005 (median 24-hour sample of .005 μg/m³) to 2013–2015 but increased from 2015 (median of 0.001 μg/m³) to 2018 (median of 0.005 μg/m³). This was attributed to greater road dust resuspension into air due to increased traffic on the nearby interstate freeway, since traffic near the site was relatively constant before 2013, but increased considerably from 2013 to 2018 (Farahani et al., 2021). For context, this increase is substantially less than the overall decline of airborne Pb concentrations near roads with heavy traffic since leaded gasoline was phased out (Section 1.4.4). Wiseman et al. (2021) estimated that 90 ± 23 kg of Pb in road dust was resuspended into air annually in Toronto, Canada, an amount corresponding to 22% of air releases from Toronto industrial facilities. Limitations identified in this study were identified as uncertainties associated with aging of street sweeping equipment, street sweeping frequency, and particle size distribution assumptions.

1.2.6. Volcanoes

The 2006 Pb AQCD (U.S. EPA, 2006) included an estimate of 540 to 6000 metric tons per year for the range of global Pb emissions from volcanoes (Nriagu and Pacyna, 1988). More recently, the Masaya volcano in Nicaragua was estimated to emit 1 ton of Pb per year (Liotta et al., 2021). In two recent studies, Pb concentrations measured at volcanic sources ranged from 0.055 to 0.75 μg/m³ for samples collected at the main active vent during the 2018 eruption of Kilauea on the island of Hawaii (Mason et al., 2021), and 0.14 to 0.27 μg/m³ for samples collected at the rim of a crater of the Masaya Volcano in April 2000 (Liotta et al., 2021). Concentrations at the upper ends of these ranges are comparable to some of the highest currently observed Pb monitoring network concentrations (Section 1.5). Airborne Pb concentrations associated with the eruption of Kilauea were higher than concentrations at nearby populated areas (Ilyinskaya et al., 2021). During the week of the 1991 eruption of Mt. Hudson in southern Chile, observed Pb concentrations more than 2000 miles away on King George

Island in the Southern Ocean were higher than before or after the eruption ([Evangelista et al., 2022](#)). Highly elevated Pb concentrations associated with the eruption were also observed in lake sediment profiles ([Evangelista et al., 2022](#)).

Pb can be emitted in both particulate form ([Liotta et al., 2021](#)), and as a volatile gas at high temperatures ([Edmonds et al., 2022](#); [Liotta et al., 2021](#)), and emissions result in the formation of particulate volcanic plumes downwind of active volcanoes ([Edmonds et al., 2022](#)). Recent research suggests that emissions of Pb from volcanoes might be underestimated. [Ilyinskaya et al. \(2021\)](#) observed that deposition of Pb and other metals were depleted more rapidly from the volcanic plume of Kilauea than more widely studied species such as sulfur, and that Pb concentrations in nearby communities during the 2018 eruption did not change as much as the concentrations of other species. They recognized that volatile metals like Pb, Cd, and Se were emitted as gases in high temperature volcanic vents and formed soluble chlorides, sulfates, and sulfides that were rapidly removed by wet deposition in the vicinity of the source by the rapidly condensing water in the humid environment created by the high abundance of water vapor emitted from the vent or otherwise present in the humid environment near the source ([Ilyinskaya et al., 2021](#)). They contrasted this with more refractory elements such as magnesium (Mg) and iron (Fe) that are not emitted as gases and noted that Pb was depleted from the volcanic plume 100 times faster than these elements ([Ilyinskaya et al., 2021](#)). This is consistent with results from [Liotta et al. \(2021\)](#), who observed enrichment of Pb in rainwater in comparison to volcanic rock at the Masaya Volcano in Nicaragua. There is some evidence of differences in volatility of Pb emitted from different volcanoes ([Liotta et al., 2021](#)). [Ilyinskaya et al. \(2021\)](#) concluded that emissions of Pb and other volatile metals from volcanoes, as well as their concentration and deposition in the immediate vicinity of volcanoes might be underestimated ([Ilyinskaya et al., 2021](#)).

1.2.7. Legacy Sources

Contemporary U.S. emissions of airborne Pb described in Sections 1.2.1 through 1.2.6 do not provide a complete picture of all contributions to ambient air Pb, because Pb emitted from past sources can become resuspended. Current air emissions are considerably smaller than historical emissions. Numerous studies of historical records have been reconstructed from sediment and peat cores as well as long-term soil concentration measurements from many North American locations including Virginia, the Northeast United States, the St. Lawrence Valley, and northern Alberta (Section 1.3.3.4). Most of these studies show evidence of decreasing Pb concentrations after the 1970s due to elimination of leaded gasoline and reductions in industrial emissions ([Balascio et al., 2019](#); [Shotyk et al., 2016](#); [Sarkar et al., 2015](#); [Richardson et al., 2014](#); [Pratte et al., 2013](#)). An exception was a sinkhole near Lake Marion SC, where sediment Pb concentrations increased continuously during the past 60 years ([Edwards et al., 2016](#)). This recent research adds to an even larger body of literature summarized in the 2013 Pb ISA and previous AQCDs that atmospheric Pb concentrations and atmospheric deposition have decreased steadily

since the 1970s ([U.S. EPA, 2013](#)). Pb isotope ratios from some of these studies suggest that historical sources are an important if not dominant contributor to Pb in North American soil and sediments.

Leaded gasoline has been a major contributor to Pb in the environment, particularly in roadside and urban soils. An estimated 5.4 million metric tons of Pb additives were used in leaded gasoline in the United States between 1927 and 1994 ([Mielke et al., 2010](#)), peaking between 1968 and 1972 at more than 200,000 metric tons per year ([U.S. EPA, 2013](#)). Pb additive use subsequently declined by 92% from 1970 to 1990 due to health concerns and leaded gasoline was finally banned in the United States in 1996. Leaded gasoline is a prominent source in sedimentary and other historical records of atmospheric Pb pollution ([U.S. EPA, 2013](#)) and is still relevant near aviation fueling stations. Recent studies investigating Pb isotope ratios continue to show that leaded gasoline was the principal source of atmospheric Pb ([Pratte et al., 2013](#)) and the dominant source of Pb in samples of North American sediments ([Pratte et al., 2013](#)) and forest soils ([Richardson et al., 2014](#)). In the United States, emissions were concentrated in urban areas, with emissions in 90 urban areas estimated to account for about 30% of total U.S. automotive Pb emissions in 1982 ([Mielke et al., 2011](#)). In a detailed recent study in a mid-size southern U.S. city, current roadside soil concentrations decreased since the peak of leaded gasoline usage but remained higher than geologic background ([Wade et al., 2021](#)).

The United States was a leading producer of Pb in the previous century with major mining and smelting operations. High Pb concentrations in soils near smelters and other industrial operations have been observed in numerous studies ([U.S. EPA, 2013](#)). The last primary Pb smelter in the United States closed in Herculaneum, MO in 2013 ([Sullivan and Green, 2020](#)). Recent studies also found high Pb concentrations in soil near closed smelters in Tar Creek, OK; Pueblo, CO; and Eureka, NV ([Diawara et al., 2018](#); [Chaffee and King, 2014](#); [Zota et al., 2011](#)). Pb concentrations in residential soil samples in Tar Creek, OK ranged from 12 to 2436 mg Pb/kg and averaged 201 mg Pb/kg ([Zota et al., 2011](#)), and Pb concentrations in samples from Pueblo, CO ranged from 12 to 10,011 mg Pb/kg and averaged 366 mg Pb/kg ([Diawara et al., 2018](#)). Pb from closed smelters was also the dominant source of Pb in lake sediments near Tacoma, WA ([Gawel et al., 2014](#); [Gray et al., 2013](#)) and attic dust in El Paso, TX ([Van Pelt et al., 2020](#)). [Wang and Kanter \(2014\)](#) identified 229 former Pb industrial sites in urban areas of the United States.

Pb-based paint was banned in the United States in 1978. However, 15.3 million homes, 14% of the homes in the United States, have significantly deteriorated Pb-based paint according to the Department of Housing and Urban Development's American Healthy Homes Survey. The proportion of houses with deteriorating Pb-based paint increases with the age of the housing, accounting for 86% of U.S. houses built before 1940. Regionally, a greater fraction of houses in the Northeast and Midwest contains Pb-based paint than in the South and West. Housing with Pb-based paint is also unevenly distributed on a local scale, with a greater fraction of poor and non-white families living in houses with Pb-based paint ([HUD, 2011](#)). A recent county-level geospatial analysis of Pb paint hazard in homes and childcare facilities found potential Pb hazard hotspots coincided with areas of higher populations of non-

white children ([Baek et al., 2021](#)). Peeling and deteriorating paint is a source of high Pb concentrations in yard soil and house dust ([HUD, 2011](#)). In streetside, residential, and other soil samples from Durham, NC, soil Pb concentrations ranged from 6 to 8825 mg Pb/kg, with the highest Pb concentrations observed within 1 m of pre-1978 residential foundations and both foundation and yard soil Pb concentrations considerably higher around older houses ([Wade et al., 2021](#)). In urban and industrial areas and near heavily trafficked roads, historical air emissions together with Pb from deteriorating paint comprise a pool of legacy Pb in urban soil ([Wang et al., 2022](#); [Obeng-Gyasi et al., 2021](#)). The potential for the contribution of legacy Pb to ambient air through suspension and resuspension is discussed in Section 1.3.4.

1.2.8. Other Sources

Exposure to Pb from community gardens and consumer products is mainly through other media, but Pb from these sources can briefly become airborne. Pb in food from residential and community gardens has been the subject of numerous recent studies. Although additional recent research also indicates that soil Pb can be a concern for urban gardens ([Engel-Di Mauro, 2021](#); [Clarke et al., 2015](#); [Kaiser et al., 2015](#); [Wiseman et al., 2015](#)), there are ongoing research efforts to improve urban gardening by reducing Pb contamination in garden produce ([Egendorf et al., 2021](#); [Taylor et al., 2021](#); [Gallagher et al., 2020](#); [Harada et al., 2019](#); [Fitzstevens et al., 2017](#); [Brown et al., 2016](#); [Schwarz et al., 2016](#); [Spliethoff et al., 2016](#); [Kaiser et al., 2015](#)).

Pb is also a concern in a variety of consumer products. Batteries were responsible for 92% of Pb consumed in the United States in 2021 ([USGS, 2022](#)). Many of the source oriented Pb monitoring sites in the national monitoring network for Pb are near secondary smelters for battery recycling (Section 1.4.1). Recent research has focused on trends for recycling used batteries from the United States and Europe in other countries. It has been estimated that there are more than 10,000 informal industrial sites for processing used Pb-acid batteries in low- and middle-income countries, especially in East Asia, South Asia, and Africa ([Ericson et al., 2017](#)). Informal industry is defined as industry characterized by a lack of adherence to regulation, including zoning and pollution controls ([Ericson et al., 2017](#)). In a study of soils from 15 recycling plants and one battery manufacturing site in 7 countries in Africa, mean soil Pb concentrations ranged from 480 to 140,000 mg Pb/kg and averaged 23,200 mg Pb/kg inside plant sites, and ranged up to 48,000 2600 mg Pb/kg and averaged 2600 mg Pb/kg in soil samples from communities surrounding the plants ([Gottesfeld et al., 2018](#)).

By amount of Pb consumed, ammunition ranks second after batteries as an end use for Pb in the United States ([USGS, 2022](#)). The mean estimate of Pb concentrations in soils from shooting ranges in 10 studies was twice as high as Pb concentrations from non-residential Superfund sites (mean values of 3604 ppm Pb and 1868 ppm Pb, respectively) ([Frank et al., 2019](#)). Recent research has advanced our understanding of the ranges of particle size, solubility, bioaccessibility, and chemical forms of Pb in

gunshot residue particles from shooting range soils ([Schindler et al., 2021](#); [Sanderson et al., 2012](#)). There is a large body of research on the environmental and health consequences of the use of Pb in ammunition ([Arnemo et al., 2016](#)). Other consumer products that are sources of Pb are contaminated ceramic cookware, food, toys, cosmetics, antiques, and herbal medicines ([Frank et al., 2019](#)). This summary of Pb in consumer products is provided for context. Research on health or environmental effects of Pb in batteries, ammunition, food, and other consumer products is considered beyond the scope of the National Ambient Air Quality Standards (NAAQS)-related research discussed in this document.

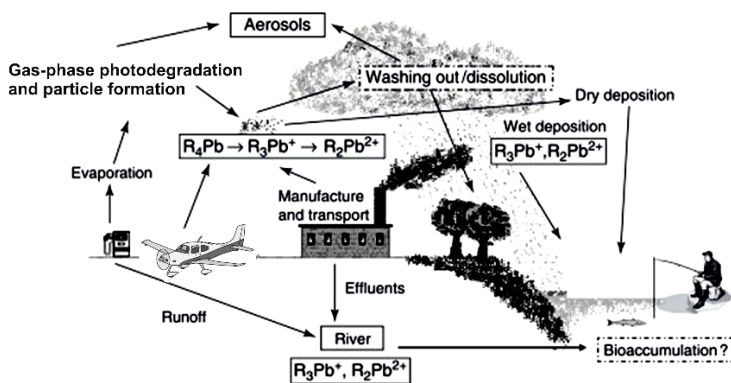
1.3 Fate and Transport of Pb Emitted into Air

Knowledge of Pb transport within and between diverse media, including air, surface water, soil, and sediment, provides a foundation for understanding the various pathways leading to atmospheric Pb exposure, as well as the atmospheric contribution to total Pb exposure discussed in Appendix 2 (<https://assessments.epa.gov/isa/document/&deid=359536>). Pb emitted into the atmosphere can be distributed into soil, water, and other media, leading to human and ecosystem contact. Understanding Pb transport in soil, water, and other media is also necessary for assessing impacts of atmospheric Pb relative to non-atmospheric sources such as wastewater discharges or mobilization from waste materials. Sections 1.3.1, 1.3.2, 1.3.3, and 1.3.4 summarize our understanding of fate and transport of Pb in air, soil, water, and urban media, respectively.

1.3.1. Fate and Transport in Air

Pb is mainly emitted in particulate form, and the fate of airborne Pb is strongly influenced by the whether it is primarily emitted in the form of ultrafine combustion particles as observed for aviation gas exhaust, or coarse particles, as observed for resuspended Pb from soil (Section 1.3.4). As described in Section 1.2.1, Pb is introduced into aviation fuel as the anti-knocking agents tetramethyl and tetraethyl Pb ([Kumar et al., 2020](#)). During engine operation, the organic functional groups of these compounds are oxidized and emitted as water and carbon dioxide. A second additive to the fuel mixture, an alkyl bromide compound, reacts with the Pb present in the combustion mix to form an array of compounds composed of Pb (II), bromide and chloride ions, molecular ammonia, and other, nonvolatile compounds that form particles. These particles are either entrained into the engine exhaust or remain in the engine's crankcase lubricant ([NCBI, 2022](#)). Unreacted tetramethyl and tetraethyl Pb have sufficiently high vapor pressures at ambient and engine operation temperatures to allow for fugitive emissions of these gases ([U.S. EPA, 1986](#)), which go on to photolyze in the presence of atmospheric ultraviolet radiation to form Pb compounds that also contribute to atmospheric PM. These Pb-containing particles are then subject to the same atmospheric processes that transport and remove other forms of PM. As discussed in Sections 1.3.1.1 and 1.3.1.2, the transport and deposition of dry particles is defined by size. Depending on the chemical counter-ion, Pb compounds vary in water solubility, determining the degree to which Pb is

removed by wet deposition. Figure 1-4 provides a general illustration of the geochemical lifecycle of Pb derived from fuel additives. Resuspension of soil bound Pb has the potential to contribute to airborne concentrations near major Pb sources and is considered in Section 1.3.4.



Source: Adapted with permission from [Encinar and Moldovan \(2005\)](#).

Figure 1-4 The biogeochemical cycle of tetramethyl/tetraethyl Pb.

1.3.1.1. Atmospheric Transport

The 2013 Pb ISA discussed in detail the available studies concerning the variables governing long-range and urban-scale transport of particle-bound Pb in the atmosphere, concluding that Pb was primarily present in submicrometer aerosols, but bimodal size distributions within this size range were frequently observed ([U.S. EPA, 2013](#)). As described in detail in Section 1.2.1, Pb (as PbBr and other halogenated forms of Pb) is primarily emitted by piston-driven aircraft in the ultrafine particle (UFP) size range (<100 nm) and larger particles formed from agglomeration of individual particles in the UFP size range ([Turgut et al., 2020](#)). Particles emitted by aircraft have been observed to be as small as 13 nm in diameter, when emitted ([Griffith, 2020](#)).

Consistent with particles from other sources, according to several studies, particle-bound Pb in fine PM is transported long distances and found in remote areas. The patterns of dispersion can be modeled using Gaussian plume models or Lagrangian and Eulerian continental transport models, indicating that Pb remains a nonvolatile, unreactive particle component. The 2013 Pb ISA also described studies that indicate that small Pb-containing particles can be scavenged by larger, soil-derived geogenic particles which can lead to chemical reactions that alter the composition and hygroscopicity of the

composite particle ([U.S. EPA, 2013](#)). This finding was supported by evidence of Pb enrichment of particles originating from Pb-free sources that were deposited in remote locations.

There has been little recent research on transport of airborne Pb, and recent studies have continued to focus on transport of Pb associated with particles smaller than 10 μm . Recent research supports previous results that Pb derived from high temperature processes such as smelting is largely emitted in the submicrometer fraction and is capable of being transported over long distances and being deposited in remote environments ([Cullen and McAlister, 2017](#)). On a smaller scale, using a generalized regression model with 4 km^2 sampling grids, [Fortuna et al. \(2020\)](#) demonstrated that Pb content of lichen samples was significantly spatially associated with dispersion modeling outcomes for Pb, and other metals primarily associated with PM_{10} emitted from a coal-fired power plant over an area of 176 km^2 , for a dispersion model developed for a time frame that corresponds to the average age of biomonitor sample material. There is also recent research on chemical transformation of Pb. In Beijing, [Peng et al. \(2020\)](#) reported complete atmospheric transformation of PbO and PbCl_2 from coal combustion to $\text{Pb}(\text{NO}_3)_2$, from a process highly dependent on NO_2 concentration and relative humidity, and especially efficient at relative humidity greater than 60% in the presence of sufficient NO_2 . This observation is important because insoluble Pb is converted into a more soluble and potentially more bioavailable form ([Peng et al., 2020](#)).

Although atmospheric lifetime depends on atmospheric conditions, UFPs quickly grow into fine particles, or particles smaller than 2.5 μm ($\text{PM}_{2.5}$), by way of gas-to-particle partitioning or coagulation with other particles before removal. Particles in the size range from 2.5 to 10 μm ($\text{PM}_{10-2.5}$) and larger are removed more quickly from the atmosphere than $\text{PM}_{2.5}$ by way of gravitational settling and deposition. This results in UFP and $\text{PM}_{10-2.5}$ concentrations having substantially greater spatial variability than $\text{PM}_{2.5}$, with higher atmospheric concentrations typically near their sources and greater spatial variability on urban and neighborhood scales ([U.S. EPA, 2009](#)). More rapid removal processes also result in shorter atmospheric lifetimes and transport distances for UFP and $\text{PM}_{10-2.5}$ than the $\text{PM}_{2.5}$ size range.

1.3.1.2. Atmospheric Deposition

The 2013 Pb ISA summarized atmospheric deposition patterns for Pb ([U.S. EPA, 2013](#)). There has been a sharply decreasing trend in Pb deposition in the United States and globally since the 1970s, corresponding to decreasing ambient air concentrations (Section 1.5.1) and decreasing traffic emissions associated with the removal of Pb from gasoline. In general, fine particulate Pb is mostly soluble and removed from the atmosphere by wet deposition, and coarse particulate Pb is mostly insoluble and removed from the atmosphere by dry deposition. Other factors also influence Pb deposition, however. The pH of precipitation can also play a role because Pb solubility increases with decreasing pH, and precipitation can also scavenge insoluble particulate Pb as an aqueous suspension. Diurnal variations in Pb deposition have been observed and attributed to differences in atmospheric structure, specifically

boundary layer height. Several U.S. studies reported substantially greater deposition rates in areas near industrial sources than in non-industrial areas, and ([U.S. EPA, 2013](#)). As a recent example, regional differences in Pb deposition patterns have also been documented in a number of studies ([U.S. EPA, 2013](#))

Several recent studies have addressed Pb deposition. [Wu et al. \(2016\)](#) used Pb isotope ratios in lichens and fungi to show that deposited Pb in bioindicators still reflected historical deposition from leaded gasoline exhaust. [Mazari and Filippelli \(2020\)](#) focused on urban atmospheric deposition patterns of Pb and other metals over a wider range of time scales by analyzing soil, bark, and leaves. They oriented sampling locations along an increasingly urban transect and found the highest Pb levels at the most urban locations. Previous observations of decreasing Pb deposition with distance from sources also supported by a recent study showing that previously remediated soil became re-contaminated following aerial deposition from a Pb smelter, with soil Pb concentrations ranging from 25–100 mg Pb/kg within years of remediation ([Bowers et al., 2014](#)). [Stankwitz et al. \(2012\)](#) investigated the effect of elevation on Pb deposition in a forested area of the Northeast United States and found deposition increased with elevation due to increasing precipitation with elevation. They also found the increase was not linear however, instead including two abrupt threshold increases associated with the two most common cloud base altitudes, which in turn corresponded to changes in vegetation. In recent research on cloud processes, [Ebert et al. \(2011\)](#) observed enrichment of Pb in ice nuclei, with a 25 times higher likelihood of Pb in ice nuclei than in interstitial aerosols by number in clouds.

Consistent with the 2013 Pb ISA, recent studies continue to show decreasing Pb deposition in various locations. For example, [Pérez-Rodríguez et al. \(2018\)](#) observed a peak in Pb concentrations in peat samples in southern Greenland that contained Pb transported from North America and Eurasia, and [Wu et al. \(2020\)](#) used bioindicators to monitor decreasing Pb deposition in Guangzhou after 2000. Other research continues to evaluate biomonitors for research on atmospheric deposition of Pb and other trace metals ([Kempter et al., 2017](#)). After deposition, resuspension of Pb in contaminated soil and road dust into air by traffic, construction, and wind is a potentially important contributor to airborne Pb (Section 1.3.4).

1.3.2. Fate and Transport in Soil

Knowledge of Pb transport in soil following wet and dry deposition is required to understand risk and exposure to human and ecological receptors following deposition of atmospheric Pb into soil. The 2013 Pb ISA summarized the long retention time and low mobility of Pb in soil and confirmed the role of soil as an overall sink for Pb even though atmospheric Pb concentrations peaked several decades ago ([U.S. EPA, 2013](#)). Pb can be deposited onto surface soils in both close proximity to and considerable distances from point sources. Once deposited in soil, subsequent fate and transport through the soil column is influenced by several physicochemical factors, including storage in leaf litter, amount, and decomposition rates of organic matter (OM), composition of organic and inorganic soil constituents,

mobile colloid abundance and composition, microbial activity, and soil pH. These physicochemical properties are based on soil forming factors: climate, organisms, parent material, relief, time, and anthropogenic input. Soils that differ in these factors will subsequently have different physicochemical properties and different trends in Pb transport. The 2013 Pb ISA summarized studies that describe the role that each of these physicochemical factors play in Pb fate and transport through soil, and more recent studies confirm conclusions from the 2013 Pb ISA ([U.S. EPA, 2013](#)).

1.3.2.1. Transport into Soil

The 2013 Pb ISA ([U.S. EPA, 2013](#)) confirmed findings from the 2006 Pb AQCD ([U.S. EPA, 2006](#)) that Pb is deposited from air onto soils in the vicinity of stationary sources and deposition decreases with increasing distance from the source. As previously discussed, Pb particles of varying size can be emitted into the atmosphere from several types of stationary sources (Section 1.2) and subsequently deposited onto soil (Section 1.3.1.2). Pb-derived spatial distribution of contaminants in soils located in the vicinity of stationary sources, such as non-ferrous smelters, depend on wind direction, size of particles emitted (smaller particles will travel further than larger particles), and mineralogical and chemical composition of particles emitted ([Ettler, 2016](#)). If soluble forms occur in the dust, greater downward leaching can occur in the soil profile following deposition ([Ettler et al., 2012](#)). Pb derived from high temperature processes such as smelting is largely emitted in the submicrometer fraction and is capable of being transported over long distances and being deposited in remote environments (Section 1.3.1.1). [Bing et al. \(2014\)](#) demonstrated the long-range transport capability of Pb emissions from industrial sources by measuring Pb concentrations and isotope ratios in soil profiles from the remote Hailuogou Glacier foreland in the Eastern Tibetan Plateau. Results revealed Pb enrichment in the O and A horizons relative to the C horizon, indicting Pb from recent atmospheric deposition rather than parent material. The binary mixing model using Pb isotope ratios reported that anthropogenic sources contributed to 45.2–61.3 % of Pb in the O horizon and 8.6–34.8% in the A horizon. Furthermore, the isotopic compositions of Pb and air mass trajectory models revealed that the major contributions of anthropogenic Pb in surface soils were from distant sources including Pb ore processing in southwest China and coal combustion in southwest China and South Asia. The study also discussed potential effects of climate change on soil properties that would result in Pb release from soils potentially affecting downstream water quality. [Bińczycki et al. \(2020\)](#) reported similar results, measuring total Pb concentrations and Pb isotope ratios in nine Podzol profiles located in high elevation remote areas of Karkonosze National Park in Poland. Results revealed high concentrations of Pb in surface horizons originating from combustion of coal in Poland and the Czech Republic followed by long-range transport. As described in the 2013 Pb ISA, Pb deposition to soils has decreased since the phase-out of on-road leaded gasoline ([U.S. EPA, 2013](#)). Reduction of Pb surface soil concentrations since the phase-out are variable, however, particularly in high altitude areas where there has been little change in O horizon Pb decreases since the phase-out. [Kaste et al. \(2011\)](#) used ^{210}Pb measurements to estimate the timescale over which Pb in canopy-derived litter is converted into mobile

colloid phases that are transported to mineral horizons. Results showed that the Pb is retained in the O horizon for longer periods of time in areas of higher elevations and latitudes. Similar results have been reported by [Zhou et al. \(2019\)](#) and [Stankwitz et al. \(2012\)](#). Longer Pb retention times in surface soils at higher elevations may be due to higher annual precipitation and cloud water depositions as well as slower OM decomposition due to lower temperatures.

1.3.2.2. Transport within Soil

The 2013 Pb ISA described a variety of complex factors influencing Pb retention and distribution in soil, including storage in leaf litter, amount and decomposition rates of OM, composition of organic and inorganic soil constituents, mobile colloid abundance and composition, microbial activity, and pH ([U.S. EPA, 2013](#)). [Zhou et al. \(2020b\)](#) evaluated the Pb adsorption capacity of acidic A and B horizon mineral soils collected from New York and Vermont. Results revealed that Pb was adsorbed more strongly in the A horizon than the B horizon soils across all samples indicating the importance of OM in Pb retention. In addition, soils collected from Vermont were able to selectively adsorb Pb more strongly than the New York samples. This increase in adsorption was attributed to higher pH, cation exchange capacity (CEC), manganese (Mn) oxide, non-crystalline Fe oxide, and OM contents in Vermont soils.

The role of leaf litter as both a contributor to Pb in surface soil and as a sink for Pb from soil in direct contact with leaves was reported in the 2013 Pb ISA ([U.S. EPA, 2013](#)). [Scheid et al. \(2009\)](#) demonstrated that total metals concentrations in leaf litter exposed to manually contaminated soils from the Swiss Federal Institute for Forest, Snow, and Landscape Research increased over the three-year duration of the study, suggesting that leaf litter that may come into contact with Pb-contaminated soil during splashing from rain events can serve as an efficient metal storage pool. [Landre et al. \(2010\)](#) compared the differences between Pb atmospheric inputs measured in bulk deposition with inputs from litterfall and throughfall (water depositing onto soil following collection onto leaves) in a remote forested catchment with limited development in Ontario Canada. Results showed that bulk deposition collectors may underestimate the amount of Pb reaching the forest floor by about 50%. More recent studies reported mixed results regarding the role of leaf litter. [Luo et al. \(2015\)](#) measured Pb in soil, litterfall, and plants in the Gongga Mountain region of Sichuan Province, China and found that both litterfall and atmospheric deposition were main contributing factors to Pb concentrations in the O horizon. In addition, this study also revealed a significant correlation between Pb concentrations in fine roots and the A horizon confirming that fine roots can adsorb and sequester Pb from soil.

After Pb is deposited onto surfaces from litterfall and atmospheric deposition, it is transported downward as decomposition slowly transforms buried leaf litter into humus. The fate of Pb in litter and subsequent release to mineral soil horizons occurs over variable timescales that may be strongly influenced by the rate of organic decomposition. [Kaste et al. \(2011\)](#) used measurements of ^{210}Pb throughout soil profiles in coniferous forests in New England and Norway to create a steady-state

transport model to quantify the fate of metals in leaf litter during OM decomposition over longer time scales that could be obtained empirically. Results showed the time scale over which canopy-derived litter was converted into mobile organo-metallic colloids ranged from 60–630 years, varying almost an order of magnitude, and was slowest in areas where decomposition was slowest. The results of this study also showed that Pb is retained by the upper litter layer and concentrations increase as litter is buried and decomposes, resulting in Pb that is enriched in the O horizon. [Zhou et al. \(2019\)](#) reported similar results in a study that measured Pb concentrations and pools in forest vegetation, litterfall, organic soil, and mineral soil. In the study, 97.3% of the pools were in litter and organic soil, with Pb concentrations in organic soil being significantly correlated with total OM in both organic and mineral soil, and transportation of Pb to mineral soil was dependent on OM decomposition.

Large surface areas with high CEC and negatively charged functional groups make organic and inorganic soil colloids capable of adsorbing Pb and thus play an important role in Pb transport. Physical factors influencing colloid mediated transport of heavy metals include flow rate, medium grain size, and influent concentration ([Xie et al., 2018](#)). Transport of colloids in soil are influenced by flow rate and the physical and chemical properties of the soil porewater and matrix. Soil porewater with a low ionic strength and increased colloid and stationary matrix surface charges are associated with colloid stabilization and maximum Pb-colloid co-migration ([Shang and Li, 2011](#)). Conversely, high ionic strength and lower colloid and surface stationary matrix surface charges are associated with destabilizing colloid conditions where colloids will tend to coagulate and adsorb onto the stationary matrix ([Shang and Li, 2011](#)). When colloids are remobilized from the stationary matrix, Pb that is bound to the colloid irreversibly is expected to remobilize along with the colloid. However, Pb that is bound via cation exchange is expected to sorb to the stationary matrix phase following colloid remobilization ([Shang and Li, 2011](#)). [Xie et al. \(2018\)](#) investigated the effects of different colloids on Pb transport under different physical conditions. Results revealed that compared with deionized (DI) water, montmorillonite, loessial, and humic acid (HA) colloids all promoted transport of Pb, with HA having the greatest influence on remobilizing Pb from quartz and sand surfaces with a 33% increase in Pb mobilization through the porous medium compared with colloid-free DI water. The enhanced mobility was attributed to the large number of organic functional groups on the surfaces of HA colloids providing large sites for Pb adsorption. Results also showed that larger matrix grain sizes led to an increase in colloid mobility due to increased outflow of the colloid in more porous media. Higher flow rate decreased Pb adsorption and colloids on quartz surfaces, thus increasing mobility of heavy metals and colloids. [Shang and Li \(2011\)](#) studied the role of rainfall on the migration of Pb-colloid complexes in farmland, floodplain, and Loess platform soils. Pb migration concentrations with colloids in farmland, Loess platform and floodplain columns were respectively, 1.12~2.25, 0.91~1.85 and 0.5~2.01 times more than migration concentration with no colloids. These results confirm the results from [Xie et al. \(2018\)](#), demonstrating that Pb migration is enhanced by colloid-Pb co-migration.

The 2013 Pb ISA described the effects of microbial activity on Pb sequestration and transport ([U.S. EPA, 2013](#)). [Perdrial et al. \(2008\)](#) observed bacterial Pb sequestration and proposed a mechanism of

Pb complexation by polyphosphate. They also postulated that bacterial transport of Pb could be important in subsurface soil environments. [Wu et al. \(2006\)](#) also concluded that Pb adsorption to the bacterial cell walls may be important with respect to Pb transport in soils. More recent studies suggest that microbial activity may enhance the release of Pb from both organic and mineral soils. [Drozdova et al. \(2015\)](#) studied the effects of both live and dead bacteria on the release of trace elements from both organic and mineral podzols (aqueous solutions in a laboratory system). Results revealed that live bacteria enhanced the release of Pb to solution, particularly in organic soils, while decreasing the release of potassium (K), calcium (Ca), strontium, Cu, titanium (Ti), Mn, Zn, and arsenic (As). The authors' noted that decreases in pH, degradation of dissolved organic carbon (DOC) and metal-organic complexes by microbial activity, element adsorption at cell surfaces, and biological uptake may occur simultaneously in the soil-bacteria suspension to both enhance and decrease the release of trace elements from the soil profiles. In the case of Pb, it is suggested that Pb is released into aqueous solution following bacterial degradation of Pb-organic complexes.

1.3.2.3. Soil Forming Factors and Land Use

The physicochemical factors influencing Pb retention and distribution throughout the soil column can vary considerably amongst soils with differences in soil forming factors (i.e., climate, organisms, parent material, relief, time, and anthropogenic input). The 2013 Pb ISA summarized Pb retention and distribution through forest soils as strongly influenced by rate of OM decomposition, depth of soil O horizon, and pH, generally concluding that atmospherically derived Pb will have a longer residence time in organic surface layers that have lower rates of OM decomposition ([U.S. EPA, 2013](#)). Therefore, Pb will be enriched in the O horizon with increased enrichment occurring in forests where climate, elevation, and vegetation (i.e., boreal forests versus deciduous forest) favor slower rates of OM decomposition. Recent literature confirms many of these findings. [Richardson et al. \(2014\)](#) resampled organic and upper two mineral horizons at 16 sites across deciduous and mixed deciduous/coniferous forests in the northeast that were previously sampled in 1980, 1990, and 2002. Results revealed that gasoline derived Pb has leached from the forest floor to mineral soil horizons across the study areas. However, the rate at which Pb is being transported from the forest floor to mineral soils varied across the 16 sites and was slowest at sites with frigid soil temperature regimes (STRs) located in the northern portions of the study area. The decreased Pb response rate and increased retention time in these soils was attributed to slower decomposition rates in frigid STR and more coniferous vegetation compared with other sites, potentially decreasing decomposition rates due to higher lignin content. [Chrastný et al. \(2012a\)](#) compared the leachability of air pollution control residues in deciduous and coniferous organic soil horizons. Results revealed higher Pb sorption onto humified OM from coniferous litter compared with deciduous litter. The increased sorption of Pb in the coniferous organic horizon was attributed to a lower pH and higher portion of fulvic acids compared with the deciduous organic horizon, which was a result of differences in chemical composition and degradability of needles and litter. These results suggest that soil in deciduous

forest may be more vulnerable to Pb mobilization compared with soils in coniferous forests. [Chrastný et al. \(2012b\)](#) compared Pb concentrations and mobility in agricultural and forested soil profiles located at varying distances from smelting and/or mining release sources. Total Pb concentrations were generally higher in forested soil profiles compared with agricultural soil profiles. However, Pb in the agricultural soil profile was found to be more mobile, confirming the important role of forest leaf litter in Pb retention. [Du et al. \(2020\)](#) investigated the effects of soil freeze thaw cycles (FTCs) on Pb sorption and desorption behavior in soils vulnerable to alternating periods of freezing and thawing. Results of the study suggested that FTCs tend to increase Pb immobilization by increasing pH with increasing FTCs, which facilitated formation of inner and outer sphere complexes. Adsorption capacity was correlated with carbonate and effects of FTC on Pb adsorption may be more dependent on carbonate and clay content than OM, CEC, or amorphous Fe.

[Burt et al. \(2014\)](#) investigated and compared the effects of different anthropogenic activities on trace metal, including Pb, fate and transport. Surface and subsurface soil samples were collected at locations throughout New York City (NYC) parks (Central Park, Pelam Park, and Van Cortlandt Park) and from areas in the Bronx Watershed for chemical extraction analysis to investigate and compare trace element extent, variability, and relationship between soil properties in the two study areas. Central Park surface samples exhibited higher trace metal concentrations compared with Pelam or Van Cortlandt Park, which may be related to proximity of Central Park sample sites to public roads and a long history of intense human activities (shanties, gardening, piggery, and villages) compared with the relatively undisturbed and mostly wooded Pelam and Van Cortlandt Parks. In the Bronx River Watershed, sum trace metal concentration was significantly higher in sample locations collected from suburban Westchester County compared with the more urbanized Bronx. The authors suggested that the lower trace element concentrations in the more urbanized area may be attributed to once industrialized land being recently converted to parkland. Together these results suggest that trace element levels may not necessarily be dependent on urbanization, current land use, or vegetation, but may be more reflective of long-term history (type, degree, and age of human disturbances) influencing soil and hydrologic processes.

Pb concentration trends in NYC parks decreased with depth confirming Pb airborne deposition from several historical point and non-point sources. Conversely, concentration trends increased with depth in the Bronx Watershed sample locations. These results were likely a result of soil formation in a mantle of construction debris covered by anthropogenically transported soil. In addition, the formation of carbonates from debris materials may have resulted in an increase in pH which increased Pb retention. The sequential extraction analysis revealed that the predominant forms of Pb were the specifically sorbed/carbonate-bound (SS/CAR) and the oxide-bound (OX) fractions, indicating that Pb is predominantly in a form containing the carbonate precipitate, metallic-organic complexes, or metal-oxides with low bonding forces (i.e., easily mobilized fractions). These results are in good agreement with a study of NYC garden soils by [Cheng et al. \(2011\)](#) that also suggested anthropogenic Pb was generally in the highly bioavailable and mobile SS/CAR and OX fractions (i.e., anthropogenic Pb in dust originating

from urban soils is more toxic and mobile than naturally occurring Pb). The authors found that the exchangeable and more mobile fractions of Pb were larger in the NYC soil compared with soils found near a Montana smelter, suggesting that the warmer and humid climate in NYC favored chemical weathering and trace element mobility. The distribution of Pb in urban soils and the exchange of Pb between urban soil and other media is further discussed in Section 1.3.4.

1.3.2.4. Summary of Pb Fate and Transport in Soils

In summary, recent literature supports the conclusions from the 2013 Pb ISA ([U.S. EPA, 2013](#)) regarding Pb fate and transport through soils. Studies continue to report higher concentrations of Pb in soils closer to stationary sources while also demonstrating the potential of Pb being deposited at considerable distances from sources via long-range transport. Once deposited onto soil, Pb is strongly retained in organic surface horizons with subsequent Pb retention and distribution in soil strongly dependent on several physicochemical properties, including storage in leaf litter, amount and decomposition rates of OM, composition of organic and inorganic soil constituents, mobile colloid abundance and composition, microbial activity, and pH. In general, leaf litter, low rates of OM decomposition, neutral pH, and soil constituents rich in charged surfaces such as OM, Fe and Mn oxides, and clay minerals will lead to increased Pb retention and sorption. Conversely, thin organic layers, increased OM decomposition, acidic pH, increases in anthropogenic Pb, and less reactive soil constituents such as quartz will tend to increase Pb leaching from soils.

1.3.3. Fate and Transport in Water and Sediments

As discussed in the 2006 Pb AQCD and the 2013 Pb ISA ([U.S. EPA, 2013, 2006](#)) atmospheric deposition, urban runoff, and industrial discharge are large contributors of Pb to surface waters with greater runoff being linked to larger storm events following a dry period. Evidence from the 2013 Pb ISA also found some evidence of a seasonal effect on runoff with greater runoff following snowmelt or rain-on-snow events. Pb transport and sedimentation within aquatic systems depends upon chemical properties including water pH and salinity, presence of OM and iron (Fe) and Mn oxides, total suspended solids (TSS), as well as mechanical processes including turbidity and flow. Previous research has also shown Pb is relatively stable in lacustrine and riverine sediments but resuspension of sediment into water or dissolution from sediment often occurs during and following storm events and can be a larger source of Pb to the water column and downstream reaches than concurrent atmospheric deposition. New research primarily provides additional support for the 2006 Pb AQCD and 2013 Pb ISA ([U.S. EPA, 2013, 2006](#)) conclusions with additional information on runoff following fire events and seasonality influence on transport and sedimentation. Furthermore, new literature provided information on temporal trends of Pb concentrations in sediments and several studies are summarized in Section 1.3.3.4 to highlight the importance of legacy Pb pools as potential “new” sources of Pb to waterways.

1.3.3.1. Biogeochemistry

1.3.3.1.1. Freshwater Biogeochemical Influences

The transport of Pb through freshwater systems is influenced by a variety of biogeochemical factors such as OM content, redox, alkalinity, and seasonality. Since the 2013 Pb ISA ([U.S. EPA, 2013](#)), new information was found for how Pb transport and availability is increased in the presence of higher nutrient levels and under anoxic conditions, while photolysis of OM reduces Pb concentration because it can be bound more to organic molecules. There is also an improved understanding of the mechanisms for how different types of OM (e.g., HAs, or amount of aromaticity) interact with Pb and how dissolved OM and PM can increase the mobility and solubility of metals in aquatic systems. An increase in DOC leads to a decrease in the amount of Pb bound to PM because Pb instead binds more to dissolved organic matter (DOM). Thus, activities that increase DOM (like surface mining or heavy rain events) can increase the mobility and solubility of metals in aquatic systems ([Guéguen et al., 2011](#)). Similarly, [Chen et al. \(2019\)](#) found that the solubility and mobilization of Pb increases through the formation of Pb-DOM complexes. As the DOMs become more allochthonous, more humic-like, more aromatic, and optically darker, the active Pb-binding fraction increases ([Chen et al., 2018](#)). Coordination chemistry has shown that Pb predominantly binds to the phenolic and carboxylic group on a salicylic-type structure or two adjacent carboxylic groups on catechol-type structures. [Cabaniss \(2011\)](#) found Pb(II) preferentially binds to strong amine-containing sites which are often located on small molecular weight (MW < 1000), and lower aromaticity molecules. There are no highly aromatic molecules acting as strong ligands for Pb(II). Pb(II) binds to phenolic groups but is more strongly bound by amine groups. At low metal loading, Pb(II) is selectively bound to very high molecular weight compounds (>2000 amu). And Pb(II) are bound by molecules with less negative overall charge (average charge of occupied ligand molecule $Z_{\text{bnd}} > -1.6$) at relatively low metal loading. At pH 7.0, Pb(II) binds in the order amines > phenols > carboxylates. [Jeremiason et al. \(2018\)](#) found that DOM mobilizes historical deposits of Pb from bog peatlands and Pb and DOC concentrations were correlated in the bog. The key factor is DOM leaching or production leading to Pb redistribution among binding sites in solid peat and the dissolved phase. The amount of Pb mobilized per unit DOC ($\mu\text{g}/\text{mg DOC}$), was greater in bogwater (0.047; range 0.037–0.067 at individual sites) than lagg water (0.033; range 0.007–0.050). Interestingly, Pb was found to preferentially adsorb onto bacterial cells (organic material) than on clay minerals ([Du et al., 2016](#)).

Suspended particulate matter (SPM) and sorption material also influence Pb transport and availability. SPM significantly influences Pb adsorption. Total Pb concentrations in water were higher when the content of the PM in the river water was high ([Milačić et al., 2017](#)). Further, the highest partitioning coefficients observed for Pb were a consequence of its high affinity to SPM and low Pb solubility in water. Pb binding to SPM in the lower Waikato River in New Zealand is predominantly via Fe-oxide surfaces and can be reliably predicted using surface complexation adsorption modeling ([Webster-Brown et al., 2012](#)).

Other metals, nutrients, and inorganic compounds in the sediment and open waters can affect Pb mobilization. High nutrient levels can increase the potentially mobile fractions of Pb ([Kang et al., 2019](#)). A significant negative relationship exists between total phosphorus (TP) and Pb concentrations per unit mass of phytoplankton in lakes ([Gormley-Gallagher et al., 2016](#)). Sulfide also showed a negative relationship with Pb, likely reflecting precipitation of Pb-sulfide complexes in sulfide-rich porewater ([Carling et al., 2013](#)). [Lombardi et al. \(2014\)](#) found that the percent labile Pb (86 %) compared with percent dissolved Pb suggests that most of the Pb was complexed with inorganic compounds. Pb was complexed preferentially with CO_3^{2-} (25 %), NO_3^- (22 %), and OH^- (19 %). Chlorophyll *a* and TSS were also correlated with most Pb fractions. Groundwater may be contaminated with Pb, and this may be due to strong correlations between Pb and Fe or Mn oxides and with total dissolved solids ([Wang et al., 2016](#)), and this study suggests that groundwater contaminant of Pb is due to natural processes and not from surface water contamination.

Pb transport and availability are influenced by redox conditions. Pb is typically released from sediments in anoxic environments and adsorbed from the overlying water in an aerobic environment ([Kang et al., 2019](#)). For the exchangeable fraction (characterized by soluble species, species with cation exchanges sites, and carbonate-bound species), Pb increased in aerobic conditions and for both high and low nutrient levels but decreased under anoxic conditions. Sediment absorbs more Pb^{2+} under aerobic conditions. Another study found that Pb can precipitate under either oxic or anoxic conditions, but due to different mechanisms. In a eutrophic lake, [Chen et al. \(2019\)](#) observed that algae degradation may decrease redox state in sediments and sulfide may be released from the degraded algae, which may promote the formation of Pb-sulfide precipitations under anoxic conditions. Whereas in oxic conditions (high redox state), Fe^{2+} and Mn^{2+} oxidation may occur in sediments and result in the adsorption or coprecipitation of Pb. Also, Pb can be confined to an immobile form (organic sulfides) at higher alkalinity in stream sediments, and gradually be released due to chemical weathering ([Pearson et al., 2019](#)). [Li et al. \(2016\)](#) found that in acid mine drainage, Pb was found to be associated with the carbonate fraction and under waterlogged conditions, dissolved Pb increased when Fe increased in concentration. In waters with acid mine drainage, Pb was predominantly present in the residual (77.7%–85%), followed by oxidizable (9.4%–12%) and reducible (5%–10%) fractions. Also, the decomposition of OM like cyanobacteria can cause a reduction in the oxidation reduction potential (ORP), which can result in an increase in Pb bound to sulfate ions ([Ni et al., 2019](#)). [Chen et al. \(2019\)](#) also found that Pb in both eutrophic and non-eutrophic lakes was commonly complexed as $\text{Pb}(\text{HS})_2$, PbCO_3 and to a lesser extent: Pb^{2+} , PbOH^+ , $\text{Pb}(\text{OH})_2$, PbSO_4 , $\text{Pb}(\text{CO}_2)_2^-$, and PbHCO_3^+ .

Temperature and seasonality also influence Pb adsorption and transport in freshwater systems. Pb showed higher concentrations during the spring than summer in river samples ([Zhang et al., 2016a](#)). [Zhang et al. \(2016a\)](#) also found that in the spring, the majority of Pb is found in the inert form (not reactive with NH_4^+ or OH^- ion exchange resins) and only ~1 to 5 % of Pb is found in the organic or labile forms. But in the summer, there were higher percentages of labile Pb ranging from ~10 to 60% in the rivers. The organic fraction was the same in both seasons, while the labile fraction increased (on average)

from 6.75 to 19.95 % between spring and summer. On average, the labile Pb fraction increased in all the rivers during summer. The increase in labile concentrations might be attributed to human activities, leading to increased potential toxicity in these rivers. In winter months, [Sun et al. \(2018\)](#) found that Pb^{2+} has a low binding energy in ice compared with other cations ($\text{Fe} > \text{Cu} > \text{Mn} > \text{Zn} > \text{Cd} > \text{Hg} > \text{Pb}$). [Lombardi et al. \(2014\)](#) found that total, dissolved, complexed, and labile Pb species were all higher in the winter, while Pb was present more in the particulate form in the summer. [Chen et al. \(2019\)](#) observed the highest dissolved Pb concentrations in July for a eutrophic lake, while the highest dissolved Pb concentrations were in January for a lake covered by floating and submersed macrophytes. The greatest increase in Pb complexation with DOM occurred in the eutrophic lake in July, while it occurred in the non-eutrophic lake in April. However, the degree of Pb complexation to DOM was significantly larger in the non-eutrophic lake in all seasons. The mobility of Pb in sediments showed significant seasonal variations, reflected by a high release of Pb during the spring and summer in the algae-dominated region and during the autumn and winter in the macrophyte-dominated region. A possible mechanism is that in the algae-dominated regions of the lakes, increased bacterial abundance in the sediments during the spring promoted microbial reduction of Fe/Mn oxides, which likely released Pb from sediments.

Pb was found to be higher during periods of extreme flooding ([Milačić et al., 2017](#)), where Pb inputs are primarily derived from heavy industrial activities or mining and metallurgy activities (depending on the site). [Valencia-Avellan et al. \(2017\)](#) also found that Pb concentrations increased with peak flow in an ephemeral tributary. This is likely because Pb is strongly associated with both particulate and colloidal Fe and Al oxides, and also cerussite (PbCO_3), SO_4^- , and DOC, which can all increase during high flood periods which are associated with the resuspension of sediments into water.

Light also has an influence on the dynamics of Pb in freshwater systems. Within an acid mine drainage impacted wetland, it was found that increased light levels caused a reduction in ferrous iron and this was associated with an increase in Pb concentration ([Duren and McKnight, 2013](#)). The mechanism for this process is the formation of superoxide radicals (O_2^-) and H_2O_2 from the photoreduction of DOM in the wetlands, where H_2O_2 reacts with Fe_2^+ and converts it to Fe_3^+ (reducing the amount of Fe_2^+ during the day). During photolysis, [Drozdova et al. \(2020\)](#) observe two simultaneously occurring processes: (1) the degradation of high molecular weight organo-mineral colloids and the formation of low molecular weight organic molecules and Pb complexes, and (2) the formation of the >0.22 μm particulate aggregates of Pb and OM. The DOM degradation produces both CO_2 and HCO_3^- whereas Pb which is initially associated with organo-ferric colloids are subjected to coprecipitation with newly formed Fe(III) oxy(hydr)oxides. Also, photolysis caused a decrease in Pb by 48% in solution and this may be because Pb is correlated to changes in concentration of Fe, DOC, and humic substances. For instance, Fe-OH and organic ligands can form ternary surface complexes with Pb. An alternative mechanism of metals removal could be their precipitation in the form of individual metal hydroxides that occurs after photo-degradation of metal-ligand (Me-L) complexes.

1.3.3.1.2. Saltwater Biogeochemical Influences

The transport of Pb through saltwater systems is influenced by a variety of biogeochemical factors such as salinity, organic matter content, redox, alkalinity, and seasonality. Since the 2013 Pb ISA ([U.S. EPA, 2013](#)), new information was found on how Pb concentrations in solution increases with increasing salinity and temperature, but decreases in the presence of DOC, Fe(III) and Mn(IV/III) (hydr)oxides, which provide important binding sites for heavy metals under high dissolved oxygen (DO; oxic) conditions. There is also more information on the role of sulfide in estuarine systems and on whether Pb comes from anthropogenic or natural sources.

Salinity of estuarine and coastal waters can have a strong influence on Pb fate and transport. ([Yao et al., 2016](#)) found that the concentration of Pb adsorbed to PM decreases with increasing salinity in the medium-low salinity of the estuary near the river mouth, indicating the release of Pb during early mixing stages in the estuary. The metal release resulted from a balance between two opposite processes: (1) metal mobilization due to ionic exchange or degradation of organic complexes and (2) metal re-adsorption onto an existing or newly formed solid phase. Basically, with increasing salinity, cations such as Na^+ , Ca^{2+} , and Mg^{2+} compete for the adsorption sites on particle surfaces, thereby decreasing adsorption and enhancing the release of sorbed Pb from the particle surfaces. Similarly, [Zhao et al. \(2013\)](#) observed that as salinity in the Yangtze Estuary increased, Pb was released from the sediments, but it was minimal (0.004–0.017%), due to preferential retention in Fe-Mn oxides and organic content. Pb cations seemed to be sorbed more specifically to sites with high dissociation constants (and high sorption energies), making them less vulnerable to leaching. ([Karbassi et al., 2014](#)) also observed greater Pb flocculation at lower salinities (0.5‰) and constant pH of 8. However, another study found the opposite pattern; while the partition coefficient K_d (L/kg), which is the relationship between the sorbed state to the dissolved state of a metal, generally decreases with salinity due to higher ionic strength and competition for sorption sites, [Alkhatib et al. \(2015\)](#) found the K_d for Pb increased with salinity (with K_d values at 234 L/kg in freshwater, 575 L/kg in brackish water, and 1341 L/kg in seawater) and this is mainly attributed to formation of insoluble metal species, like PbSO_4 , which led to higher K_d values with the increase of salinity. Another study with this pattern found that for PbS , freshwater exhibited the highest Pb release followed by seawater and estuary water ([Chou et al., 2018](#)). Clearly, other factors like the types of inorganic species and metals and other conditions must influence the impact that salinity has on the transport of Pb in saltwaters.

The presence of different minerals in estuarine and seawaters can influence the transport of Pb between sediments, saltwater, and the atmosphere. For example, [Shelley et al. \(2018\)](#) observed that Pb and Al was significantly correlated ($r^2 = 0.478$) in saltwater and that Pb solubility was greater in saltwater than in ultra-high purity water used as a control, though Pb solubilities decrease as aerosol loading increased. Fe(III) and Mn(IV/III) (hydr)oxides provide important binding sites for heavy metals under oxic conditions, and sulfide provides important binding sites for Pb under anoxic conditions ([Wang et al., 2013](#)). Consequently, the reductive dissolution of Fe(III) and Mn (IV/III) (hydr)oxides could encourage

the release of Pb into solution. But dissolved levels of Pb became undetectable within 10 days suggesting that it can be almost completely sequestered in the metal sulfide phases under sulfate-reducing conditions (during bacterial sulfate reduction activity). [Morgan et al. \(2012\)](#) found acid volatile sulfide to have a strong relationship with reactive Pb in estuaries and a strong relationship between FeS and Pb in sediments, where Pb sulfates are more likely to precipitate than FeS due to lower solubility. Thus, FeS is likely to retain Pb in estuarine sediments. [Tovar-Sánchez et al. \(2019\)](#) observed that both Pb and Fe were abundant in the sea surface microlayer. And [Keene et al. \(2014\)](#) saw a strong correlation between total Pb and reactive Fe in interfacial sediments of an estuary, with 50% of Pb being associated with reactive or “acid extractable” phases in the sediment. [Ebling and Landing \(2015\)](#) studied the Pb levels in the sea surface of the open ocean (“microlayer” – the thin layer at the boundary between the ocean and the atmosphere) and measured dissolved, labile particulate, and refractory particulate trace element concentrations of the sea surface microlayer. They found dissolved Pb to increase in the microlayer by a factor of 2–3 over time, coinciding with an increase in Fe, which may have come from precipitation. At the same time, the refractory particulate Pb increased by a factor of 23 in the microlayer. Pb in the microlayer had retention time of about 1–2 days. The enrichment factor (EF) for Pb was >1 demonstrating enrichment in the microlayer. [Cánovas et al. \(2020\)](#) observed Pb was abundant in PM (37%–59% in dissolved fraction) and that 66% of Pb was found forming Cl⁻ complexes, ~20% as CO₃⁻ complex, 5% as Free Pb, and 5% as Pb hydroxide. Pb showed a balanced speciation between the uncharged and positively charged species.

PM suspended in water has been found to strongly influence Pb transport and fractionation in seawater. [Angel et al. \(2016\)](#) reported that the amount of dissolved Pb concentrations in seawater was dependent on the concentration of precipitate present, decreasing as the precipitate concentration increased. The composition of the precipitate formed is likely to be a metastable Pb chlorocarbonate. [Feng et al. \(2017\)](#) observed how the partitioning coefficient (K_p), for the amount of Pb sorbed to SPM was highest for Pb compared with other trace metals (Ni, Cr, Cu, Hg, Zn, Cd, and As). And the K_p for Pb is higher in the SPM than for the sediment-water interface. This is because SPM has a smaller particle size, and higher specific surface area and OM content, and thus can adsorb more heavy metals. The exchangeable and carbonate fractions of Pb also had significant positive correlations with the K_p for Pb in SPM and the exchangeable, carbonate, and residual fractions of Pb had significant positive correlations with K_p for Pb in sediments. Thus, adsorption is likely to be the dominant partition process of Pb. [Burton et al. \(2019\)](#) found through a review study that the removal efficiencies (of the metal from the water column to SPM) for 7 of the 12 estuaries were at or greater than approximately 75% for Pb. And metal removal efficiency was greater for Pb than Cd and Zn, consistent with the metal’s partition coefficient. Pb accumulates more in the finer fractions of clay (<8 μm) and fine silt (8–16 μm) ([Yao et al., 2016](#)). Pb concentrations in the bulk SPM varied from 25 to 38 mg Pb/kg, with an average of 32 mg Pb/kg. Pb had an average EF value of 0.81 and were all <1.5. This indicates that the Pb concentrations originated from natural weathering processes. The EF of an element is defined as the ratio of that element to a conservative element in a sample divided by the ratio of that element to the same conservative element in a background reference sample. An EF value between 0.5 and 1.5 suggests that the trace metals may be

entirely from crustal materials or from natural weathering processes, while an EF value >1.5 suggests that a significant portion of trace metals is delivered from non-crustal materials, or nonnatural weathering processes, like anthropogenic activities ($EF = [Pb]/[Fe]_{\text{sample}} / [Pb]/[Fe]$) (Yao et al., 2016). In very polluted environments, extreme EF values for Pb can be observed. For example, an EF of approximately 600 was recently observed in a highly industrialized and urbanized area of China, indicating Pb that was dominated by anthropogenic contributions (Xing et al., 2017). One study by Holmes et al. (2014) examined the role of estuaries in modifying the adsorptive properties of new and aged plastics towards trace metals and found the absorption capacity of Pb on plastic surfaces to decrease from river water to seawater and with decreasing pH due greater competition with other cations.

Temperature, oxic conditions, and organic content influence Pb transport in saltwaters. Within estuarine waters, temperature was positively associated with free Pb concentration, with a 1°C increase corresponding to approximately a 7% increase in free Pb concentration (Dong et al., 2016). DO was also found to be dominant factor that controlled the release of Pb from coastal sediments, with increased hypoxia causing increased Pb in overlying waters compared with sediments (Liu et al., 2019). Similarly, Banks et al. (2012) observed greater dissolved Pb concentration in porewater estuarine sediments at lower DO levels, where the ratio of dissolved Pb concentration to metal concentration was 1.2 for 5% DO, 1.1 for 20% DO, and 0.9 for 75% DO. In anoxic conditions the presence of wetland plants, like *S. alterniflora*, could lead to higher concentrations of Pb in the sediments, via pumping oxygen into the rhizosphere, which can cause the release of Pb to sulfates (Wang et al., 2013). Similar to freshwater systems, within estuarine waters, DOC and free Pb concentration had a negative relationship, indicating organic ligands in the water column were more important binding agents for free Pb ions relative to particulate organic ligands (Dong et al., 2016). Also, the presence of HA showed inhibition effects on its metal release of Pb from PbS (Chou et al., 2018). Carbon dioxide (CO_2) also influences Pb; a model predicted that under scenarios of increasing CO_2 , free Pb could increase from 9%–97% and organically bound could increase by 5%–43% (Stockdale et al., 2016).

Several studies also found that within saltwater systems, pH has a negative impact on free Pb concentrations. Vasyukova et al. (2012) also found that % dissolved Pb decreases as pH increases, and Pb is an element strongly associated with colloids and exhibits significant increases of relative proportion of colloidal forms with pH increase. Another study found that the partition coefficient K_d (L/kg), which is the relationship between the sorbed state to the dissolved state of a metal, was greatest for Pb at pH 7, at 16434 L/kg, indicating that more sorbed Pb was present at neutral pH (Alkhatib et al., 2015). When assessing the precipitation of Pb from PbS, there was minimal release of Pb from PbS at pH 8, intermediate Pb released at pH 7 (213 mg/L/m^2) and even more Pb released at pH 5 (386 mg/L/m^2), which suggests that H^+ plays a role in the oxidative dissolution of Pb sulfides (Chou et al., 2018).

Seasonality, rainfall, and tidal flows can influence Pb dynamics in estuaries and coastal waters. In the study by Hierro et al. (2014), Pb was found primarily in PM (average of $825 \mu\text{g/L}$). Pb-PM concentrations (per volume) were 2–3 times higher in PM carried by ebbing tide compared with the rising

tide, due to increased PM when there is a fall in sea level. Often, Pb sorbed/coprecipitated with Fe hydroxides, and highest particulate concentrations coincided with the estuarine maximum turbidity zone. In terms of rainfall, one study found that increased rainfall resulted in lower free Pb concentrations, likely due to dilution ([Dong et al., 2016](#)), while another study found higher levels of Pb in the spring when the rainfall amounts were larger compared with summer months ([Xing et al., 2017](#)). Additionally, this study found strong correlations between crustal-derived elements (Al, Fe) and anthropogenic elements (Pb, Cd, Zn) likely due to both being influenced by air deposition rainwater runoff ([Xing et al., 2017](#)). Also, during seawater-freshwater interaction from seawater intrusion to an aquifer, it was observed that Pb exhibited significant correlation with colloids and was thus sensitive to the flow of the colloidal fraction where seawater and freshwater are interacting ([Tan et al., 2017](#)).

1.3.3.2. Transport into Water (including Runoff)

The 2006 Pb AQCD concluded Pb in runoff was mostly in the particulate fraction and identified runoff as being dependent on storm intensity and time between rain events ([U.S. EPA, 2006](#)). The 2013 Pb ISA provided information on Pb runoff from roadways, urban areas, and snow melt into watersheds ([U.S. EPA, 2013](#)). New research provides additional support for both the 2006 Pb AQCD and 2013 Pb ISA conclusions with additional information on runoff following fire events and urban sources of Pb unique to city history and planning.

1.3.3.2.1. Urban

Pb in runoff in urban areas is correlated with surrounding land use characteristics such as impervious surface area and road density. In a study that examined Pb concentration and distribution in bed sediments of the Palolo drainage basin in Hawaii, [Hotton and Sutherland \(2016\)](#) found of the three streams that comprise the basin, Palolo had Pb concentrations of 134 mg Pb/kg compared with Pukele (24 mg Pb/kg) and Waiomao (7 mg Pb/kg). Furthermore, Palolo had high concentrations along its entire length whereas Pukele and Waiomao showed highest concentrations downstream. This high Pb concentration along Palolo was correlated with urban land-use characteristics including street length, storm drain length, the number of storm drain inlets and outlets, as well as vehicle counts and overall population. Urban development around Palolo was higher than around the other two streams in the drainage basin. In a similar study, sediment Pb concentration was measured in highly urbanized watersheds across several U.S. cities ([Nowell et al., 2013](#)). Pb was positively correlated with local urban factors and study area variables including population density, urban land cover, road density, and amount of impervious surface area as well as total organic carbon. Boston had higher Pb concentrations than other cities with comparable urbanization and sediment total organic carbon and the authors highlight this higher Pb concentration in Boston likely reflects the city's long history of industrial activity and high-density development. [McKenzie and Young \(2013\)](#) examined Pb water column fractions following storm

events in creeks draining different surrounding land-use areas. Highways and urban areas had higher runoff loads compared with agricultural and natural sites. Agricultural storm loadings were similar to those in natural systems and irrigation loadings were less than storm loadings. Pb was primarily associated with suspended sediments so would have low mobility and bioavailability. Highway runoff, on the other hand, had high levels of dissolved Pb.

Several recent studies highlight urban-specific sources of Pb to city waterways due to city design and historical pollution. For example, a study by [Coxon et al. \(2016\)](#) examined and mapped the contamination histories of the rivers that drain the lower western Chesapeake Bay basin. Sources of contamination have changed over Virginia's history and reflect the development of the area. Western mountain reaches have elevated Pb levels due to lithology and historical mining while agriculture and urbanization contribute to Pb enrichment across the drainage basin. Norfolk naval base and shipyard is a current and significant source of metal enrichment, as are incinerators, older office buildings with Pb paint, and ordnance storage. Furthermore, changes in urban land-use management have led to legacy Pb pools becoming a new source and Pb enrichment downstream of urban areas is high—with sediments downstream of Richmond showing particularly high Pb enrichment levels. Overall, fuel combustion, street dust, and highly contaminated urban soils are the contemporary suppliers of Pb to the Virginia Chesapeake waterways. In the Gwynns Falls watershed area in Baltimore, Pb concentration in riparian sediments decreased with increasing distance from the city center (when normalized for sediment surface area). Also of note, three hotspots of contamination in the urban system occurred adjacent to areas that had been identified in 1979 as artificially filled ([Bain et al., 2012](#)). A non-U.S. study found that despite restoration efforts enacted 30 years prior, Pb sediment contamination in an urban lagoon in Sardinia exceeded 100 mg Pb/kg at 22 of 34 monitoring locations ([Atzori et al., 2018](#)). High Pb concentrations were not correlated with OM content and showed similar contamination patterns with mercury (Hg). Instead, Pb (and Hg) peaks were in sites with proximity to a chlor-alkali plant and an airport. In a study that examined trace metal export in relation to soil concentrations, soil and water properties, and watershed land use across several New England watersheds, Pb export rates varied from 0.03 to 0.37 kg Pb/year/km² ([Richardson, 2021](#)). Dissolved Pb concentration was not correlated with soil Pb concentration but was positively correlated with aquatic Zn and DOC concentrations. Furthermore, dissolved Pb export was positively correlated with watershed cover of wetlands and negatively correlated with the percentage of forest cover. The author suggests the positive correlation with wetland cover may be due to wetlands serving as a reservoir of historic pollution and the negative correlation with forests is due to there being less development and therefore less pollution, as well as potentially higher retention of trace metals (Cu, Pb, and Zn) by soil iron oxides. Another recent study sought to assess the trace metal loading rates in the Great Lakes basin and estimated results found Pb inputs to Lakes Superior and Michigan were primarily atmospheric while Lakes Erie and Ontario received proportionally more Pb from tributary inputs and to a less degree, from connecting lake channels. Lake Huron, being in the middle, unsurprisingly receives Pb from atmospheric deposition and tributaries in relatively more equivalent contributions ([Bentley et al., 2022](#)). Lastly, another study examined the effects of road salts and deicers on metal mobilization within the soil profile ([Schuler and Relyea, 2018](#)). Sodium (Na) can

displace Ca and Mg in the soil which can increase porosity of the soil structure leading to mobilization of metals. Salts can also mobilize Pb by breaking down the organic-rich colloidal structures that often bind Pb within the soil matrix. Salts can also displace metals, including Pb, from binding with organic compounds because the binding affinity is higher for Na, Ca, and Mg than it is for heavy metals. Although this study did not measure Pb concentration in water or stream sediments, it highlights how salts and road deicers can increase Pb mobility into water systems through the physical and chemical changes to the soil matrix—an interaction effect unique yet widespread in urban systems.

1.3.3.2.2. Non-Urban

As in urban environments, Pb in runoff in non-urban areas is primarily within sediments and runoff into waterways is driven by storm events and overall precipitation patterns. A European study examined trace metal budgets across 14 forested catchments over the period of 1997–2011 ([Bringmark et al., 2013](#)). Due to high anthropogenic deposition for decades, Pb accumulation in catchment soils was high. Pb is bound to soil OM in these soils leading to high retention of Pb in the system. At higher altitude sites which experience greater precipitation, retention is lower due to greater runoff and transport of PM out of the system. In a similar study in England, while Pb deposition has decreased in recent decades, legacy Pb in peat catchments is a continuing source of Pb to waterways ([Rothwell et al., 2011](#)). Atmospheric deposition was measured at 34 gPb/ha/year while fluvial outputs were 316 gPb/ha/year. Following storm events, Pb runoff into waters occurs primarily as suspended particles (261 gPb/ha/year) with a smaller aqueous portion (55 gPb/ha/year). In the Snowy Mountains of Southeast Australia, down-catchment reservoirs with large catchment size showed comparable sediment metal enrichment values to soil enrichment values indicating the soil surface which contains metal values reflective of anthropogenic deposition is the source of sediment to reservoirs, not eroded subsoils (which is less contaminated) ([Stromsoe et al., 2015](#)). However, Pb (and chromium) are depleted in reservoir sediments compared with soils, indicating these more particle-reactive materials are bound up within the soil matrix and are not being washed into down-catchment reservoirs.

In waterways draining the Alberta badlands, total Pb concentration frequently exceeded Alberta guidelines for freshwater biota ([Kerr and Cooke, 2017](#)). However, Pb concentration was positively correlated with TSS due to an increase in sediment mass, not due to increased sediment Pb concentration, highlighting the importance of erosion and precipitation interactions in arid systems. In contrast, a study in Brazil found metal fluxes, including Pb, were highest during the dry season compared with the wet season and were due to suspended sediments ([Bezerra da Silva et al., 2015](#)). Unlike the studies measuring flux in the badlands of Alberta, this increase was not due to bedload but due to a lack of dilution. The watershed included agricultural and industrial sources as inputs and Pb was likely from coal combustion, solid waste incineration, and legacy Pb from petroleum but sources could also include pesticide use, sewage sludge runoff and agricultural wastewater.

Pb runoff and accumulation from soils into lakes is also influenced by snow and ice melt. Overall, three catchments in the Pyrenees have greater Pb concentration in lake sediments than surrounding soil and bedrock ([Bacardit et al., 2012](#)). Lakes within the two watersheds above 2000 meters above sea level had lower Pb concentrations than lakes within the lowest watershed (1655 meters). The lower Pb accumulation in these high elevation lakes may be due to snowmelt moving soil bound Pb further down this catchment and bypassing the lakes altogether due to lake ice. [Kim et al. \(2015\)](#) measured dissolved Pb (and other trace elements) from melting glaciers along the Antarctic coastline in Marian Cove and determined glacier meltwater is a significant source of Pb to the cove. In ice, Pb was measured at values between 90–920 pM and 88–550 pM in snow. Pb ranged from 30–120 pM in seawater and Pb concentration decreased with increasing salinity in seawater samples.

As described in Section 1.2.4, fires are a large and increasing contributor to ambient air Pb concentrations. A few recent studies have specifically examined Pb (and other metals) movement following fires. Overall, metal mobility to waterways following a burn event is largely dependent upon the first storm event following the fire. A review of metal mobilization following fire found fires can lead to mobilization of Pb into waterways ([Abraham et al., 2017](#)). Pb bound within the soil matrix, in vegetation, or other burned materials, is released following a burn and is readily washed into downstream waterbodies with rainfall. [Burton et al. \(2016\)](#) found the total Pb (unfiltered) median water concentrations downstream of the Station Fire in California was higher than concentrations outside the burn area and higher than concentrations measured prior to storm events. Furthermore, these post-fire total Pb concentrations exceeded the recommended aquatic use criteria (CCC) following storm events. The authors suggest these higher Pb concentrations within burned areas were likely due to ash runoff because Pb concentration in ash samples was higher than soil samples. Pb source in the ash was primarily vegetative or biogenic in origin but Pb in ash collected from residential burn areas was higher. A 2011 global review that examined water quality in forested catchments following wildfire reported Pb exceeded water quality guidelines in Australia and the United States and is associated with high suspended solids concentrations following post-fire rainfall events ([Smith et al., 2011](#)).

1.3.3.3. Sedimentation, Transport, and Flux in Water and Sediment

As in the 2006 Pb AQCD and the 2013 Pb ISA ([U.S. EPA, 2013, 2006](#)), chemical and physical characteristics of the water such as pH, salinity, and flow rate as well as the chemical and physical properties of the suspended sediments determine the fate of Pb and therefore influence rates of sedimentation and flux as well as transport downstream. Recent publications provide additional support regarding Pb adsorption onto organic-rich or small colloid particles as well as the importance of water flowrate in settlement and downstream transport. Literature since the previous ISA provides new detail of the effects of seasonality on Pb fate and transport in water. Seasonal patterns of precipitation can lead to differences in runoff, flowrate, and turbidity, for example, which can subsequently alter sedimentation rates, transport downstream, and flux from sediments.

1.3.3.3.1. Urban

Within urban environments, city infrastructure can lead to increased loading and movement into downstream reaches. In an urban Baltimore area watershed, sediment concentrations of metals including Pb increased with urbanization ([Bain et al., 2012](#)). Stormwater flow and well-drained soils with low OM interact to increase runoff and downstream movement of Pb. In an arid California watershed, urban infrastructure allows for the quick movement of water away from urban areas resulting in increased Pb concentrations in receiving water bodies following rain events ([McKee and Gilbreath, 2015](#)). Pb concentration was correlated with water turbidity due to Pb being primarily within the particulate fraction. Another study examined the influence of runoff and other diffuse pollution sources on lake water and sediment chemistry of Hough Park Lake in Central Missouri ([Ikem and Adisa, 2011](#)). The lake is surrounded by a golf course with little natural buffering between the course and the lake. Average lake Pb concentrations in sediments were 11.05 mg Pb/kg for littoral zone sediment and 0.79 mg Pb/kg in pelagic zone sediment. Total Pb in the water column was 0.0004 mg/L in the spring. Pb content was primarily in the residual phase (75%) and the authors suggest since all heavy metals were primarily within the residual phase (lowest mobility phase), the source of heavy metals is likely due to erosion and runoff of parent rock material.

Seasonal and local weather patterns interact with other factors such as soil and sediment physical and chemical characteristics to transport Pb into and within water bodies. One study sampling water column and surface sediment Pb concentrations in Lake Pontchartrain along I-10 shows seasonal differences ([Zhang et al., 2016b](#)). Spring sediment concentrations ranged from 16.42–28.25 mg Pb/kg and from 6.94–21.79 mg Pb/kg during the summer. Water column Pb concentrations in spring ranged from 4.65–7.4 µg Pb/L and from 4.7–10.4 µg Pb/L during the summer. The higher sediment concentrations in spring and higher water column concentrations in summer may be due to warmer summer water temperatures releasing more Pb from sediments. Differences between spring and summer could also be due to less precipitation and sediment disturbance via turbidity during cooler months. Pb in sediments was primarily in the stable residual fraction. In the San Juan River delta of Lake Powell, sediment loading and associated Pb contamination in the downstream reaches reflect an interaction of seasonality and precipitation ([Frederick et al., 2019](#)). During the spring, high sustained flow from snowmelt occurs at high elevation tributaries with a history of mining. This increased flow in the spring contributes more Pb-contaminated sediment to the downstream delta area. Tributaries that contribute greater sediment during short rainfall events have lower Pb concentrations.

Transport and settlement patterns of Pb are also a function of sediment particle size. In a study examining the downstream transport of heavy metals from the superfund site Iron Mountain into the Sacramento River, Pb enters the Keswick Reservoir primarily in the dissolved form and is precipitated or adsorbed into the particulate phase ([Taylor et al., 2012](#)). However, Pb does not settle out of the water column and is instead transported far downstream due to particle association with the colloid phase. This transport of fine contaminated particles occurs during both high and low flow conditions. In the Miami

River in Florida, Pb was negatively correlated with sediment particle size ([Tansel and Rafiuddin, 2016](#)). As particle size decreased, Pb content increased with 900 mg Pb/kg found within the fine sediment fraction. Due to Pb being bound to finer sediments, turbidity from boating, tidal action, and rain events are of concern for resuspension and mobilization of Pb within the water column. Following a dam removal on the Pawtuxet River in Rhode Island, fluxes of all metals including Pb increased in response to river flow ([Katz et al., 2017](#)). As river flow increased, sediments were resuspended into water and this particle-bound Pb moved downstream into Narragansett Bay. [Sebastiao et al. \(2017\)](#) examined Pb (and other metals) in the river sediments at two paved river fords in suburban Philadelphia and across seasons. Pb was found in higher concentrations in April, July, and in December, but these higher values were not correlated with any rain event. Pb was positively correlated with organic content but only at the ford that was less used. The authors suggest this relationship occurs due to less water movement from traffic which in turn allows Pb to adhere to organic particles and settle out of the water column. Furthermore, since sediment Pb concentration was still high during the winter when the fords are closed to traffic, Pb persistence in this system is not seasonal.

1.3.3.3.2. Non-Urban

Seasonal effects such as snowmelt can impact Pb movement. Anthropogenic Pb per unit area in high elevation lake sediments in the Pyrenees was lower than in the surrounding catchments, and this is potentially due to Pb deposition largely accumulating in snowpack followed by melting and outwash into lower elevation systems before the ice on the high elevation lakes can melt and incorporate this deposition portion as happens at lower elevation lakes ([Bacardit et al., 2012](#)). In a study that measured Pb in surface sediment at the river mouth of the Papaloapan River across a gradient of increasing water depth in the SW Gulf of Mexico, Pb was positively correlated with organic carbon but only during the winter months ([Rosales-Hoz et al., 2015](#)). During the summer, Pb was strongly positively correlated with Al₂O₃ (also during the winter months though not as strongly). Pb concentration increased with water depth as did the muddy proportion in sediments. Muddy sediment output from the river was greater during the summer.

As in urban aquatic environments, environmental and physical drivers of water flow patterns largely govern the transport of Pb within non-urban aquatic environments with additional influence of sediment and water chemistry. Pb water concentration at European bog and peaty riparian sites was positively correlated with DOC (particularly at the bog location) ([Broder and Biester, 2017](#)). However, at this location, Pb concentrations in water were lowest during the spring snowmelt likely due to a dilution effect whereas during high rainfall flow events, amounts exported increase while water concentrations decrease. Pb was more likely mobilized due to OM decomposition than affinity for forming Pb-OM complexes since all elements showed similar patterns regardless of OM affinity. Pb concentrations in water were highest during the fall when dry periods were followed by high rain events. High elevation peat mires, soils, and down-catchment reservoirs were sampled in the Snowy Mountains in southeast Australia ([Stromsoe et al., 2015](#)). Pb input to peat mires is dominated by atmospheric deposition and

showed greater enrichment of Pb compared with down-catchment reservoirs. Down-catchment reservoirs had depleted Pb levels in comparison due to a dilution effect of soil-bound Pb and large catchment areas.

In an arctic peatland, Pb aqueous concentrations were 2–3 times higher in the spring compared with the summer ([Stolpe et al., 2013](#)). Pb concentrations were correlated with DOM. Pb was also primarily in the 0.5–4 nm colloid fraction. During the spring melt in an arctic peatland, pH and high dissolved DOC occur due to erosion of acidic OM and fine particles while concurrently diluting the contribution of the bicarbonate parental material to waterways. During the summer, alkalinity increases while DOC decreases because water inputs shift to groundwater source. A European study examined trace metal budgets across 14 forested catchments over the period of 1997–2011 ([Bringmark et al., 2013](#)). Due to high anthropogenic deposition for decades, Pb accumulation in catchment soils was high. Pb is bound to soil OM in these soils leading to high retention of Pb in the system. At higher altitude sites which experience greater precipitation, retention is lower due to greater runoff and transport of PM out of the system. In a similar study in England, while Pb deposition has decreased in recent decades, legacy Pb in peat catchments is a continuing source of Pb to waterways ([Rothwell et al., 2011](#)). Atmospheric deposition was measured at 34 gPb/ha/year while fluvial outputs were 316 gPb/ha/year. Following storm events, Pb runoff into waters occurs primarily as suspended particles (261 gPb/ha/year) with a smaller aqueous portion (55 gPb/ha/year).

1.3.3.4. Temporal Trends Documented in Sediments

Temporal trends of Pb deposition in sediment show distinct leaded gasoline peaks in the United States. These peaks are found globally, corresponding to the specific phase-out periods for multiple countries. Patterns of increasing Pb concentration occurring from the mid-19th century through the mid-20th century due to early industry as well as agriculture, weathering, and mining operations are identifiable in North American lake and reservoir sediments. Following the peak deposition period in the 1960s due to leaded gasoline in North America, widespread decreases in Pb concentration in sediments are seen over the following half century, but concentration values are still higher than background levels showing continued deposition, non-point contamination, and/or legacy Pb runoff contributions.

Sediment dating of a mill pond in eastern Virginia shows local Pb sources (weathering and coal combustion) were the primary inputs to Lake Matoaka during the years 1700–1775 ([Balascio et al., 2019](#)). In 1780, Pb accumulation decreased slightly, possibly due to a decline of industry which coincides with the capital of Virginia moving from nearby Williamsburg to Richmond. Over the following two centuries, Pb accumulation increased, and sources were from regional mining and Pb ore smelting activities. Pb concentrations continue to increase during the 1900s to a peak maximum in 1975 followed by a sharp decline. This rise and fall of Pb accumulation reflect the increase in coal combustion, smelting, and use of leaded gasoline. Sediment records in Lake Anna in Virginia have higher Pb concentrations in the downstream portion of the reservoir (often exceeding 50 mg Pb/kg) in comparison to the upper reaches

([Odhiambo et al., 2013](#)). Furthermore, these higher concentrations in the downstream portions were limited to the younger surface sediments. Lake Anna sits in a rural watershed and sediment cores do not show the typical increase followed by sharp decrease indicative of leaded gasoline deposition. Instead, sediment enrichment of Pb in addition with cadmium (Cd), Cu, and Zn point to mining runoff as the source of Pb enrichment in sediments. An old sulfur (S) mine operated in the area until 1877, and a pyrite, Cu, and Fe mine until 1920. All other mines ceased operation in the 1990s. A study that measured heavy metal, polychlorinated biphenyl, and polycyclic aromatic hydrocarbon concentrations in dated sediments of the lower Anacostia River in Washington D.C. found Pb concentration had two peaks: the first occurred at corresponding depth of 1943 and the second in 1984 ([Velinsky et al., 2011](#)). The cause for the early 20th century peak is not clear, as Pb sources in the area included both agriculture and industry. The second peak in 1984 and subsequent decrease likely corresponds to the use and then phase-out of leaded gasoline. A location near the Navy Yard and Government Services Administration showed an increase in Pb concentration again over the years of 1989–2000, and the authors note this sampling location is close to large storm water and sewer drainages.

In Horseshoe Lake near St. Louis, three main periods of variable Pb pollution were identified. The first period was dated as pre-settlement, had low Pb concentration and the lowest $^{206}\text{Pb}/^{207}\text{Pb}$ ratio and is representative of background parental material and deposition from flooding of the Mississippi River basin ([Brugam et al., 2012](#)). The second period dated as post 1750 had increasing Pb concentration, and the $^{206}\text{Pb}/^{207}\text{Pb}$ ratio diverges from the ratio in the first period. The $^{206}\text{Pb}/^{207}\text{Pb}$ ratio increases and matches Missouri ore samples, and this period coincides with the start of Pb mining in the region. The third period dated from 1915 to the present also contained high Pb concentrations but a lower $^{206}\text{Pb}/^{207}\text{Pb}$ ratio than period two. The source of Pb in this sediment layer is less clear because the $^{206}\text{Pb}/^{207}\text{Pb}$ ratio is similar to vehicle exhaust values of leaded gasoline but is also similar to a nearby old Pb smelter. The lower ratio but high concentrations may also be reflecting erosion and settling of upstream agricultural runoff. The parental material upstream under agriculture has a lower ratio than silt from the Mississippi River but a higher Pb concentration due to agriculture. Lake Whittington, an oxbow lake, was created in 1937 by the U.S. Army Corps of Engineers off the Mississippi River. Flooding of the Mississippi River is the main source of sediment to Lake Whittington ([Van Metre and Horowitz, 2013](#)). Sediment analysis within the lake shows Pb concentration increased from 1938 to the 1970s followed by a decrease. The increase is due, in part, by greater sediment contribution from polluted up-river watersheds of the upper Mississippi and Ohio rivers and less contribution from the cleaner Missouri River watershed which had extensive damming in the 1950s. The concentration decrease post 1970s is explained by reduction in leaded gasoline emissions.

Sediments were sampled and dated in an oxbow lake in southwestern Pennsylvania to establish historical contamination in an area of the country with a long pollution exposure history ([Ostrofsky and Schworm, 2011](#)). Pb concentrations increased from 1915 to 1938 corresponding to the opening Donora Zinc Works. Pb levels decrease during the 1940s corresponding depth layer which the authors suggest reflects either a decrease in production or improvement in recovery methods. This downward trend

continues through the 1950s (Donora Zinc Works closed in 1957), but Pb concentration increases shortly thereafter around the time a coal powerplant opened nearby. Pb concentration decreases again in the 1980s—perhaps in response to the cessation of leaded gasoline. However, As, Cd, and Zn concentrations also decrease suggesting the Pb pollution patterns in this area during this time are instead linked to the coal powerplant ([Rossi et al., 2017](#)). In Sandy Lake, Pennsylvania, Pb levels increase alongside Fe, Mn, and S from approximately 1770 until the 2000s. The increase in concentrations seen in Pb and other elements corresponds with the opening of a coal mine which directly contaminated Sandy Lake with acid mine drainage in the late 1800s. The decrease in Pb levels in the 2000s likely reflects the decrease in deposition from leaded gasoline. In another study, Pb sediment concentrations in Little Lake Bonnet in Florida increased over the period of 1874 to 1920 with a peak of ~28 mg Pb/L ([Escobar et al., 2013](#)). Concentrations increased further to ~38 mg Pb/L in 1949 with an overall peak in 1990 of ~72 mg Pb/L. Pb concentration then declined after 2001 to ~60 mg Pb/L. Little Lake Jackson in Florida showed similar patterns with a peak between mid-1970 and early 1980s. Isotope ratio analysis ties Pb peak patterns with leaded gasoline. The general increasing concentrations in the lakes during the 20th century correspond with broad regional industrialization during this period including pesticide and fertilizer use on golf courses, Pb-As insecticide use on nearby citrus groves, and proximity of coal power plants.

A detailed sediment analysis from Vermillion Lake in Sudbury, Ontario, Canada linked Pb concentration to historical industry and leaded gasoline ([Schindler and Kamber, 2013](#); [Wiklund et al., 2012](#)). Pb concentrations first started increasing in the late 19th century at a time when logging in the area first started. Pb concentrations increased until a peak in the late 1960s into the 1970s. The subsequent decrease in concentration corresponds to the phase-out of leaded gasoline in Canada in 1976 and union strikes at nearby mines, resulting in low production. Pb ratios indicated multiple sources of Pb. The parent rock and ores have a unique $^{206}\text{Pb}/^{207}\text{Pb}$ ratio and patterns in this ratio combined with increasing nickel (Ni) concentrations over the period of 1905–1919 indicating Pb level was primarily due to mining contamination. The continuing increase in Pb concentrations after this period would likely reflect greater deposition from nearby smelters and refineries which has a similar ratio profile as leaded gasoline. [Child et al. \(2018\)](#) examined sources and geographic extent of atmospheric metal deposition across eastern Washington lakes within 50 km from the Trail smelter in British Columbia. Pb isotopes and deposition profiles indicate the Trail smelter as a primary source of atmospheric trace metal deposition including a lake outside the 50 km radius and upwind ([Louchouart et al., 2012](#)). A study by [Dunnington et al. \(2020\)](#) examined Pb trends using sediment dating in multiple lakes across northeastern North America. Sampled lakes included locations in the Adirondacks (northeast New York), lakes across Vermont, New Hampshire, and Maine, as well as several lakes in Nova Scotia. In general, Pb concentrations decreased from west to east. Sediment dating reveals anthropogenic Pb concentrations began increasing first in the Adirondack region in 1859 followed by the VT-NH-ME region in 1874, and finally in Nova Scotia in 1901. Authors acknowledge early Pb emissions were likely due to coal combustion in the Adirondack and New England lakes, but with the increase in Nova Scotia lakes after 1923, Pb from gasoline was likely an important deposition source to all lakes in this study. Furthermore, looking across the whole sediment

core, Pb in youngest sediment is still higher than pre-industrial levels—an indication of continued contamination and loading from legacy Pb in runoff.

In a review by [Marx et al. \(2016\)](#), global contamination records of Pb were examined using sediment, peat, and ice cores from across North and South America, Europe, Asia, Australia, and both polar regions. In North America, Pb contamination dating back to 6500 BCE was found and the authors link this early contamination to pre-historic Cu use. Enrichment in this core increases between 1300 CE and 1500 CE, where enrichment doubles, corresponding to the start of the industrial revolution. By the 1960s CE, enrichment peaks are followed by a decline to 2002 (though enrichment is still well above the 1500 CE values). A peat and lake core in Canada record enrichment starting much later (1800s CE) and linking it to coal mining. The peat core shows Pb enrichment peak in 1910 while the lake core peaks in the 1970s. Overall, Europe and North America have higher enrichment values than Australia and Antarctica. Globally, Pb enrichment starts in pre-historic era in Europe, North America, and east Asia while in South America, enrichment starts during the Middle Ages. However, by the latter half of the 1800s, Pb enrichment is globally well above background levels, increasing until the 1970s when enrichment declines in Europe and North America but continues to increase in east Asia and Australia. A global study by [Zhou et al. \(2020a\)](#) sampled 168 rivers and 71 lakes from 1972 to 2017 to examine global patterns in heavy metal pollution. Pb levels globally increased during the 1970s and 1980s to a peak level of 257 µg/L in the 1990s. Pb levels decreased slightly during the 2000s with a slight increase in the 2010s. Pb levels were highest in South American water bodies (~333 µg Pb/L) and lowest in Europe (~14 µg Pb/L). Potential sources included rock weathering, fertilizer and pesticide application, mining and manufacturing, and waste discharge. Across the decades, the primary source of Pb was determined to be from mining and manufacturing.

1.3.3.5. Sediment Pb Pools as Potential Sources to Surface Waters

The removal or breaching of worn-down dams, such as old mill dams, in the eastern United States are a potential new source of legacy Pb for downstream waterways. One study by ([Niemitz et al., 2013](#)) found higher Pb sediment levels above a former mill dam draining former and current agricultural lands compared with dammed sediment above a forested catchment within the upper reach of the Yellow Breeches Creek watershed in Pennsylvania. Sediments at both locations, however, contained legacy Pb from gasoline emissions. In another study, while Pb flux initially increased following the removal of Pawtuxet River dam and was positively correlated with river flow, SPM concentration decreased and remained lower than pre-removal levels for the duration of the study ([Katz et al., 2017](#)). This decrease in SPM concentration, however, is potentially due to increased contribution of low-contamination level soils previously above the flood zone downstream of the dam site, and sediment cores taken in multiple locations upstream exceeded sediment quality criteria. Therefore, while removal of a dam may lead to a dilution effect on downstream waters, pools of legacy Pb upstream of a dam will still move into downstream waterways with the post-removal associated increase in water flow. Furthermore, these

contaminated sediments can transform to more biologically available forms as they contribute to increased turbidity with increased water flow and salinity as with the Yellow Breeches and Pawtuxet River's flow to the Atlantic (Chesapeake and Narraganset Bay, respectively). Interestingly, in a study examining the effect of beaver dams on heavy metal retention and sediment contamination found Pb aqueous concentration to be lower in the outflow because the dammed water acts as an oxidation pond and results in sorption of Pb to iron oxides ([Shepherd and Nairn, 2020](#)). In another study that examined trace metals in surface sediments of a tidal tributary of the Chesapeake Bay, Pb concentrations were above threshold effects levels at 44% of sites sampled. The Chester River watershed is a forested and agricultural watershed and metal accumulation within riverine sediments is likely due to a combination of multiple non-point source runoff as well as tidal exchange with the Chesapeake—highlighting metal pollution transport can occur upstream in estuarine environments ([Krahforst et al., 2022](#)). Hurricane Sandy associated storm surge resuspended Barnegat Bay sediments rich in metal contaminants and transported them northward within the Bay ([Romanok et al., 2016](#)). The source of metal contaminants within sediment silt comes from runoff from inundated urban lands, wetlands, estuaries, streams, and from the resuspension into water of estuarine sediments that may have previously been considered pools of legacy contaminants—including Pb from upstream deposits. Similarly, as discussed in Section 1.3.3.2.1, runoff and sediment concentrations have been linked to characteristics of urbanization suggesting urban areas are a potential source of resuspended Pb in water from sediments following storm or high-flow events.

1.3.3.6. Summary of Pb Fate and Transport in Aquatic Systems

In summary, literature since the 2013 Pb ISA supports previous conclusions regarding the physicochemical drivers of Pb fate and transport in aquatic systems. Studies continue to report runoff from urban or historically industrial areas contain higher Pb concentrations than non-urban areas with new information highlighting relationships between street length and density, population density, and land cover with runoff. Recent studies expand on the influence of seasonality and precipitation events on runoff as well as transport and sedimentation. Timing of snow and ice melt can alter down-catchment transport of Pb in high elevation watersheds, for example, while another study found water column concentrations differed between summer and winter—possibly due to differences in precipitation patterns influencing sedimentation and resuspension into water. A collection of recent studies linked Pb concentration peaks in lacustrine and riverine sediment cores to national and global patterns of industrialization in the late 19th and early 20th century, to increased vehicle abundance and associated leaded gasoline in the mid-20th century, followed by a decline in Pb concentration coinciding with the phase-out of leaded gasoline and stricter emissions regulations. Furthermore, new literature also addressed the importance of turbidity and resuspension into water in relation to legacy Pb pools. While Pb deposition has decreased in the last half century with the phase-out of leaded gasoline and stricter regulation, Pb sediment pools in areas with a history of industry and urbanization are vulnerable to

resuspension into water and both down and upstream movement following a disturbance event. Dam removal or other disturbances to streams in the eastern United States can lead to resuspension in water and dissolution of Pb-contaminated sediment that was previously deposited. Lastly, with the predicted increase in drought alongside less frequent but more severe precipitation patterns across most of the United States, the potential for remobilization of legacy Pb is a growing area of concern and consideration.

1.3.4. Fate and Transport in Urban Media

Additional media besides air, water, and soil are useful for understanding how Pb moves and changes over time in the urban environment. These can include urban soil (Section 1.2.7), resuspended airborne dust, road dust (Section 1.2.5), and house dust, between which Pb can be transported or cycled. Pb concentrations are characteristically higher in urban soil than other soils. [Frank et al. \(2019\)](#) reported the mean estimate of Pb concentration in urban residential soils was 3 times greater than for non-urban soils in a meta-analysis of recent studies. [Obeng-Gyasi et al. \(2021\)](#) estimated that urban soil Pb concentrations were approximately 7 times U.S. background levels (Section 11.1.3) through a comparison of an analysis 84 studies of U.S. soil Pb with a U.S. Geological Survey study of U.S. background soil Pb concentrations ([Datko-Williams et al., 2014](#); [Smith et al., 2013](#)). [Datko-Williams et al. \(2014\)](#) concluded that there had been little change in urban U.S. soil Pb concentrations from 1970 to 2012. The highest concentrations often occur in roadside soil and near buildings, reflecting the proximity to legacy Pb from leaded gasoline and deteriorating paint, respectively ([Obeng-Gyasi et al., 2021](#)), although [Frank et al. \(2019\)](#) reported lower soil Pb concentrations for roadside soils than for residential urban soils in their meta-analysis of studies on soil Pb concentrations in the United States. The 2013 Pb ISA also reviewed observations of decreasing soil Pb concentrations with distance from a road ([U.S. EPA, 2013](#)). There is some evidence that the pattern of decreasing soil Pb concentrations with road distance are paralleled by near-road air Pb concentrations (Section 1.2.6).

Pb has a very long residence time in soil, with models predicting more than a century until soil concentrations return to steady-state levels ([Harris and Davidson, 2005](#)). This is consistent with the slow transport rates typically observed for a range of conditions (Section 1.3.2) and facilitates the persistence of long-term hot spots. For example, as described in Section 1.2.7, soil Pb in Durham NC ranged from 6–8825 mg Pb/kg and soil Pb concentrations were higher around older homes, indicating contribution from leaded paint ([Wade et al., 2021](#)). Home age accounted for 40% of the variance in foundation soil Pb, with soil near painted houses containing significantly higher soil Pb than for brick homes ([Wade et al., 2021](#)). Studies in East Chicago IL, Greensboro NC, Brooklyn NY, and Philadelphia PA have explored the high spatial variability of urban soil Pb concentrations, with hot spots related to income and racial disparities ([Caballero-Gómez et al., 2022](#); [Pavilonis et al., 2022](#); [Haque et al., 2021](#); [Obeng-Gyasi et al., 2021](#)). Urban and neighborhood-scale spatial variability of ambient air Pb concentrations have been observed in recent studies, but not directly related to urban soil (Section 1.5.2).

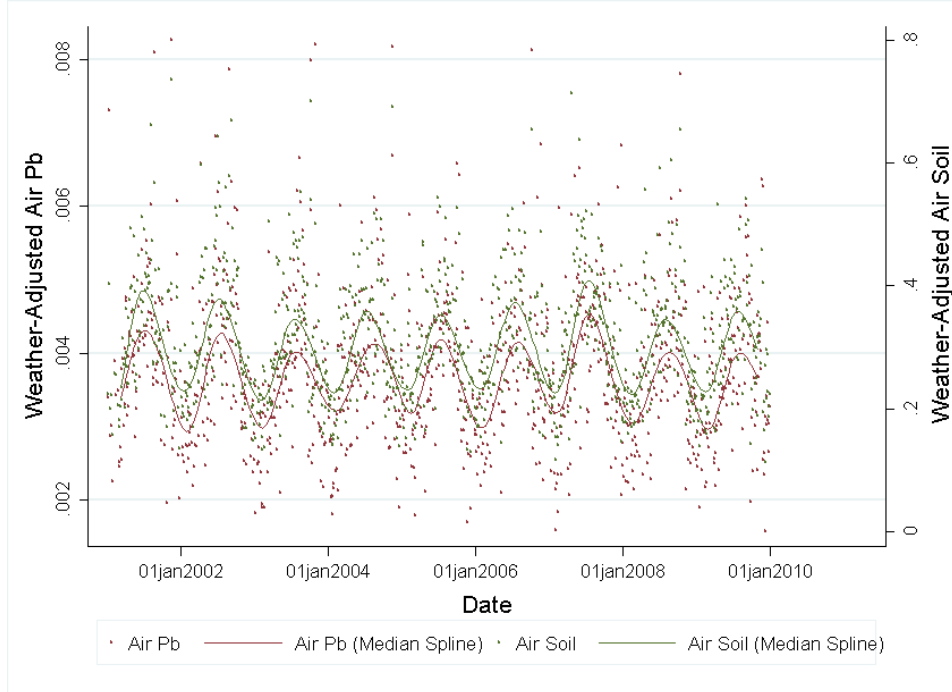
Resuspension of Pb in contaminated soil and road dust by traffic, construction, and wind has been described as a potential contributor to airborne Pb under some circumstances ([U.S. EPA, 2013](#)). The 2013 Pb ISA reported that contaminants associated with particles with diameters up to about 100 μm can typically become resuspended into air, but particles larger than 10–20 μm typically do not remain airborne long enough for appreciable transport ([U.S. EPA, 2013](#); [Nicholson, 1988](#); [Gillette et al., 1974](#)). However, the extent of resuspension of contaminants in surface soil and dust particles into air depends strongly on landscape, geology, particle size and wind speed. The 2013 Pb ISA summarized factors influencing resuspension into air in a complex urban landscape with heavy traffic, buildings, pavement and above- and below-ground infrastructure ([U.S. EPA, 2013](#)). The critical diameter at which resuspension into air occurs is the diameter at which the particle settling velocity becomes equal to the friction velocity of air needed to move the particle at rest. Although this was estimated at roughly 20 μm in an open landscape ([U.S. EPA, 2013](#); [Gillette et al., 1974](#)), a higher friction velocity is expected for urban environments with traffic-induced turbulence ([Britter and Hanna, 2003](#)). This could result in resuspension of somewhat larger particles into air in an urban setting with heavy traffic ([Nicholson and Branson, 1990](#)). Near-road observations indicate that the fraction of total particulate Pb associated with particles larger than 10 μm can be 15% or more ([U.S. EPA, 2013](#)).

Pb particles from soil and dust occur at sizes ranging from 0.1–10 μm , a size range with potential for resuspension into air and inhalation ([O’Shea et al., 2021](#)). Laboratory studies and sampling in areas with previous major emissions sources suggests the potential for resuspension of near-surface soil-bound Pb to contribute to airborne concentrations in those areas ([Pingitore et al., 2009](#); [U.S. EPA, 2006](#)). A previously reported modeling study estimated up to 90% of Pb emissions in Southern California are attributed to Pb resuspension from soil and road dust into air ([Harris and Davidson, 2005](#)), though [Lankey et al. \(1998\)](#) noted a smaller estimate of 43%. With estimated annual emissions of 54,000 kg airborne Pb in 2001, modeled resuspension was identified as the largest source of airborne Pb in the Southern California region ([Harris and Davidson, 2005](#)). Although Pb from contemporary sources can also be resuspended into air, emissions from historical sources were considerably greater, and substantial Pb from sources like leaded gasoline and historical industrial emissions or from non-atmospheric sources like paint have accumulated in soil over many years, particularly in urban areas (Section 1.2.7).

Correlations between soil Pb concentrations and atmospheric Pb concentrations have been observed in recent studies. [Laidlaw et al. \(2014\)](#) reported atmospheric Pb loadings increased by 0.066 $\mu\text{g}/\text{m}^2/28$ days for every mg Pb/kg increase in soil Pb. Another study found that a 1% increase in estimated resuspended soil concentration in air corresponded to a 0.39% increase in atmospheric Pb concentration (95% CI, 0.28 to 0.5%) ([Zahran et al., 2013](#)). The isotopic composition of Pb in airborne particles is consistent with that of road dust and topsoil, with significant contributions (a binary mixing model found from 32 ± 10 to $43 \pm 9\%$) of Pb from leaded gasoline ([Resongles et al., 2021](#)). Atmospheric soil and Pb aerosols are 3.15 and 3.12 times higher, respectively, during weekdays than weekends, suggesting traffic as a major driver of Pb resuspension into air ([Laidlaw et al., 2012](#)). In London, 450–650 kg/year of Pb is emitted as resuspended dust, a similar magnitude as primary Pb air emissions in

urban locations ([Resongles et al., 2021](#)). Additionally, Pb isotopic composition was similar for particles collected at ground-level and building height, suggesting Pb is well mixed throughout the vertical column in urban environments ([Resongles et al., 2021](#)). Dust emissions are significant and represent missing sources in the emission inventories ([Xu et al., 2019](#)). To reduce national-scale bias of modeled Pb concentrations, a fivefold increase in anthropogenic emissions of Pb was necessary to achieve agreement between simulated and observed ambient air Pb concentrations ([Xu et al., 2019](#)). While these studies suggest that resuspension Pb from soil into air is a potentially important local source of Pb in ambient air, it appears to be a much smaller contributor to current ambient air Pb concentrations than leaded gasoline exhaust was in previous decades. Airborne Pb monitoring was originally required for urban National Core multipollutant monitoring network (NCore) multipollutant monitoring network sites (Section 1.4) but was discontinued in 2016 because concentrations were consistently much lower than NAAQS levels (40 Code of Federal Regulations (CFR) Part 58, Appendix A). Moreover, at five Pb monitoring sites near roads with heavy traffic, ambient air Pb concentrations decreased from more than 1 $\mu\text{g}/\text{m}^3$ in 1979 to less than 0.03 $\mu\text{g}/\text{m}^3$ in 2010 ([U.S. EPA, 2013](#)).

Several studies have reported seasonal patterns of resuspension from soil into air, with highest resuspension occurring in summer and autumn when soils are driest ([Resongles et al., 2021](#); [Mielke et al., 2019](#); [Laidlaw et al., 2017](#); [Laidlaw et al., 2016](#); [Laidlaw et al., 2014](#)). In Detroit, atmospheric Pb is 44.8% higher in August than January (Figure 1-5) ([Zahran et al., 2013](#)). This seasonal pattern is also observed in measurements of children's blood levels ([Laidlaw et al., 2017](#); [Mielke et al., 2017](#); [Laidlaw et al., 2016](#); [Zahran et al., 2013](#)) and is discussed in detail in Section 2.4. National scale modeling of heavy metal concentrations with the chemical transport model GEOS-Chem indicated that simulated heavy metal concentrations in $\text{PM}_{2.5}$ over continental North America were consistent with monitoring observations in winter, but generally low in other seasons, suggesting that contributions of missing sources of Pb follows a seasonal pattern similar to that observed for airborne soil components ([Xu et al., 2019](#)).



Source: Reprinted with permission from [Zahran et al. \(2013\)](#). Copyright 2013, American Chemical Society. Air soil refers to the estimated ambient air concentration of soil-derived PM based on crustal element concentrations. Weather-adjusted concentrations are concentrations that have been adjusted for relative humidity, pressure, temperature, visibility, and wind speed using their known relationships with air Pb and air soil to determine their seasonality independent of short-term weather conditions. The median spline is a smoothing function based on a polynomial fit.

Figure 1-5 Ambient air Pb and air soil concentrations and median splines in $\mu\text{g}/\text{m}^3$ from Detroit, Michigan.

Though rare, extreme weather events can alter soil Pb concentrations drastically. Following Hurricane Katrina in New Orleans, soil Pb decreased from 285 to 55 mg Pb/kg on public land and from 710 to 291 mg Pb/kg on private land ([Mielke et al., 2017](#)). These observed effects are likely due to result in decreased resuspension into air following flooding, as well as transport of soil from outside the city covering Pb-contaminated urban soil ([Mielke et al., 2017](#)). Recent Pb isotopic aerosol signatures show origins from leaded gasoline, suggesting Pb sources have not changed substantially since the removal of leaded gasoline ([Resongles et al., 2021](#)). Pb in PM_{10} samples collected in London ranges from 3.9–19.4 ng/m^3 , with deposition rates of 11,700–45,800 $\text{ng}/\text{m}^2/\text{day}$ for Pb associated with total suspended particulate (TSP) matter ([Resongles et al., 2021](#)). Thirty-one percent of PM_{10} particles measured were attributed to resuspended road dust in air ([Resongles et al., 2021](#)).

The larger size of resuspended dust particles compared with typical atmospheric particle size distributions makes the atmospheric lifetimes and travel distances of the airborne dust Pb potentially shorter than those expected for $\text{PM}_{2.5}$ or PM_{10} ([U.S. EPA, 2013](#)). As a result, resuspension of large amounts of soil Pb into air does not appear to be an efficient process for Pb removal from a neighborhood. However, resuspension followed by relatively rapid deposition provides a potential process for Pb to translocate within neighborhoods, reducing high concentrations near busy roads while increasing it in

other areas. This pattern of evening out soil Pb concentrations in city centers over long time scales has been described by [Laidlaw and Filippelli \(2008\)](#).

Association with airborne dust also provides Pb with a transport pathway indoors, where it deposits as house dust. Along with urban soil, house dust has been a particular concern for accumulation of Pb from deteriorating paint ([Lanphear et al., 1998](#)). The evidence for the link between atmospheric Pb and house dust Pb near large industrial sources can be strong enough that urban-scale house dust Pb concentrations have been used to effectively track changes in atmospheric deposition patterns caused by the addition of a tall stack to a smelter ([Van Pelt et al., 2020](#)). Since there are also other processes for transport of Pb between soil and house dust, an unknown portion of the Pb in house dust becomes airborne after its release into the environment. However, there is potential for Pb resuspension into air to serve as a source of both ambient air Pb and house dust Pb. In a recent study of childhood leukemia risk from carpet dust, mean dust loadings were 24.5 and 15.3 $\mu\text{g}/\text{ft}^2$ in homes of children with and without leukemia, respectively ([Whitehead et al., 2015](#)). These results compare to [Frank et al. \(2019\)](#), who reported a mean of 13 $\mu\text{g}/\text{ft}^2$ for 535 floor samples and 214 $\mu\text{g}/\text{ft}^2$ for 380 windowsill samples in a meta-analysis of studies published between 1999 and 2015. [Gillings et al. \(2022\)](#) observed that Pb in both house dust and surface soil decreased with distance from mining areas. The decline with distance was steeper for soil than for house dust ([Gillings et al., 2022](#)). Whether soil Pb was removed or buried deeper under the surface was not discussed. There is also evidence for Pb-contaminated dust deposition onto roofs, which could then undergo resuspension into the air during demolition ([Caballero-Gómez et al., 2022](#)).

Recent research supports prior information on the influence of legacy Pb from leaded gasoline, past industrial emissions, and deteriorating paint on soil Pb concentrations in some areas, with the highest concentrations near roads and buildings. Within urban soil there appears to be gradual Pb transport away from roads and buildings, and a slow reduction of soil Pb concentration gradients over time, potentially due at least in part to cycles of resuspension into air, atmospheric transport, and deposition. There is also transport between soil and other compartments, namely house dust, road dust, and air. Overall, transport rates are extremely slow, and changes in concentration gradients near sources and hot spots are very gradual, apparently remaining for decades without intervention or other external disturbances like hurricanes or floods. Current research is taking place toward understanding rates of Pb transport and their influencing factors either among compartments or among different locations in the same medium (i.e., soil, road dust). One salient observation is that the extremely slow movement of Pb through the urban environment facilitates persistent hot spots of high soil Pb and house dust Pb concentrations. There is little data on whether hot spots of high soil Pb and dust Pb concentrations also lead to pockets of high ambient air concentrations, with the exception of near-road observations. Although not all urban Pb transport involves air, there is evidence that resuspension of Pb in urban soil may contribute to airborne Pb concentrations in some locations.

1.4 Monitoring of Pb in Ambient Air

This section describes advances in development and evaluation of sampling and analytical methods for monitoring and measurement of airborne Pb. Section 1.4.1 describes national monitoring networks currently in operation. Section 1.4.2 describes recent research to evaluate the performance of the Federal Reference Method (FRM) for Pb in ambient air. Section 1.4.3 provides a summary of network monitoring challenges related to Pb airborne Pb sampling. Section 1.4.4 describes recent advances in sampling and analysis of airborne Pb in monitoring and research.

1.4.1. Network Monitoring

Four national monitoring networks collect data on Pb concentrations in ambient air and report it to the Air Quality System (AQS). Up-to-date network descriptions and monitor locations for the Pb state and local air monitoring stations (SLAMS), Chemical Speciation Network (CSN), Interagency Monitoring of Protected Visual Environments (IMPROVE), National Air Toxics Trends Stations (NATTS), and NCore networks are available in “Overview of Lead (Pb) Air Quality in the United States” ([U.S. EPA, 2023c](#)). Measurements between networks are not directly comparable because of PM size range differences and other differences in sampling and analytical methods.

The SLAMS network shown in Figure 1-6 is operated by state and local agencies and monitors are sited in compliance with regulatory requirements ([U.S. EPA, 2023c](#)). Although data are used for other scientific purposes, the SLAMS network is designed primarily with the goal of evaluating compliance with the Pb NAAQS. As described in the 2013 Pb ISA, new monitoring requirements that were revised over the period from 2008 to 2010 expanded the number of SLAMS monitors ([U.S. EPA, 2013](#)). Source-oriented monitors are required near sources of Pb air emissions which are expected to or have been shown to contribute to ambient air Pb concentrations exceeding the NAAQS. At a minimum there must be one source-oriented site located to measure the maximum Pb concentration in ambient air resulting from each non-airport Pb source estimated to emit 0.50 tons of Pb per year or more and from each airport estimated emit 1.0 tons of Pb per year or more. These thresholds were established to ensure monitoring takes place near Pb air sources with the greatest potential to cause ambient air concentrations to exceed the Pb NAAQS.

In addition to the SLAMS network, Pb is monitored in several monitoring networks designed for non-regulatory purposes described in Figure 1-7. Pb is also measured within the CSN, the IMPROVE network, and the NATTS network. These networks are designed to meet other objectives besides NAAQS attainment evaluation. Pb in PM_{2.5} is monitored in the CSN and IMPROVE networks. The purpose of the CSN is to monitor PM_{2.5} species to help understand spatial and temporal variations in PM_{2.5} chemistry, including annual, seasonal, and sub-seasonal trends. Pb is one of 33 elements collected on Teflon filters every third day and analyzed by energy-dispersive X-ray fluorescence spectrometry (ED-XRF).

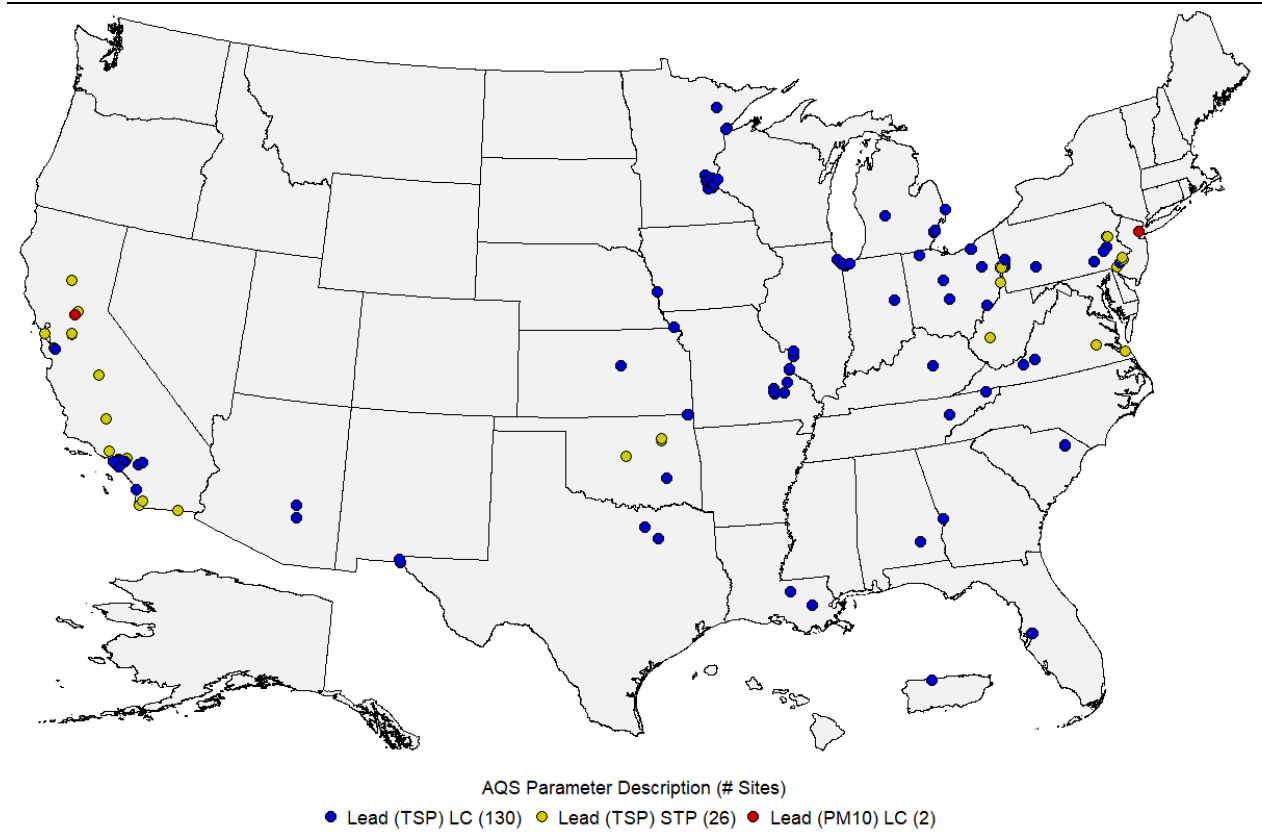
IMPROVE network monitors are operated mostly in rural locations by the National Park Service and other agencies for establishing current visibility conditions, tracking changes in visibility, and determining causal mechanisms of visibility impairment in national parks and wilderness areas. As for CSN samples, Pb in PM_{2.5} sampled in the IMPROVE network is analyzed by ED-XRF.

As shown in Figure 1-7, Pb is also monitored in the NATTS network, designed to monitor concentrations of hazardous air pollutants (HAPs). The NATTS is intended to provide model input, to observe long-term trends in HAP concentrations, and to examine emission control strategies. Pb is one of seven core inorganic HAPs collected in PM₁₀ on Teflon filters and typically analyzed by IC-PMS. Up-to-date maps of monitor locations for the Pb SLAMS, CSN, IMPROVE, NCore, and NATTS networks are available at <https://www.epa.gov/air-quality-analysis/lead-naaqs-review-analyses-and-data-sets>.

Although not required, some monitoring agencies also conduct non-source-oriented Pb monitoring at National Core multipollutant monitoring network (NCore) sites. There are 60 such urban NCore sites in Core Based Statistical Areas (CBSA) with a population of 500,000 or more. For these non-source-oriented monitors, the main objective is to gather information on neighborhood scale Pb concentrations that are typical of urban areas to better understand ambient air-related exposures of populations in these areas. The NCore network is a multi-pollutant monitoring network with advanced measurement systems for particles, pollutant gases, and meteorology. It is designed to support timely reporting of data to the public, development of emission strategies, and long-term health assessments. Monitoring network maps shown in Figure 1-6 and Figure 1-7 are annually updated at <https://www.epa.gov/air-quality-analysis/lead-naaqs-review-analyses-and-data-sets>. Monitoring for Pb was required at some NCore monitoring sites when the network was initiated in 2011.

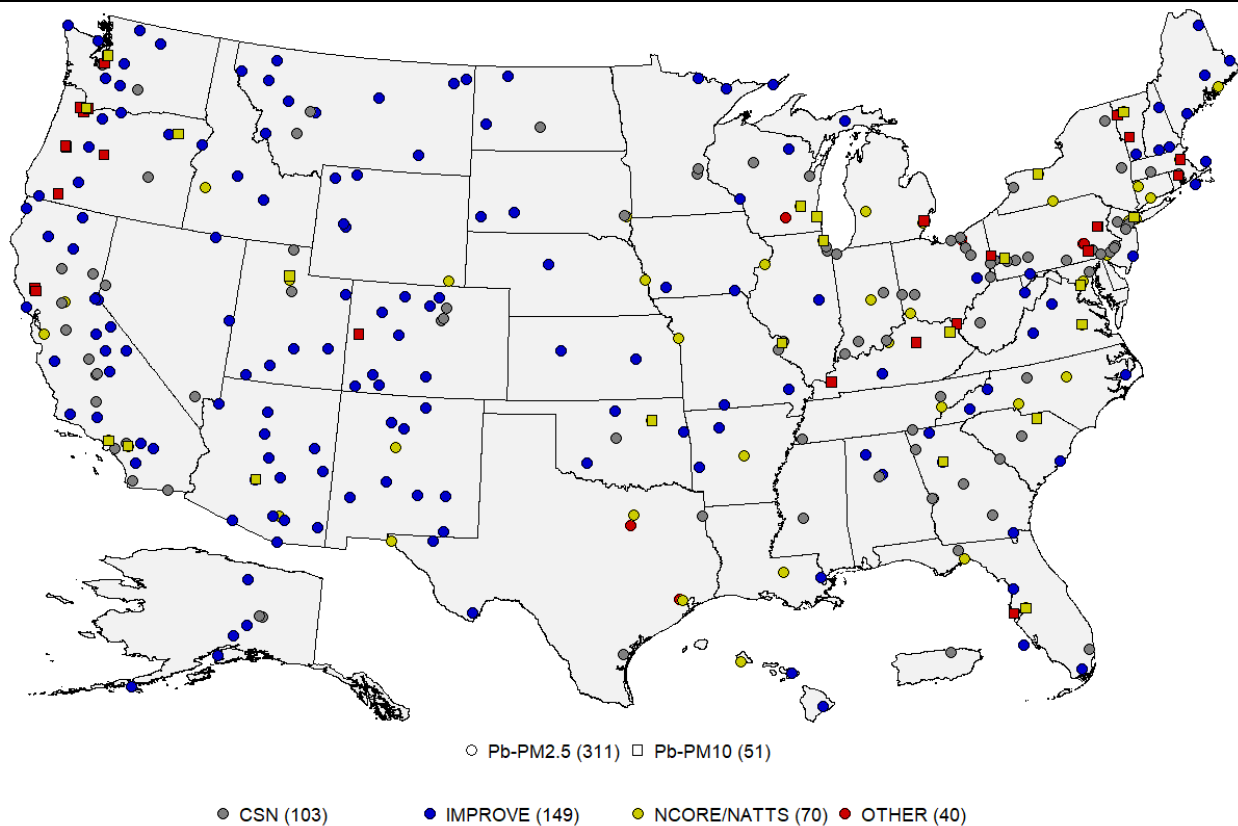
The number of Pb FRM and Federal Equivalent Method (FEM) monitors has decreased steadily since 1985, with a brief uptick corresponding to the NCore monitoring requirement for Pb from 2011 to 2016 (see Section 1.4.1, Figure 1-11). The long-term decrease in the number of monitors is due in part to criteria established to allow Pb monitoring to be discontinued. Requests for discontinuation, subject to the review of the Regional Administrator, will be approved for any state and local monitoring station monitor which has shown attainment during the previous five years, that has a probability of less than 10% of exceeding 80% of the applicable NAAQS during the next three years based on the levels, trends, and variability observed in the past, and which is not specifically required by an attainment plan or maintenance plan (40 CFR Part 58.14c). The requirement for monitoring Pb near sources may also be waived by the Regional Administrator if the state or local agency can demonstrate that the Pb source will not contribute to a maximum Pb concentration in ambient air in excess of 50% of the NAAQS based on historical monitoring data, modeling, or other means, and the waiver must be renewed once every 5 years. Concentrations fell below this level at many source-oriented monitors after the source was eliminated or emissions reduced. Concentration at non-source-oriented monitors in the U.S. are often extremely low. For example, the maximum rolling 3-month average Pb concentration over a three-year period never reached 50% of the NAAQS concentration for any of the 23 NCore monitors for which design values

were reported for at least some period between 2011 and 2023, and only 4 NCore Pb monitors ever reported a rolling 3-month average concentration greater than $0.01 \mu\text{g}/\text{m}^3$, barely above the detection limit of $0.0075 \mu\text{g}/\text{m}^3$ for the Pb-TSP FRM, for any three-month period ([U.S. EPA, 2023b](#)).



Source: ([U.S. EPA, 2023c](#)).

Figure 1-6 Map of U.S. ambient air monitoring sites reporting regulatory Pb data to U.S. EPA during the 2020–2022 period.



Source: [\(U.S. EPA, 2023c\)](#).

Figure 1-7 Map of U.S. ambient air monitoring sites reporting non-regulatory Pb data to U.S. EPA during the 2020–2022 period.

1.4.2. Federal Reference Methods

In order to be used in regulatory decisions judging attainment of the Pb NAAQS, ambient air Pb concentration data must be obtained through the FRM, or an FEM defined for this purpose. Accordingly, for enforcement of the air quality standards set forth under the Clean Air Act, the U.S. EPA has established provisions in the Code of Federal Regulations under which analytical methods can be designated as FRM or FEM. FRMs and FEMs for the Pb NAAQS exist for both sample collection and sample analysis. There are two FRMs for Pb sampling in ambient air: (1) Reference Method for the Determination of Lead in Suspended Particulate Matter Collected from Ambient Air (40 CFR part 50 Appendix G), and (2) Reference Method for the Determination of Lead in Particulate Matter as PM₁₀ Collected from Ambient Air (40 CFR part 50, Appendix G). The Pb-TSP FRM sample collection method measures Pb-associated TSP and is required for all source-oriented NAAQS monitors, and the FRM for Pb- PM₁₀ is accepted for Pb NAAQS monitoring at non-source-oriented monitors in specified situations [\(U.S. EPA, 2013\)](#).

The Pb-TSP FRM sample collection method specifies use of a high-volume TSP sampler that meets specified design criteria (40 CFR part 50 Appendix B). Ambient air PM is collected on a glass fiber filter for 24 hours using a high-volume air sampler. Variability in high-volume TSP sampler collection efficiency associated with effects of wind speed and wind direction for particles larger than 10 μm has been documented since the sampler was first implemented for TSP and Pb-TSP sampling and was a major focus of the 2013 Pb ISA ([U.S. EPA, 2013](#)).

To provide informative background for addressing sampling issues associated with particles larger than 10 μm , the 2013 Pb ISA reviewed historical research on large particle sampling as well as recently developed low-volume samplers with manufacturer-designated TSP inlets. The 2013 Pb ISA concluded that a high degree of variability had been observed between different models of manufacturer-designated TSP samplers, that no alternative to the FRM TSP sampler had yet been identified, and that there was still a need to assess the feasibility of a revised TSP sampling method for efficient collection particles larger than 10 μm ([U.S. EPA, 2013](#)).

The low-volume Pb-PM₁₀ FRM sample collection method specifies use of a low-volume PM₁₀ sampler that meets specified design criteria (40 CFR part 50, Appendix Q). Ambient air PM is collected on a polytetrafluoroethylene (PTFE) filter for 24 hours using active sampling at local conditions with a low-volume PM₁₀ sampler and analyzed by XRF. Use of the FRM for Pb-PM₁₀ is allowed in certain instances where the expected Pb concentration does not approach the NAAQS and in the absence of nearby sources of Pb associated with particles greater than 10 μm diameter.

In addition to FRMs used in the SLAMS network, other methods are used in the CSN, IMPROVE and NATTS networks, as well as in field studies unrelated to network applications. The most relevant of these methods are listed and described in the 2013 Pb ISA ([U.S. EPA, 2013](#)). In the CSN and IMPROVE networks, Pb in PM_{2.5} is collected on Teflon filters by low-volume samplers and analyzed by XRF ([U.S. EPA, 2013](#)). Other sampling approaches, including cascade impactor sampling for Pb particle size distributions, saturation samplers, and passive samplers to provide high-density coverage for evaluation of spatial variability were reviewed in the 2013 Pb ISA ([U.S. EPA, 2013](#)), and recent applications to Pb spatial variability and size distributions are reported in Section 1.5. Other analytical methods applied to Pb were also reviewed in the 2013 Pb ISA, including inductively coupled plasma atomic emission spectroscopy, ED-XRF, proton induced X-ray emission spectroscopy, X-ray photoelectron spectroscopy, Pb speciation methods including X-ray absorption fine structure as well as gas chromatography and high performance liquid chromatography combined with mass spectrometry, ICP-MS, Pb isotope ratio analysis, and continuous Pb monitoring methods ([U.S. EPA, 2013](#)). Few new advances related to Pb analysis have been reported for these methods, but recent applications of some are reported in Section 1.5.

1.4.3. Sampling Considerations

When the Pb NAAQS was revised in 2008, revision of the FRM from a method sampling Pb-TSP to a method sampling PM less than or equal to 10 μm in diameter (Pb-PM₁₀) was also considered because of poor precision and variable collection efficiencies with wind speed and direction for larger particle sizes associated with the Pb-TSP FRM. The Pb-TSP FRM was developed in the 1950s for collection of TSP. It has been the FRM for airborne Pb since 1973, but over the first decade after its designation as the Pb FRM, at least twelve studies reported variable sampler performance depending on several factors, particularly particle size, wind speed, sampler orientation with respect to wind direction, and extent of passive collection ([Krug et al., 2017](#)). Variations in Pb-TSP FRM sampler performance could be due in part to broad acceptable performance ranges and the lack of a strictly defined performance standard for evaluating TSP samplers ([Krug et al., 2017](#)).

The Pb-PM₁₀ FRM is not as vulnerable to sampling errors associated with the Pb-TSP FRM because it is based on a strictly defined performance standard. Transition to a Pb-PM₁₀-based NAAQS was not supported, however, because Pb associated with particles larger than 10 μm in diameter can be an important contributor to airborne Pb exposure, in part because of potential resuspension of Pb in urban or industrial soil or road dust into air in some locations (Section 1.3.4). Additionally, Pb-PM₁₀ can only be used as a surrogate for Pb-TSP if the loss of particles larger than 10 μm in diameter can be compensated by firmly establishing a quantitative adjustment factor based on concurrent Pb-TSP and Pb-PM₁₀ sampling that exhibits long-term stability over time ([Krug et al., 2017](#)). On the grounds of limited comparisons of Pb-TSP and Pb-PM₁₀ available at the time, it was judged that more data sets were needed before either national or site-specific relationships between Pb-TSP and Pb-PM₁₀ could be established. Thus, the Pb-TSP sampling method was retained as the FRM because of the importance of including Pb associated with particles larger than 10 μm in diameter and the lack of a quantitative adjustment factor. However, a Pb-PM₁₀ FRM was developed and permitted for non-source-oriented monitoring sites, where rolling 3-month average Pb-TSP concentrations were less than 0.1 $\mu\text{g}/\text{m}^3$ and Pb associated with particles larger than 10 μm was not anticipated.

Although the term TSP implies collection of airborne particles of all sizes, there is evidence that the Pb-TSP sampler could still miss particles with diameters larger than certain upper limits for efficient sampling. Although a TSP sampler collects more particulate mass than a PM₁₀ sampler, a substantial fraction of airborne PM could be missed by both samplers if the size range of Pb-associated particles extends beyond both of their practical size limits for efficient sampling. As described in the 2013 Pb ISA ([U.S. EPA, 2013](#)), in previous observations the TSP sampling efficiency of 97% for 5 μm particles dropped to 35% for 15 μm particles under the same conditions ([U.S. EPA, 2013](#); [Wedding et al., 1977](#)), and the cut-point for 50% sampling efficiency was observed to decrease from 50 μm at a 2 km/hour wind speed to 22 μm at 24 km/hour ([Rodes and Evans, 1985](#)). This suggests that at least under some circumstances resuspended Pb at the high end of the Pb particle size distribution relevant for resuspension into air might be collected with less than 50% efficiency. Insufficient data on size distributions of

airborne resuspended Pb beyond the size range efficiently collected by the Pb-TSP sampler makes it difficult to assess either the fraction of Pb potentially missed by a Pb-TSP sampler or the contribution of Pb from this size range to total airborne Pb. An additional challenge to measuring Pb over its entire PM size range is that spatial variability is greater for coarse than for fine particles. As described in the 2019 PM ISA ([U.S. EPA, 2019](#)), PM_{2.5} concentrations on an urban scale are more uniform than for PM_{10-2.5}. By extension, including a substantial amount of mass for particles larger than PM₁₀ is potentially representative over a smaller area containing a smaller population.

1.4.4. Recent Advances in Sampling and Analysis

The 2013 Pb ISA described several new developments in sampling and analysis of airborne Pb, including the addition of new FRMs and FEMs ([U.S. EPA, 2013](#)). Advances in the development of new sampling and analytical methods described here stem in part from 2008 revisions of the Pb NAAQS. Specifically, the 2008 revisions described conditions under which a Pb-PM₁₀ FRM could be used as an alternative to the original Pb-TSP FRM. The trade-off between missing Pb from Pb-TSP from upper end sampling bias and uncertainty versus the potential for missing a large fraction of airborne Pb using the Pb-PM₁₀ FRM continues to be a driving force for further research. In addition, the lower NAAQS level established by the 2008 revisions triggered a need for alternative analytical methods like ICP-MS with better performance characterization at lower concentrations. Recent publications provide essential characterization and comparisons of both old and new measurement methods. These include advanced wind-tunnel studies of the original Pb-TSP FRM (40 CFR Part 50 Appendix B) ([Vanderpool et al., 2018](#)) and other TSP samplers ([Krug et al., 2017](#)), a detailed field comparison of collocated Pb-PM₁₀ versus Pb-TSP performance ([Ward et al., 2019](#)), use of particle-size-fractionated airborne lead ([Meng et al., 2014](#)), performance evaluation and interlaboratory comparison of the recently designated ICP-MS FRM (FR 78, page 40,000) ([Harrington et al., 2014](#)), and development of relevant reference materials in a suitable concentration range for XRF and ICP-MS analysis of airborne Pb ([Yatkin et al., 2016](#)).

Following a surge of studies immediately after its development, little new work to further evaluate Pb-TSP FRM sampler performance was carried out until [Krug et al. \(2017\)](#) summarized and compared results from the previous evaluations of sampler performance conducted under various conditions, and used up-to-date methods to quantify the effects of environmental and operational factors affecting sampler performance in a controlled wind-tunnel setting using isokinetic samplers operating alongside the sampler. [Krug et al. \(2017\)](#) reported that: 1) sampling effectiveness ranged from 42% to 92% based on particle diameter, across orientations and wind speeds, an effectiveness range that is comparable to those reported in some previous studies and smaller than those reported in others; 2) sampling effectiveness is a near monotonic decreasing function of aerodynamic particle size, as predicted by sampling theory; 3) wind speed plays a significant role in sampling effectiveness; and 4) sampling effectiveness varies with sampler orientation to the wind and the variability increases with wind speed, but not to the extent observed in previous studies.

Several low-volume, portable commercial samplers have been widely referred to as TSP samplers because of their lack of internal size fractionation. Described as samplers with manufacturer-designated TSP inlets in the 2013 Pb ISA ([U.S. EPA, 2013](#)), these devices also have potential for airborne Pb sampling, but have not been as extensively evaluated for collection efficiency as a function of particle size as the Pb-TSP FRM. Some early efforts to characterize alternative low-volume TSP samplers were summarized in the 2013 Pb ISA, and the value of testing them as potential replacements for high-volume TSP sampling was discussed ([U.S. EPA, 2013](#)). This testing has now been completed by [Vanderpool et al. \(2018\)](#), who conducted a study specifically to evaluate size-selective performance of six low-volume manufacturer-designated TSP samplers at different wind speeds in a controlled wind-tunnel setting. Like the Pb-TSP FRM, sampling performance generally decreased with both particle diameter and wind speed for each of the inlets evaluated, and all sampling inlets exhibited some degree of measurement bias for larger particles and at higher wind speeds ([Vanderpool et al., 2018](#)). On average over most wind speeds, most samplers collected 75% to 95% of particulate mass expected for particle diameters ranging up to 30 μm ([Vanderpool et al., 2018](#)). However, these would still need to be evaluated more extensively before approval as a FRM or FEM and use in the NAAQS monitoring network.

Other recent research includes a detailed assessment of collocated Pb-TSP and Pb-PM₁₀ monitoring results to expand on the limited available data for understanding the relationship between Pb-TSP and Pb-PM₁₀ concentrations and to assess the suitability of a site-specific adjustment factor. Pb-TSP and Pb-PM₁₀ data were collected every sixth day for more than three years from a monitor adjacent to the Walkill secondary smelter in New York, which had been recently equipped with a wet electrostatic precipitator to reduce emissions of larger particles. Data from the two samplers were strongly correlated with an adjustment factor of 1.49, somewhat lower than previous observations for primary smelters from a small number of samples ([Ward et al., 2019](#)). [Ward et al. \(2019\)](#) confirmed that implementation of a Pb-PM₁₀ monitor at their source-oriented location would lead to underestimation of the total ambient air Pb concentration without the application of an adjustment factor relating Pb-PM₁₀ to Pb-TSP. They also suggested that development of a generic adjustment factor for all Pb monitoring locations was probably not possible because of differences in particulate Pb characteristics between different locations and source emissions. These results indicate that in addition to non-source-oriented sites where the Pb-PM₁₀ FRM is currently used, there is also potential to obtain high quality data using Pb-PM₁₀ samplers at some source-oriented sites. However, this approach also requires demonstration of a stable relationship between Pb-PM₁₀ and Pb-TSP over time, which has yet to be evaluated.

Revision of the Pb NAAQS in 2008 resulted in a NAAQS level that approached the limit of quantitation for the Pb analysis FRM based on flame atomic absorption spectroscopy (FAAS). Improvements in sensitivity, precision, throughput capability, and extraction efficiency since the development of the original FRM provided additional motivation for development of a new FRM ([Harrington et al., 2014](#)). To address these changes, a new Pb analysis FRM based on ICP-MS was introduced in 2013 (40 CFR Part 50 Appendix G). The new FRM includes two extraction methods: hot block HNO₃ extraction and ultrasonic extraction in a HNO₃/HCl mixture. The FRM was evaluated in a

multi-laboratory study that demonstrated acceptable sample stability after extraction; acceptable equivalency with the FAAS FRM; acceptable intra- and interlaboratory precision; comparability across relevant filter media; acceptable accuracy for analysis of botanical, geological, and industrial standard reference materials; and method detection limits of less than 5% of the 2008 NAAQS levels ([Harrington et al., 2014](#)). Considering these results, the ICP-MS-based FRM for Pb-TSP is considered more appropriate for the 2008 NAAQS level than the previous FAAS-based FRM for Pb-TSP because of its good performance at significantly lower ambient air Pb-TSP concentrations ([Harrington et al., 2014](#)).

Another useful recent advance for ambient air Pb measurement was the development of new reference materials suitable for XRF analysis, which is used as an FEM for Pb NAAQS monitoring as well as for quantifying Pb concentrations in the CSN and IMPROVE monitoring networks. The new reference materials are useful for laboratory audits, federal equivalency method evaluation, calibration, and quality control. They were generated by aerosol deposition over a range of Pb concentrations on PTFE filters used for ambient air sampling, and good long-term stability was demonstrated ([Yatkin et al., 2016](#)). The new reference materials fill a gap in commercially available reference materials because previously available reference materials were not similar to filter media used for collection or the PM matrix and contained Pb amounts that were not similar to typical ambient air Pb samples. [Yatkin et al. \(2016\)](#) also used the new reference materials to conduct an interlaboratory comparison of XRF analysis methods and to establish equivalence between XRF and ICP-MS Pb analysis methods.

Several advances have also recently taken place in research instrumentation to improve time resolution. Performance was evaluated for an updated version of the Semi-continuous Elements in Aerosol Sampler (SEAS-III). With this sampler, a high volume of sample is collected in a slurry for analysis by ICP-MS. A collection efficiency of $87 \pm 16\%$ was reported and collocated precision was better than 25% for 20 elements. For Pb, the collocated precision was 33% for sample concentrations averaging 4 ng/m^3 , or about 5 times the reported minimum detection limit of 0.79 ng/m^3 ([Pancras and Landis, 2011](#)). A portable XRF monitor with subdaily time resolution has also been evaluated and applied to field measurements of airborne PM ([Sofowote et al., 2019](#); [Tremper et al., 2018](#); [Furger et al., 2017](#)). Extractive electrospray ionization combined with Time-of-flight mass spectrometry has also been developed for real-time measurement of Pb in ambient air ([Giannoukos et al., 2020](#)).

1.5 Ambient Air Pb Concentration Trends

This section summarizes ambient air Pb concentrations and trends. The 3-month average ambient air Pb concentrations presented here were created using a simplified approach of the procedures detailed in 40 CFR part 50 Appendix R and, as such, cannot be directly compared with the Pb NAAQS for determination of compliance. Section 1.5.1 presents nationwide ambient air Pb concentration trends. Figure 1-11 summarizes results from numerous, mostly local studies on urban and neighborhood spatial

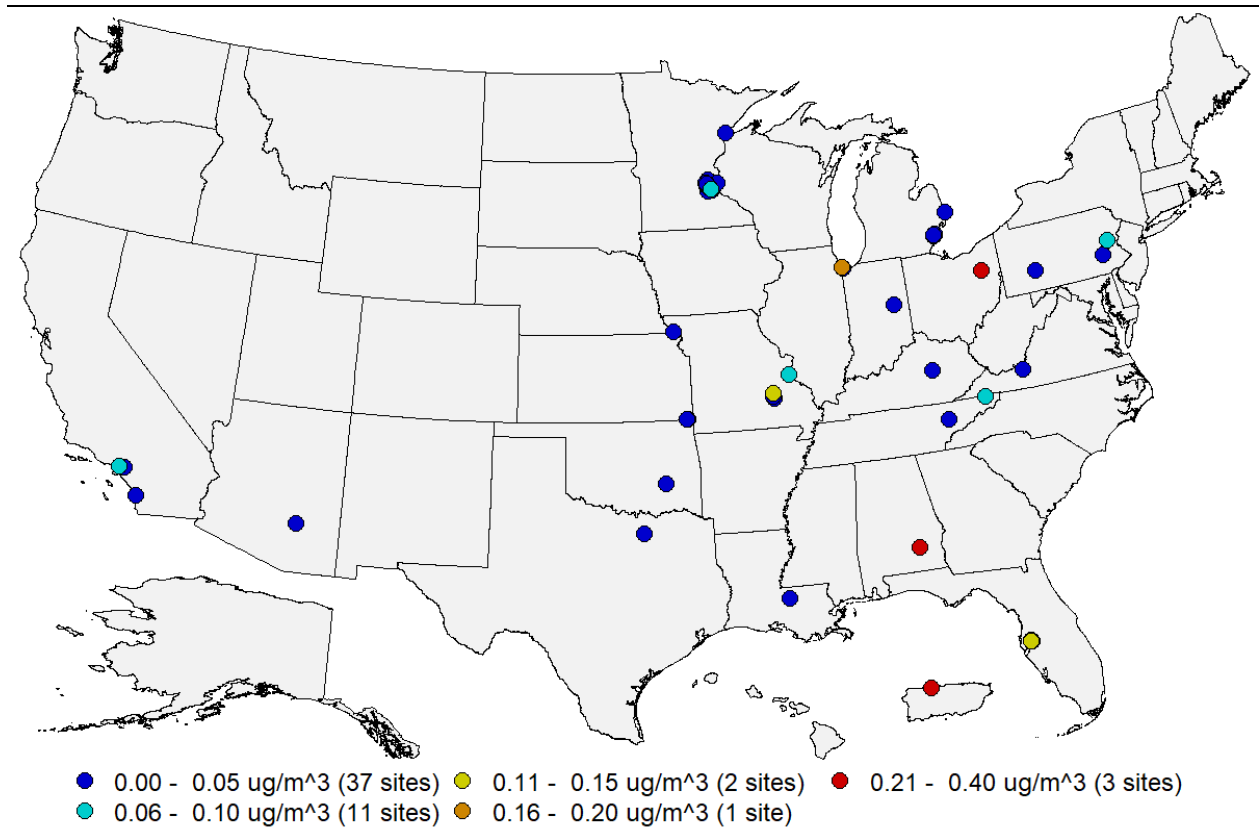
scale variability. Sections 1.5.2, 1.5.3, and 1.5.4 report the latest results on seasonal/diurnal trends, size distributions, and background concentrations of Pb in ambient air PM from diverse locations.

1.5.1. National Scale Ambient Air Concentrations and Long-Term Trends

Figure 1-8 is a national map of maximum rolling 3-month average Pb concentrations in counties with Pb-TSP monitors during the period 2020–2022 ([U.S. EPA, 2023c](#)). Elevated 3-month average Pb concentrations were observed in several U.S. locations during the period. Maximum rolling 3-month average Pb concentrations for the period 2020–2022 exceeded $0.15 \mu\text{g}/\text{m}^3$ for Canton/Stark County OH ($0.40 \mu\text{g}/\text{m}^3$), Arecibo PR ($0.35 \mu\text{g}/\text{m}^3$), Troy/Pike County AL ($0.22 \mu\text{g}/\text{m}^3$), and Hammond/Lake County IN ($0.16 \mu\text{g}/\text{m}^3$). In each of these locations, daily concentrations occasionally reached or exceeded $1 \mu\text{g}/\text{m}^3$. For example, in 2022 the daily Pb concentration reached or exceeded $1 \mu\text{g}/\text{m}^3$ for 1 day in Arecibo and Troy AL, and for 2 days in Canton OH and Hammond IN. In Iron County MO, no rolling 3-month average greater than $0.15 \mu\text{g}/\text{m}^3$ was observed during 2020–2022, but in 2022 the daily concentration exceeded $1 \mu\text{g}/\text{m}^3$ on 7 days. The 2020–2022 maximum rolling 3-month average Pb concentration was less than $0.15 \mu\text{g}/\text{m}^3$ and the daily Pb concentration was less than $1 \mu\text{g}/\text{m}^3$ at all other monitoring sites in the United States. In cases where the highest concentrations were observed or where concentrations exceeded $0.15 \mu\text{g}/\text{m}^3$ for the first time, additional actions were taken. For example, in Canton OH, where the highest maximum rolling 3-month average Pb concentration for 2020–2022 was observed, as well as in Hammond IN, where a maximum rolling 3-month average Pb concentration greater than $0.15 \mu\text{g}/\text{m}^3$ was observed for the first time during the 2020–2022 period, local sources were sent notices of violations in 2018. In Hammond IN, an area near the source was also designated as a Superfund site in 2023.

A detailed summary of Pb concentrations measured in the U.S. from monitors used for regulatory compliance (see Section 1.4.1) is provided in Table 1-3. These are compared to Pb concentrations from non-regulatory monitoring networks (see Section 1.4.1) in Table 1-4. Maps and tables like Figure 1-8 and Table 1-3 and Table 1-4 for the most recently available 3-year period will be updated annually and made available at <https://www.epa.gov/air-quality-analysis/lead-naaqs-review-analyses-and-data-sets>. Although maximum and 99th percentile concentrations in Table 1-3 and Table 1-4 exceed $0.15 \mu\text{g}/\text{m}^3$, median (p50) concentrations are under $.010 \mu\text{g}/\text{m}^3$ for all monitors, including both source and non-source-oriented monitors. These concentrations are low enough to make trends difficult to discern, especially for non-source-oriented monitors, and many of the Pb monitors installed at NCore monitoring sites (see Section 1.4) were later removed after consistent observations of Pb concentrations well below NAAQS levels. As described in Section 1.2.1, ambient air Pb measurements were also required at 17 U.S. airports with estimated Pb emissions between 0.50 and 1.0 tons Pb per year for a full year ending in December of 2013, in addition to airports already required to meet ambient air Pb monitoring requirements because of estimated Pb emissions greater 1.0 tons Pb per year. Airport Pb emissions depend on the level of piston-

aircraft activity and patterns of runway use. Maximum 3-month average Pb concentrations ranged from 0.1 to 0.33 $\mu\text{g}/\text{m}^3$ and exceeded 0.15 $\mu\text{g}/\text{m}^3$ at 2 of the 17 airports ([U.S. EPA, 2015](#)).



Source: ([U.S. EPA, 2023c](#)).

Figure 1-8 Pb maximum rolling 3-month average in $\mu\text{g}/\text{m}^3$ for the 2020–2022 period.

Table 1-3 Distribution of regulatory Pb-total suspended particle concentrations in $\mu\text{g}/\text{m}^3$ for 2020–2022

metric	quarter	N.sites	N.obs	mean	SD	min	p1	p5	p10	p25	p50	p75	p90	p95	p98	p99	max	max.site
daily	all	130	25,155	0.023	0.079	0.000	0.000	0.001	0.001	0.003	0.006	0.016	0.045	0.086	0.178	0.295	2.923	290930021
daily	1st quarter	127	6,276	0.022	0.072	0.000	0.000	0.001	0.001	0.002	0.006	0.016	0.041	0.082	0.174	0.293	2.019	290930021
daily	2nd quarter	129	6,165	0.027	0.100	0.000	0.000	0.001	0.002	0.003	0.007	0.018	0.053	0.100	0.214	0.344	2.923	290930021
daily	3rd quarter	129	6,489	0.022	0.069	0.000	0.000	0.001	0.002	0.003	0.007	0.017	0.045	0.083	0.160	0.265	2.370	391510024
daily	4th quarter	128	6,225	0.022	0.073	0.000	0.000	0.001	0.001	0.002	0.006	0.015	0.041	0.080	0.171	0.289	1.710	391510024
monthly	all	130	4,131	0.019	0.046	0.000	0.001	0.001	0.002	0.003	0.008	0.018	0.040	0.071	0.131	0.196	1.123	290930021
monthly	1st quarter	127	1,057	0.018	0.042	0.000	0.001	0.001	0.002	0.003	0.007	0.017	0.040	0.061	0.137	0.211	0.583	290930021
monthly	2nd quarter	129	1,013	0.023	0.064	0.000	0.001	0.001	0.002	0.003	0.008	0.020	0.041	0.083	0.144	0.313	1.123	290930021
monthly	3rd quarter	129	1,040	0.017	0.031	0.000	0.000	0.001	0.002	0.003	0.008	0.017	0.040	0.064	0.105	0.139	0.520	391510024
monthly	4th quarter	128	1,021	0.019	0.041	0.000	0.001	0.001	0.002	0.003	0.008	0.017	0.039	0.075	0.135	0.182	0.633	290930016
3-month	all	129	4,116	0.019	0.037	0.000	0.001	0.001	0.002	0.004	0.009	0.019	0.043	0.071	0.126	0.209	0.534	290930021
3-month	1st quarter	127	1,053	0.019	0.035	0.000	0.001	0.001	0.002	0.003	0.008	0.018	0.043	0.066	0.143	0.208	0.361	290930016
3-month	2nd quarter	126	1,003	0.022	0.049	0.000	0.001	0.001	0.002	0.004	0.009	0.020	0.044	0.074	0.199	0.275	0.534	290930021
3-month	3rd quarter	128	1,037	0.019	0.034	0.000	0.001	0.002	0.002	0.004	0.009	0.018	0.041	0.074	0.108	0.152	0.396	391510024
3-month	4th quarter	126	1,015	0.018	0.029	0.001	0.001	0.002	0.002	0.004	0.009	0.019	0.044	0.073	0.105	0.137	0.324	290930016

N.sites = number of sites; N.obs = number of observations; SD = standard deviation; min = minimum; p1, p5, p10, p25, p50, p90, p95, p98, p99 = 1st, 5th, 10th, 25th, 50th, 90th, 95th, 98th, 99th percentiles; max = maximum; max.site = AQS ID number for the monitoring site corresponding to the observation in the max column. 1st quarter = January/February/March; 2nd quarter = April/May/June; 3rd quarter = July/August/September; 4th quarter = October/November/December.

Source = ([U.S. EPA, 2023c](#)).

Table 1-4 Distribution of Pb concentrations for various types of measurements and monitoring site locations in $\mu\text{g}/\text{m}^3$ for 2020–2022

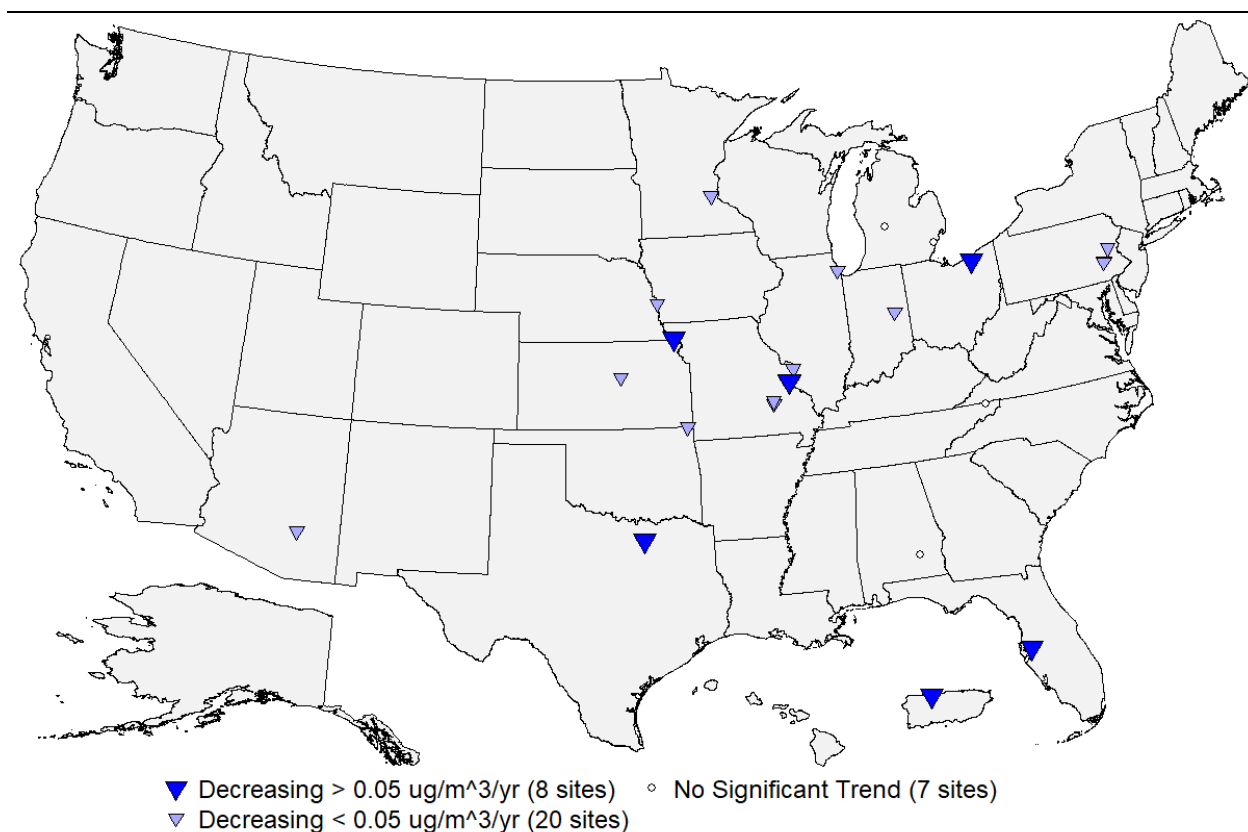
metric	measurement	network	N.sites	N.obs	mean	SD	min	p1	p5	p10	p25	p50	p75	p90	p95	p98	p99	max	max.site
daily	Pb-TSP	Source	83	16,901	0.030	0.095	0.000	0.000	0.001	0.002	0.003	0.008	0.021	0.061	0.114	0.238	0.363	2.923	290930021
daily	Pb-TSP	Non-Source	73	10,331	0.008	0.019	0.000	0.000	0.001	0.001	0.002	0.004	0.008	0.017	0.029	0.059	0.088	0.444	060250005
daily	Pb-PM10	All Sites	48	7,625	0.003	0.008	0.000	0.000	0.000	0.001	0.002	0.003	0.005	0.008	0.016	0.025	0.319	420250300	
daily	Pb-PM2.5	Urban	159	36,800	0.003	0.006	-0.012	-0.007	-0.005	-0.003	-0.001	0.002	0.005	0.009	0.012	0.016	0.019	0.360	060250005
daily	Pb-PM2.5	Rural	150	45,756	0.001	0.002	-0.009	0.000	0.000	0.000	0.000	0.000	0.001	0.001	0.002	0.004	0.007	0.099	511630003
monthly	Pb-TSP	Source	83	2,597	0.026	0.056	0.000	0.001	0.001	0.002	0.004	0.011	0.024	0.056	0.094	0.176	0.283	1.123	290930021
monthly	Pb-TSP	Non-Source	73	2,147	0.008	0.012	0.000	0.001	0.001	0.001	0.002	0.004	0.008	0.017	0.025	0.039	0.052	0.226	060250005
monthly	Pb-PM10	All Sites	48	1,547	0.003	0.004	0.000	0.000	0.001	0.001	0.001	0.002	0.003	0.005	0.008	0.015	0.022	0.078	420250300
monthly	Pb-PM2.5	Urban	159	4,947	0.003	0.004	-0.008	-0.003	-0.001	0.000	0.001	0.002	0.004	0.006	0.008	0.011	0.014	0.077	060250005
monthly	Pb-PM2.5	Rural	150	4,814	0.001	0.001	-0.001	0.000	0.000	0.000	0.000	0.000	0.001	0.001	0.002	0.004	0.006	0.015	511630003
3-month	Pb-TSP	Source	82	2,581	0.026	0.045	0.000	0.001	0.002	0.002	0.005	0.012	0.027	0.059	0.091	0.173	0.258	0.534	290930021
3-month	Pb-TSP	Non-Source	72	2,088	0.008	0.010	0.000	0.001	0.001	0.002	0.002	0.005	0.008	0.017	0.025	0.037	0.047	0.119	191550011
3-month	Pb-PM10	All Sites	48	1,445	0.003	0.003	0.000	0.001	0.001	0.001	0.001	0.002	0.003	0.006	0.008	0.012	0.019	0.046	420250300
3-month	Pb-PM2.5	Urban	151	4,618	0.003	0.002	-0.002	-0.001	0.000	0.001	0.001	0.002	0.004	0.005	0.007	0.009	0.012	0.033	060250005
3-month	Pb-PM2.5	Rural	149	4,513	0.001	0.001	0.000	0.000	0.000	0.000	0.000	0.000	0.001	0.001	0.002	0.004	0.006	0.010	010730023

N.sites = number of sites; N.obs = number of observations; SD = standard deviation; min = minimum; p1, p5, p10, p25, p50, p90, p95, p98, p99 = 1st, 5th, 10th, 25th, 50th, 90th, 95th, 98th, 99th percentiles; max = maximum; max.site = AQS ID number for the monitoring site corresponding to the observation in the max column. Source = Source-Oriented Sites; Non-Source = All Other Sites; Urban = CSN, NCore, and NATTS sites; Rural = IMPROVE sites.

Source = ([U.S. EPA, 2023c](#)).

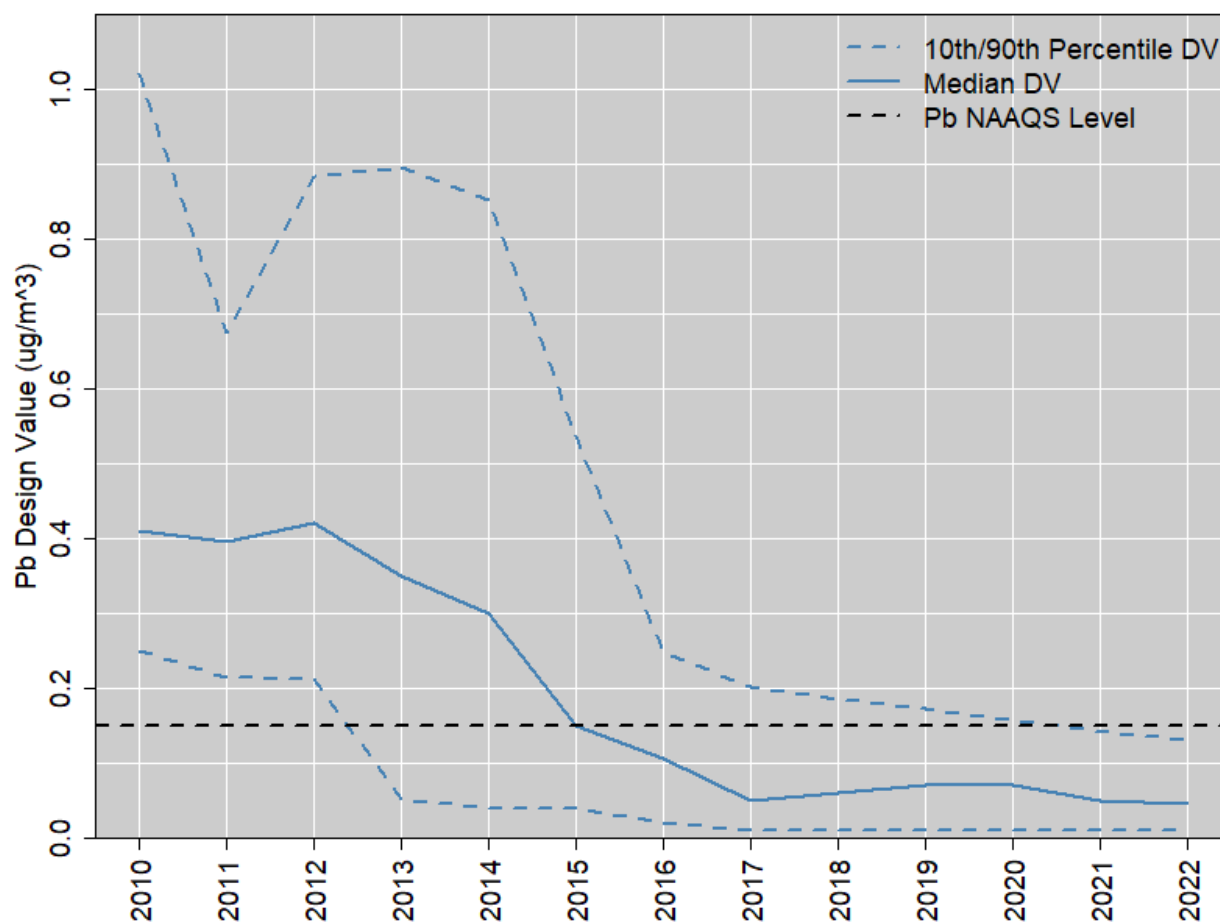
Pb concentrations in ambient air in the United States have decreased since the 1970s, mainly due to the phase-out of Pb in gasoline. In some cases, there has been a more recent period of continued decline corresponding to reductions in Pb emissions from local and regional industrial sources. A quantitative description of the trend based on monitoring network data is problematic for two reasons. First, Pb concentration reporting requirements changed in 2010 from measured Pb concentration at standard and temperature and pressure to Pb concentration measured concentration under local conditions. As a result, daily concentration and design value data from before 2010 are not directly

comparable to data from after 2010. Second, as numerous monitors have been discontinued because of declining Pb concentrations, the proportion of monitors that are located near sources has increased. Figure 1-9 is a national map and Figure 1-10 a time series plot showing how maximum rolling 3-month average Pb concentrations in counties with Pb-TSP monitors changed during the periods 2010–2012 and 2020–2022 for all monitors that operated during both periods (U.S. EPA, 2023c). Pb concentrations decreased for most monitors, in some cases by more than $0.05 \mu\text{g}/\text{m}^3$. Up-to-date graphics of annual maximum 3-month average Pb concentration trends are available in “Overview of Lead (Pb) Air Quality in the United States” (U.S. EPA, 2022a), and updated annually at <https://www.epa.gov/air-quality-analysis/lead-naaqs-review-analyses-and-data-sets>.



Source: (U.S. EPA, 2023c).

Figure 1-9 Site-level trends in maximum rolling 3-month average Pb concentrations for 2010–2022.

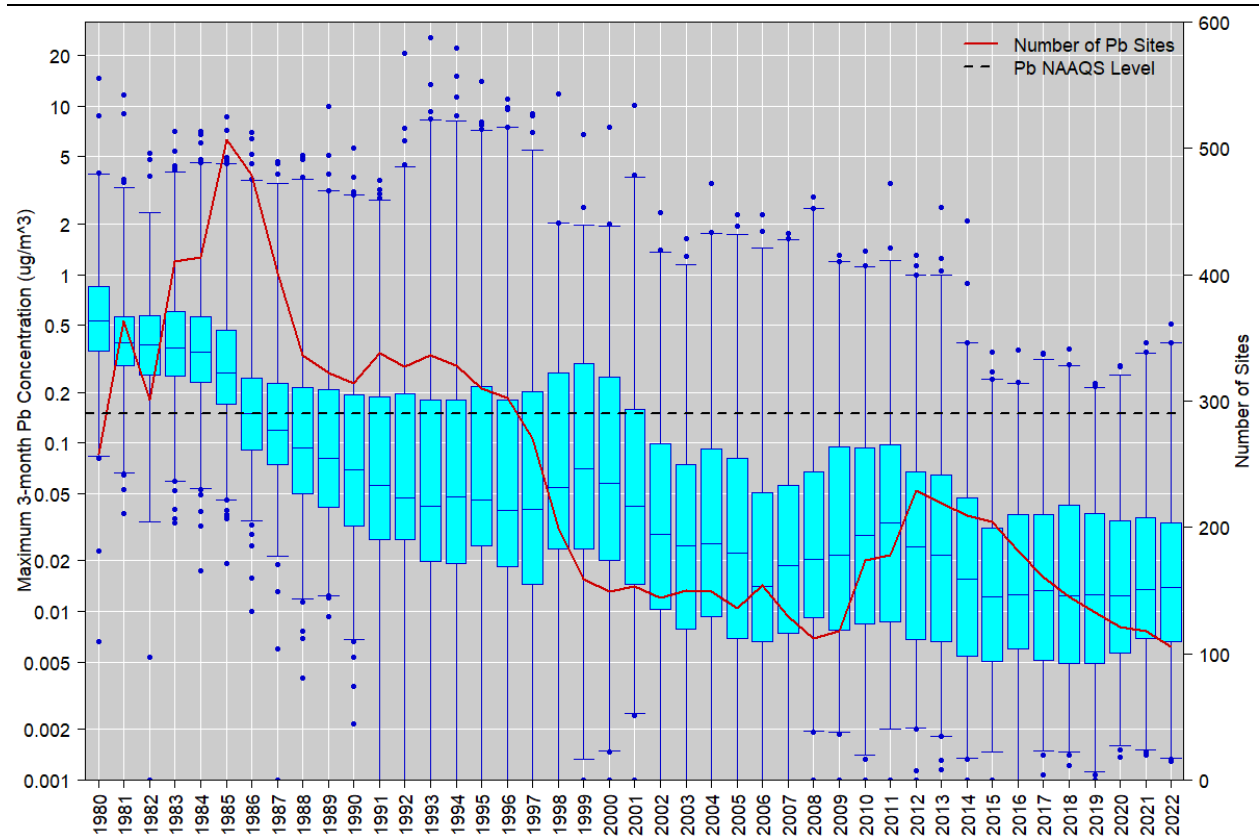


Source: (U.S. EPA, 2023c).

Figure 1-10 National trend in Pb annual maximum 3-month average concentrations in $\mu\text{g}/\text{m}^3$, 2010 to 2022.

These national trends of decreasing ambient air Pb concentrations are a continuation of longer-term trends that can be traced back to the removal of Pb from gasoline in the 1970s and later reductions of industrial use and processing of Pb in some areas and have been extensively documented in the 2013 Pb ISA (U.S. EPA, 2013) and earlier assessments. Figure 1-11 shows the extended trend of the distribution of maximum rolling 3-month average Pb concentrations across all monitors operating in each year from 1980–2022 (U.S. EPA, 2023c). Instead of limiting the data to monitors operating over the entire period as in Figure 1-9 and Figure 1-10, in Figure 1-11 the population of monitors changes with each year due to retirement of old monitors and implementation of new monitors, and reported concentrations change from standard temperature and pressure to local conditions in 2010. This overall trend will be updated annually at <https://www.epa.gov/air-quality-analysis/lead-naaqs-review-analyses-and-data-sets>. The trend is generally reflected in long-term local and regional observations of Pb concentrations in the United States and Canada for diverse locations and conditions, including monitoring sites in New York state (Buckley and Mitchell, 2011), urban Baltimore (Lin et al., 2022), Montreal (Bagur and Widory, 2020) and

Edmonton ([Bari and Kindzierski, 2016](#)), and high traffic areas of Cincinnati ([Grinshpun et al., 2014](#)). It is also reflected in long-term sediment records from numerous locations in the United States, as described in Section 1.2.3. In general, there was a steep decline in ambient air Pb concentrations in the 1970s and 1980s corresponding to the phase-out of Pb in gasoline, and in some cases a more recent period of continued decline corresponding to reductions in Pb emissions from local and regional industrial sources. In general, both AQS data and more detailed North American field studies usually support continuing national and local long-term trends of decreasing ambient air Pb concentrations.



Source: ([U.S. EPA, 2023c](#)).

Note: Boxes represent the median and interquartile range, whiskers extend to the 1st and 99th percentiles, and values outside this range are shown as circles. The red line shows the number of sites reporting regulatory data to the U.S. EPA in each year. The concentrations on the left-hand y-axis are shown on a logarithmic scale.

Figure 1-11 Distribution of annual maximum 3-month concentrations measured at regulatory Pb monitoring sites, 1980 to 2022.

1.5.2. Urban and Neighborhood Spatial Variability

The 2013 Pb ISA contains a comparison of Pb concentrations across six counties and past literature on spatial distribution of airborne Pb in urban centers illustrating intra-urban variability ([U.S. EPA, 2013](#)). These examples show that both point and non-point sources along with wind strength and direction can play a role in distributing Pb across urban areas and create spatial variability. The 2006 Pb AQCD ([U.S. EPA, 2006](#)) contains additional information on Pb transport in the environment. Ambient air Pb across urban and neighborhood scales may not be captured by national monitoring networks because of contributions from more local emission sources ([Yu et al., 2011](#)). In particular, high-emitting Pb sources may create local hotspots of elevated Pb in environmental media (Section 1.3.4). Since the publication of the 2013 Pb ISA, additional studies have been published illustrating Pb concentrations across urban centers. Recent studies on near-road spatial variability are discussed together with traffic and road sources in Section 1.2.6. More general aspects of urban and neighborhood spatial variability are described in this section.

Spatial variability of ambient air Pb across New York City has been investigated in several studies. A study of PM_{2.5} measurements across four boroughs of New York City found that spatial patterns varied by season with the highest concentrations of Pb observed during the summer (7.94 ng/m³). The sites within lower Manhattan had the highest concentrations Pb for both seasons. The authors attributed Pb concentrations in lower Manhattan to waste incineration and traffic-related sources but mention that Pb may be a poor tracer for incineration ([Peltier and Lippmann, 2011](#)). In a study of PM_{2.5} samples used in a land-use regression model from 150 street-level sites across New York City, Pb was found to have a mean value of 3.40 ng/m³ with a standard deviation of 1.52 ng/m³ and spatial coefficient of variation of 0.45. Pb was attributed most strongly to boilers burning residual oil, which was correlated with other elements consistent with emission factors data, results from combustion experiments, and characterization of residual oil fly ash ([Ito et al., 2016](#)).

Other urban centers have also been investigated for spatial variability of ambient air Pb. Particles between 2.5 and 10 μm were collected at ten sites in the greater Los Angeles area. The annual average Pb concentration did not vary greatly between the Los Angeles (1.3 ng/m³), Long Beach (1.3 ng/m³), Riverside (0.8 ng/m³), and Lancaster (0.5 ng/m³) sites. Principle component analysis revealed that Pb was present most commonly with other elements that are tracers of abrasive vehicular emissions such as Sb, Ba, Mo, Cu, Rh, and Fe ([Pakbin et al., 2011](#)). In another study spatial variations of trace elements in PM₁₀ around Paterson, NJ were investigated. Among 199 samples taken, there was an average Pb concentration of 5.37 ng/m³ with a standard deviation of 5.07 ng/m³ ([Yu et al., 2011](#)). In a study of trace metals concentrations across four sites in St. Louis the authors found that annual median air Pb concentrations in PM₁₀ ranged from 6.01 ng/m³ (S.D. = 10.10 ng/m³) at a suburban site ~10 km away from the urban core to 8.96 ng/m³ (S.D. = 16.00 ng/m³) at an urban site 3 km north of the urban core. Conditional probability function plot graphs revealed that all sites were affected by Pb from a source to the south. A local smelting plant was identified as the possible source ([Yadav and Turner, 2014](#)).

[Stevens et al. \(2014\)](#) investigated Pb-PM_{2.5} concentrations across six sites in Detroit, Michigan that were part of the Detroit Exposure and Aerosol Research Study. The authors found that Pb concentrations in PM_{2.5} were heterogeneous across sites, with the highest mean concentrations of Pb for outdoor, indoor, and personal exposures occurring at two heavily industrial areas focusing on steel manufacturing and automobiles. In another study spatial variability of PM_{2.5} metals in Massachusetts was modeled. Pb was estimated to be most heavily concentrated in areas of high roadway density in downtown Boston, similar to areas high in Al, Fe and Ti, indicating that the source of Pb was likely from road dust and soil particles. The mean value for Pb among 62 sites was 4.5 ng/m³ with a predicted coefficient of variation of 0.467 ([Requia et al., 2019](#)).

[Upadhyay et al. \(2011\)](#) investigated Pb in PM_{2.5} and PM₁₀ around three sites in Phoenix, Arizona. Two sites were located south of Phoenix Sky Harbor International Airport representing a mix of urban residential and industrial use while a control site was located east of the airport with no local point sources present. The two sites closest to the airport had the highest mean air Pb concentrations among the three sites, 4.6 ng/m³ and 4.7 ng/m³ versus 2.0 ng/m³ for Pb-PM_{2.5} and 6.3 ng/m³ and 5.6 ng/m³ versus 3.3 ng/m³ for Pb-PM₁₀, similar to other U.S. cities. Principle component analysis revealed that Pb in PM_{2.5} was grouped with elements Cu and Zn, suggesting mobile sources and Pb in PM₁₀ was grouped with As and Cr, suggesting combustion processes as a source. Pb concentrations also peaked on January 1st, suggesting the influence of local fireworks.

Researchers may also use biological organisms as bioindicators for Pb concentrations in ambient air. Pigeons were used in a New York City study. Samples of pigeons' blood revealed that the highest Pb concentrations were found in the Soho/Greenwich Village neighborhood (mean = 23.121 µg Pb/dL) and other neighborhoods of downtown Manhattan ([Cai and Calisi, 2016](#)). In another study, 26 lichen samples and four atmospheric PM measurements were collected around Middletown, Ohio. Pb concentrations in lichen samples reached a high of 151.27 ppm nearest the local steel plant but showed large heterogeneity across samples with the lowest Pb concentration at 11.30 ppm found in a lichen sample outside the general area, used as a background. Isotopic analysis of Pb species indicates that the Pb in these lichen samples are a mix of coal fly ash and traffic-related PM, with some possible contribution from steel plant emissions ([Kousehlar and Widom, 2020](#)).

[Jovan et al. \(2022\)](#) and [Kondo et al. \(2022\)](#) used local youth to collect moss samples around the industrially adjacent South Park and Georgetown neighborhoods in Seattle, WA. [Jovan et al. \(2022\)](#) found that the 79 samples collected by youth with minimal supervision had highly significant agreement (p = 0.001) to 19 expert-collected samples. Pb concentrations peaked along the industrial core separating the two communities. Among all samples there was a median value of 18.1 mg Pb/kg and minimum and maximum values of 5.9 and 110.6 mg Pb/kg respectively. [Kondo et al. \(2022\)](#) assessed the spatial predictors of metal concentrations found in 61 of the moss samples. Traffic volume and block-group level percent people of color were found to be the spatial predictors significantly associated with higher Pb concentrations in moss.

1.5.3. Seasonal and Diurnal Trends

The 2013 Pb ISA ([U.S. EPA, 2013](#)) briefly illustrates that, depending on the measurement location, there can be seasonal variation for Pb in ambient air. Seasonal variability can depend heavily on local meteorological conditions including mixing height, wind direction, precipitation, and humidity ([U.S. EPA, 2006](#)). [Levin et al. \(2020\)](#) discusses several additional factors that may contribute to local trends in ambient air Pb. As explored in Section 1.3.4, resuspension of Pb in soil can contribute Pb into air, with the highest contributions in dry summer months. Wildfires, which occur most often during the summer and into fall, can remobilize Pb deposited in the natural environment and Pb contained in man-made structures (Section 1.2.4). The 2013 Pb ISA ([U.S. EPA, 2013](#)) includes past research that has identified seasonal variation of ambient air Pb in various locations. There was no research captured by the literature screening for this document that contained information on ambient air Pb diurnal trends.

Seasonal variation of Pb concentrations has been investigated in several studies of various locations since the 2013 Pb ISA ([U.S. EPA, 2013](#)). These studies have varied in their design with some measuring trends over a period of several years while others only measure a one-year period, and some have presented averages of Pb concentrations while others have presented more detailed monthly data of Pb concentrations. Table 1-5 below details study conditions and findings of seasonal variations from these studies.

Table 1-5 Seasonal variations in Pb concentration in ambient air

Study	Location	Time Period	Seasons (Months)	Source Attribution of Pb	Findings of Seasonal Variations
(Pakbin et al., 2011)	Greater Los Angeles Area	2008–2009	All Seasons	Abrasive vehicular emissions with some contributions from soil dust and vehicular catalytic converter wear	Average ambient air Pb concentrations highest in the winter for the more urban Los Angeles (1.3 ng/m ³ in winter versus 1.0 ng/m ³ in summer) and Long Beach (1.8 ng/m ³ in winter versus 0.8 ng/m ³ in summer) sites. Average ambient air Pb concentrations were higher in the summer for the semirural Riverside (0.5 ng/m ³ in winter versus 0.8 ng/m ³ in summer) and desert Lancaster (0.2 ng/m ³ in winter versus 0.7 ng/m ³ in summer) sites.
(Peltier and Lippmann, 2011)	New York City, NY	2008	Winter (January–March), Summer (May–July)	Incineration and Biomass Burning	Highest concentrations of Pb measured were found in lower Manhattan during the summer months, suggesting a highly localized source of Pb only present during this time. Pb concentrations were near 1 ng/m ³ with hot spot concentrations, on average, at 5 and 10 ng/m ³ during the winter and summer, respectively.

Study	Location	Time Period	Seasons (Months)	Source Attribution of Pb	Findings of Seasonal Variations
(Song and Gao, 2011)	Carlstadt, NJ	2007–2008	Winter (December–February), Summer (July)	Brake wear, direct vehicle emissions, other urban sources	Higher concentrations of Pb in winter for both coarse (2.04 ng/m ³ in winter versus 1.41 ng/m ³ in summer) and fine (2.82 ng/m ³ in winter vs. 1.27 ng/m ³ in summer) despite overall aerosol mass being lower in winter than summer.
(Yu et al., 2011)	Paterson, NJ	2005–2006	All Seasons	Traffic-related and industrial emissions	Pb concentrations highest in the winter and second highest in the fall for mobile, industrial, and commercial sites. Pb concentrations were highest in winter and summer for the background site.
(Grinshpun et al., 2014)	Cincinnati, OH	2010–2011	Fall, Winter, Summer (months not specified)	Traffic-related emissions	Pb concentration was higher in the fall than winter and summer in a downtown Cincinnati location.
(Kundu and Stone, 2014)	Iowa	2009–2012	All Seasons	Diesel combustion, gasoline combustion, biomass burning, industry	There were no consistent seasonal patterns for Pb concentrations across sites measured.
(Prabhakar et al., 2014)	Southern Arizona	1988–2009	Summer (April–June), Fall (October–November), Monsoon (July–September), Winter (December–March)	Smelting operations and traffic-related emissions	Seasonal patterns were found to vary across sites, indicative of local conditions. Phoenix was impacted more heavily by traffic-related emissions, being an urban center, while Tonto National Monument was more affected by related smelting operations.
(Stevens et al., 2014)	Detroit, Michigan	2004–2007	Summer, Winter (months not specified)	Traffic-related and industrial emissions	Outdoor mean Pb concentrations were found to be slightly higher in summer for four sites. In contrast, site 5, a heavily industrial site had much a higher average Pb winter value (42 ng/m ³) than summer value (15 ng/m ³).

Study	Location	Time Period	Seasons (Months)	Source Attribution of Pb	Findings of Seasonal Variations
(Li and McDonald-Gillespie, 2020)	Tulsa, OK and Picher, OK	2010–2016	All Seasons	Atmospheric Pb blown from nearby chat piles	Picher showed strong seasonal Pb mass concentration peaks during the period of January–March and September, likely due to Pb blown from nearby chat piles. Tulsa did not show any strong seasonal variation over the measurement period.

NJ = New Jersey; NY = New York; OH = Ohio; OK = Oklahoma; Pb = lead.

1.5.4. Particle Size Characteristics

The size distribution of Pb-containing particles differs depending on source type and the collection efficiency of Pb-TSP samplers. [Cho et al. \(2011\)](#) found that most studies included in their review and published after 1986 indicated a shift in Pb particle size distribution from the fine fraction to coarse fraction with the primary mode rising to 2.5–10 µm from a previous estimation of it being below 2.5 µm. Studies used to evaluate this shift ranged from sampling near roads, near industrial sources, offshore in a lake environment, rural locations, and urban locations, within the United States and the European Union. The elimination of the combustion of tetramethyl- and tetraethyl Pb in automobiles as the dominant source of Pb-PM in the atmosphere, as indicated in Section 1.2, has led to larger Pb-containing particles on average. However, coarse particles have higher settling velocities than fine fraction or ultrafine fraction particles, resulting in measured concentrations of coarse or ultracoarse (particles greater than 10 µm diameter) particles being spatially and temporally heterogeneous, as these particles may drop out before they are collected by a TSP sampler. These topics have been discussed in previous assessments ([U.S. EPA, 2013, 2006](#)) as well as in Sections 1.3.1.1 and 1.4.3.

The literature search and screening process for the current iteration of the ISA did not find many published studies containing information on Pb particle size distributions beyond what was included in the 2013 Pb ISA ([U.S. EPA, 2013](#)). To briefly summarize information from the 2013 Pb ISA, near-roadway emissions may be the result of emissions directly from vehicular combustion or parts such as brakes or wheel weights, sources near the roadway that are not related to traffic, or traffic-induced turbulence causing resuspension of deposited Pb-bearing particles originating from wheel weights, industrial emissions, or historic sources into air. [Sabin et al. \(2006\)](#) mentioned that freeways tend to be a source of very large particles dispersed by turbulence from vehicular traffic and found a bimodal distribution of particles at a near-road site in Los Angeles with a mode in the largest size fraction sampled.

Other near-road studies in the 2013 Pb ISA ([U.S. EPA, 2013](#)) found a mix of size distributions at near-road sites subject to different meteorological conditions and measurement techniques. [Hays et al. \(2011\)](#) measured Pb in ambient air particles 20 meters north of a major interstate in Raleigh, NC. Pb was

found in $PM_{10-2.5}$, $PM_{2.5-0.1}$ and $PM_{0.1}$ size fractions, at 50 mg Pb/kg in each size fraction. Ambient air Pb concentrations appeared unimodal and normally distributed over the accumulation mode with $0.4 \pm 0.4 \text{ ng/m}^3$, $1.4 \pm 0.6 \text{ ng/m}^3$, and $0.1 \pm 0.02 \text{ ng/m}^3$ for $PM_{10-2.5}$, $PM_{2.5-0.1}$, and $PM_{0.1}$ size fractions, respectively. Daily concentration changes were heavily correlated with traffic, including Pb- PM_{10} samples highly correlated with As samples, most likely resuspended from contemporary roadway sources. [Song and Gao \(2011\)](#) collected measurements of ambient air PM using a sampling site approximately 5 meters from the New Jersey Turnpike. The Pb mass size distribution had a bimodal concentration distribution in summer and a trimodal distribution in winter with 47% and 58% of Pb mass measured in fine particles in summer and winter, respectively (Pb mass concentration values mentioned in Table 1-5). Factor analysis attributed the source of Pb to brake wear, fuel combustion, and urban pollution.

[Masri et al. \(2015\)](#) collected both fine-mode and coarse mode ambient air PM at the Harvard supersite in Boston, MA. This site is located atop a six-story building within one block of a four-lane roadway and two major highways. Trace amounts of Pb were found to be exclusively associated with fine-mode particles. Positive Matrix Factorization analysis was used to associate these particles across a wide range of possible sources from regional pollution, motor vehicles, crustal or road dust, oil combustion and wood burning.

Size distributions have also been recorded at other sites as well, reflecting spatiotemporal variability within and near cities. [Gonzalez et al. \(2021\)](#) analyzed data from five sites (Manila, Philippines; Marina, CA; Tucson, AZ; Hayden, AZ; Mt. Lemmon, AZ) that measured both submicrometer and supermicrometer particles (range 0.056–18.0 μm) which were then extracted for further analysis. Pb mass concentrations within the submicrometer and supermicrometer ranges were found to vary by site with Manila, Tucson, and Hayden (the location of an active metals smelter) having higher mass concentrations in the submicrometer range while Marina and Mt. Lemmon had higher Pb mass concentrations in the supermicrometer range. The Marina and Manila sites were also separated by fire and non-fire-influenced datasets which showed the presence of a submicrometer mode for Pb mass concentration in the fire-influenced data that was not present in the non-fire-influenced data. [Upadhyay et al. \(2011\)](#) measured ambient air PM in Phoenix, Arizona both south and east of the Phoenix Sky Harbor International Airport. The authors found Pb to be associated with both fine and coarse particles at three sites in Arizona, with $PM_{2.5}:PM_{10}$ ratios between 0.5 and 0.7 for Pb at the three sites tested, indicating that a substantial fraction of Pb was associated with both fine and coarse particles at each site. [Youn et al. \(2016\)](#) performed chemical speciation on aerosol samples collected at an active smelting site in Hayden AZ and an urban background site in Tucson AZ. The particle size distribution of Pb mass found at the active smelting site was bimodal with a large peak at 0.32 μm , and a smaller peak at 5.6 μm . The background site was trimodal with peaks at 0.1 μm , 0.32 μm , and a smaller peak at 3.2 μm . Submicrometer particles were attributed to the condensation and coagulation of smelting vapors, whereas coarse particles were attributed to fugitive dust, including from mine tailings. Ambient air Pb concentration values at the active smelting site were higher than in samples from the background site.

1.5.5. Background Concentrations

A small fraction of Pb in ambient air in the United States cannot be reduced by domestic emission controls or domestic interventions within the United States. According to the 2013 Pb ISA, natural sources of Pb to ambient air include suspension of surface soil containing natural Pb and wind erosion of natural Pb-containing rocks. Previous assessments have suggested the evidence to indicate a plausible range of natural background Pb concentration is 0.02 to 1 ng/m³ (U.S. EPA, 2013; NRC, 1980). As described in the 2013 Pb ISA (U.S. EPA, 2013), average concentrations in this range have been measured at remote monitoring sites such as Crater Lake, OR and Lassen Volcanic National Park, CA. In addition to natural sources, intercontinental transport of Asian dust could also make a substantial contribution to total atmospheric Pb, but generally less than 1 ng/m³ (U.S. EPA, 2013). The 2013 Pb ISA reviewed evidence for intercontinental transport of Pb in African dust to the Southeastern United States and described mixed results concerning whether intercontinental transport or natural sources contributed the most to atmospheric Pb. The 2013 Pb ISA concluded that estimates of background Pb concentrations in ambient air were well below current concentrations (U.S. EPA, 2013). No new studies on background Pb concentrations in the United States since the last NAAQS review were identified in our literature search and screening process.

1.6 Summary and Conclusions

Pb emissions and ambient air concentrations in the United States continue to steadily decline. Major industrial sources have either reduced their emissions or closed, resulting in the emergence of aviation gas as the dominant contemporary source. However, resuspension of soil containing Pb from legacy sources has the potential to contribute to atmospheric Pb in some locations, and high concentrations of Pb associated with wildfires have been observed. Pb from these sources continues to have potential health and ecological effects after atmospheric deposition to soil and water. A substantial fraction of airborne Pb can be associated with PM larger than 10 µm in some locations. Bias and uncertainty associated with sampling these large particles in Pb-TSP sampling are still an issue, although it has become better understood and there have been several improvements in measurement tools, including development of an ICP-MS-based FRM for Pb analysis, and introduction of reference materials for analysis on filters. Overall, there have been substantial improvements in our understanding of and research capabilities for airborne Pb.

1.7 References

- [Abraham, J; Dowling, K; Florentine, S. \(2017\)](#). Risk of post-fire metal mobilization into surface water resources: A review [Review]. *Sci Total Environ* 599-600: 1740-1755. <http://dx.doi.org/10.1016/j.scitotenv.2017.05.096>.
- [Alexakis, DE. \(2020\)](#). Suburban areas in flames: Dispersion of potentially toxic elements from burned vegetation and buildings. Estimation of the associated ecological and human health risk. *Environ Res* 183: 109153. <http://dx.doi.org/10.1016/j.envres.2020.109153>.
- [Alkhatib, E. id; Akhdhar, A; Altirad, F. \(2015\)](#). Prediction of metal remobilization from sediments under various physical/chemical conditions: Design of experiment for Cd, Co, Pb, and Zn [Abstract]. *Abstr Pap Am Chem Soc* 249: 141.
- [Alshetty, D; Shiva Nagendra, SM. \(2022\)](#). Urban characteristics and its influence on resuspension of road dust, air quality and exposure. *Air Qual Atmos Health* 15: 273-287. <http://dx.doi.org/10.1007/s11869-021-01102-x>.
- [Angel, BM; Apte, SC; Batley, GE; Raven, MD. \(2016\)](#). Lead solubility in seawater: An experimental study. *Environ Chem* 13: 489-495. <http://dx.doi.org/10.1071/EN15150>.
- [Anttila, P; Makkonen, U; Hellen, H; Kyllonen, K; Leppanen, S; Saari, H; Hakola, H. \(2008\)](#). Impact of the open biomass fires in spring and summer of 2006 on the chemical composition of background air in south-eastern Finland. *Atmos Environ* 42: 6472-6486. <http://dx.doi.org/10.1016/j.atmosenv.2008.04.020>.
- [Arnemo, JM; Andersen, O; Stokke, S; Thomas, VG; Krone, O; Pain, DJ; Mateo, R. \(2016\)](#). Health and environmental risks from lead-based ammunition: Science versus socio-politics. *Ecohealth* 13: 618-622. <http://dx.doi.org/10.1007/s10393-016-1177-x>.
- [ASTM. \(2021\)](#). ASTM D910-21: Standard specification for leaded aviation gasolines [Standard]. West Conshohocken, PA: ASTM International. <https://standards.globalspec.com/std/14392908/astm-d910-21>.
- [Atzori, G; Aru, V; Marincola, FC; Chiarantini, L; Medas, D; Sarais, G; Cabiddu, S. \(2018\)](#). Sediments distribution of trace metals in a coastal lagoon (Southern Sardinia, Mediterranean Sea): Assessment of contamination and ecological risk. *Chem Ecol* 34: 727-746. <http://dx.doi.org/10.1080/02757540.2018.1491557>.
- [Aucott, M; Caldarelli, A. \(2012\)](#). Quantity of lead released to the environment in New Jersey in the form of motor vehicle wheel weights. *Water Air Soil Pollut* 223: 1743-1752. <http://dx.doi.org/10.1007/s11270-011-0979-2>.
- [AVweb. \(2013\)](#). Shell announces unleaded 100-octane fuel (updated). Available online at <https://www.avweb.com/news/shell-announces-unleaded-100-octane-fuel-updated/> (accessed August 22, 2023).
- [Bacardit, M; Krachler, M; Camarero, L. \(2012\)](#). Whole-catchment inventories of trace metals in soils and sediments in mountain lake catchments in the Central Pyrenees: Apportioning the anthropogenic and natural contributions. *Geochim Cosmo Acta* 82: 52-67. <http://dx.doi.org/10.1016/j.gca.2010.10.030>.
- [Baek, M; Outrich, MB; Barnett, KS; Reece, J. \(2021\)](#). Neighborhood-level lead paint hazard for children under 6: A tool for proactive and equitable intervention. *Int J Environ Res Public Health* 18: 2471. <http://dx.doi.org/10.3390/ijerph18052471>.
- [Bagur, M; Widory, D. \(2020\)](#). Characterising the levels and sources of the historical metal contamination in the atmosphere of Montreal (Canada) from 1973 to 2013 by coupling chemistry and Lead and Osmium isotope ratios. *Atmos Res* 235: 104794. <http://dx.doi.org/10.1016/j.atmosres.2019.104794>.
- [Bain, DJ; Yesilonis, ID; Pouyat, RV. \(2012\)](#). Metal concentrations in urban riparian sediments along an urbanization gradient. *Biogeochemistry* 107: 67-79. <http://dx.doi.org/10.1007/s10533-010-9532-4>.
- [Balascio, NL; Kaste, JM; Meyer, MG; Renshaw, M; Smith, K; Chambers, RM. \(2019\)](#). A high-resolution mill pond record from eastern Virginia (USA) reveals the impact of past landscape changes and regional pollution history. *Anthropocene* 25: 100190. <http://dx.doi.org/10.1016/j.ancene.2019.100190>.

- [Banks, J; Ross, DJ; Keough, MJ. \(2012\).](#) Short-term (24 h) effects of mild and severe hypoxia (20% and 5% dissolved oxygen) on metal partitioning in highly contaminated estuarine sediments. *Estuar Coast Shelf Sci* 99: 121-131. <http://dx.doi.org/10.1016/j.ecss.2011.12.025>.
- [Bari, MA; Kindzierski, WB. \(2016\).](#) Eight-year (2007-2014) trends in ambient fine particulate matter (PM_{2.5}) and its chemical components in the Capital Region of Alberta, Canada. *Environ Int* 91: 122-132. <http://dx.doi.org/10.1016/j.envint.2016.02.033>.
- [Bentley, C; Junqueira, T; Dove, A; Vriens, B. \(2022\).](#) Mass-balance modeling of metal loading rates in the Great Lakes. *Environ Res* 205: 112557. <http://dx.doi.org/10.1016/j.envres.2021.112557>.
- [Bortorelli, P. \(2021\).](#) GAMI awarded long-awaited STC for unleaded 100-octane avgas. Available online at <https://www.avweb.com/aviation-news/gami-awarded-long-awaited-stc-for-unleaded-100-octane-avgas/> (accessed August 22, 2023).
- [Bezerra da Silva, YJA; Cantalice, JRB; Singh, VP; do Nascimento, CW; Piscoya, VC; Guerra, SMS. \(2015\).](#) Trace element fluxes in sediments of an environmentally impacted river from a coastal zone of Brazil. *Environ Sci Pollut Res Int* 22: 14755-14766. <http://dx.doi.org/10.1007/s11356-015-4670-9>.
- [Bińczycki, T; Weber, J; Mielnik, L; Asensio, C. \(2020\).](#) Lead isotope ratios in Podzol profiles as a tracer of pollution source in the subalpine zone of the Karkonosze National Park, Sudety Mts (south-western Poland). *Catena* 189: 104476. <http://dx.doi.org/10.1016/j.catena.2020.104476>.
- [Bing, H; Wu, Y; Zhou, J; Ming, L; Sun, S; Li, X. \(2014\).](#) Atmospheric deposition of lead in remote high mountain of eastern Tibetan Plateau, China. *Atmos Environ* 99: 425-435. <http://dx.doi.org/10.1016/j.atmosenv.2014.10.014>.
- [Boaggio, K; LeDuc, SD; Rice, RB; Duffney, P; Foley, K; Holder, A; McDow, S; Weaver, CP. \(2022\).](#) Beyond particulate matter mass: Heightened levels of lead and other pollutants associated with destructive fire events in California. Manuscript submitted for publication.
- [Bowers, T; Drivas, P; Mattuck, R. \(2014\).](#) Prediction of soil lead recontamination trends with decreasing atmospheric deposition. *Soil Sediment Contam* 23: 691-702. <http://dx.doi.org/10.1080/15320383.2013.857294>.
- [Bray, CD; Battye, W; Uttamang, P; Pillai, P; Aneja, VP. \(2017\).](#) Characterization of particulate matter (PM_{2.5} and PM₁₀) relating to a coal power plant in the boroughs of Springdale and Cheswick, PA. *Atmosphere (Basel)* 8: 186. <http://dx.doi.org/10.3390/atmos8100186>.
- [Bringmark, L; Lundin, L; Augustaitis, A; Beudert, B; Dieffenbach-Fries, H; Dirnböck, T; Grabner, MT; Hutchins, M; Kram, P; Lyulko, I; Ruoho-Airola, T; Vana, M. \(2013\).](#) Trace metal budgets for forested catchments in Europe: Pb, Cd, Hg, Cu and Zn. *Water Air Soil Pollut* 224: 1502. <http://dx.doi.org/10.1007/s11270-013-1502-8>.
- [Britter, RE; Hanna, SR. \(2003\).](#) Flow and dispersion in urban areas. *Annu Rev Fluid Mech* 35: 469-496. <http://dx.doi.org/10.1146/annurev.fluid.35.101101.161147>.
- [Broder, T; Biester, H. \(2017\).](#) Linking major and trace element concentrations in a headwater stream to DOC release and hydrologic conditions in a bog and peaty riparian zone. *Appl Geochem* 87: 188-201. <http://dx.doi.org/10.1016/j.apgeochem.2017.11.003>.
- [Brown, MJ; Raymond, J; Homa, D; Kennedy, C; Sinks, T. \(2011\).](#) Association between children's blood lead levels, lead service lines, and water disinfection, Washington, DC, 1998-2006. *Environ Res* 111: 67-74. <http://dx.doi.org/10.1016/j.envres.2010.10.003>.
- [Brown, SL; Chaney, RL; Hettiarachchi, GM. \(2016\).](#) Lead in urban soils: A real or perceived concern for urban agriculture? [Review]. *J Environ Qual* 45: 26-36. <http://dx.doi.org/10.2134/jeq2015.07.0376>.
- [Brugam, RB; Ketterer, M; Maines, L; Lin, ZQ; Retzlaff, WA. \(2012\).](#) Application of a simple binary mixing model to the reconstruction of lead pollution sources in two Mississippi River floodplain lakes. *J Paleolimnol* 47: 101-112. <http://dx.doi.org/10.1007/s10933-011-9562-5>.
- [Buckley, SM; Mitchell, MJ. \(2011\).](#) Improvements in urban air quality: Case studies from New York State, USA. *Water Air Soil Pollut* 214: 93-106. <http://dx.doi.org/10.1007/s11270-010-0407-z>.

- [Burt, R; Hernandez, L; Shaw, R; Tunstead, R; Ferguson, R; Peaslee, S.](#) (2014). Trace element concentration and speciation in selected urban soils in New York City. *Environ Monit Assess* 186: 195-215. <http://dx.doi.org/10.1007/s10661-013-3366-1>.
- [Burton, CA; Hoefen, TM; Plumlee, GS; Baumberger, KL; Backlin, AR; Gallegos, E; Fisher, RN.](#) (2016). Trace elements in stormflow, ash, and burned soil following the 2009 Station Fire in southern California. *PLoS ONE* 11: e0153372. <http://dx.doi.org/10.1371/journal.pone.0153372>.
- [Burton, GA, Jr; Hudson, ML; Huntsman, P; Carbonaro, RF; Rader, KJ; Waeterschoot, H; Baken, S; Garman, E.](#) (2019). Weight-of-evidence approach for assessing removal of metals from the water column for chronic environmental hazard classification [Review]. *Environ Toxicol Chem* 38: 1839-1849. <http://dx.doi.org/10.1002/etc.4470>.
- [Caballero-Gómez, H; White, HK; O'Shea, MJ; Pepino, R; Howarth, M; Gieré, R.](#) (2022). Spatial analysis and lead-risk assessment of Philadelphia, USA. *Geohealth* 6: e2021GH000519. <http://dx.doi.org/10.1029/2021GH000519>.
- [Cabaniss, SE.](#) (2011). Forward modeling of metal complexation by NOM: II. Prediction of binding site properties. *Environ Sci Technol* 45: 3202-3209. <http://dx.doi.org/10.1021/es102408w>.
- [Cahill, TA; Barnes, DE; Lawton, JA; Miller, R; Spada, N; Willis, RD; Kimbrough, S.](#) (2016). Transition metals in coarse, fine, very fine and ultra-fine particles from an interstate highway transect near Detroit. *Atmos Environ* 145: 158-175. <http://dx.doi.org/10.1016/j.atmosenv.2016.09.023>.
- [Cai, F; Calisi, RM.](#) (2016). Seasons and neighborhoods of high lead toxicity in New York City: The feral pigeon as a bioindicator. *Chemosphere* 161: 274-279. <http://dx.doi.org/10.1016/j.chemosphere.2016.07.002>.
- [Campos, I; Abrantes, N; Keizer, JJ; Vale, C; Pereira, P.](#) (2016). Major and trace elements in soils and ashes of eucalypt and pine forest plantations in Portugal following a wildfire. *Sci Total Environ* 572: 1363-1376. <http://dx.doi.org/10.1016/j.scitotenv.2016.01.190>.
- [Cánovas, CR; Basallote, MD; Borrego, P; Millán-Becerro, R; Pérez-López, R.](#) (2020). Metal partitioning and speciation in a mining-impacted estuary by traditional and passive sampling methods. *Sci Total Environ* 722: 137905. <http://dx.doi.org/10.1016/j.scitotenv.2020.137905>.
- [Carling, GT; Richards, DC; Hoven, H; Miller, T; Fernandez, DP; Rudd, A; Pazmino, E; Johnson, WP.](#) (2013). Relationships of surface water, pore water, and sediment chemistry in wetlands adjacent to Great Salt Lake, Utah, and potential impacts on plant community health. *Sci Total Environ* 443: 798-811. <http://dx.doi.org/10.1016/j.scitotenv.2012.11.063>.
- [Carr, E; Lee, M; Marin, K; Holder, C; Hoyer, M; Pedde, M; Cook, R; Touma, J.](#) (2011). Development and evaluation of an air quality modeling approach to assess near-field impacts of lead emissions from piston-engine aircraft operating on leaded aviation gasoline. *Atmos Environ* 45: 5795-5804. <http://dx.doi.org/10.1016/j.atmosenv.2011.07.017>.
- [Chaffee, MA; King, HD.](#) (2014). Geochemistry of soil contamination from lead smelters near Eureka Nevada. *Geochemistry: Exploration, Environment, Analysis* 14: 71-84. <http://dx.doi.org/10.1144/geochem2011-104>.
- [Chen, M; Ding, S; Lin, J; Fu, Z; Tang, W; Fan, X; Gong, M; Wang, Y.](#) (2019). Seasonal changes of lead mobility in sediments in algae- and macrophyte-dominated zones of the lake. *Sci Total Environ* 660: 484-492. <http://dx.doi.org/10.1016/j.scitotenv.2019.01.010>.
- [Chen, WB; Guéguen, C; Smith, DS; Galceran, J; Puy, J; Companys, E.](#) (2018). Metal (Pb, Cd, and Zn) Binding to Diverse Organic Matter Samples and Implications for Speciation Modeling. *Environ Sci Technol* 52: 4163-4172. <http://dx.doi.org/10.1021/acs.est.7b05302>.
- [Cheng, Z; Lee, L; Dayan, S; Grinshtein, M; Shaw, R.](#) (2011). Speciation of heavy metals in garden soils: Evidences from selective and sequential chemical leaching. *Journal of Soils and Sediments* 11: 628-638. <http://dx.doi.org/10.1007/s11368-011-0351-6>.
- [Child, AW; Moore, BC; Vervoort, JD; Beutel, MW.](#) (2018). Tracking long-distance atmospheric deposition of trace metal emissions from smelters in the upper Columbia River valley using Pb isotope analysis of lake sediments. *Environ Sci Pollut Res Int* 25: 5501-5513. <http://dx.doi.org/10.1007/s11356-017-0914-1>.

- [Cho, SH; Richmond-Bryant, J; Thornburg, J; Portzer, J; Vanderpool, R; Cavender, K; Rice, J. \(2011\). A literature review of concentrations and size distributions of ambient airborne Pb-containing particulate matter. Atmos Environ 45: 5005-5015. <http://dx.doi.org/10.1016/j.atmosenv.2011.05.009>.](#)
- [Chou, PI; Ng, DQ; Li, IC; Lin, YP. \(2018\). Effects of dissolved oxygen, pH, salinity and humic acid on the release of metal ions from PbS, CuS and ZnS during a simulated storm event. Sci Total Environ 624: 1401-1410. <http://dx.doi.org/10.1016/j.scitotenv.2017.12.221>.](#)
- [Chrastný, V; Vaněk, A; Komárek, M; Farkaš, J; Drábek, O; Vokurková, P; Němcová, J. \(2012a\). Incubation of air-pollution-control residues from secondary Pb smelter in deciduous and coniferous organic soil horizons: Leachability of lead, cadmium and zinc. J Hazard Mater 209-210: 40-47. <http://dx.doi.org/10.1016/j.jhazmat.2011.12.072>.](#)
- [Chrastný, V; Vaněk, A; Teper, L; Cabala, J; Procházka, J; Pechar, L; Drahota, P; Penížek, V; Komárek, M; Novák, M. \(2012b\). Geochemical position of Pb, Zn and Cd in soils near the Olkusz mine/smelter, South Poland: effects of land use, type of contamination and distance from pollution source. Environ Monit Assess 184: 2517-2536. <http://dx.doi.org/10.1007/s10661-011-2135-2>.](#)
- [Clarke, LW; Jenerette, GD; Bain, DJ. \(2015\). Urban legacies and soil management affect the concentration and speciation of trace metals in Los Angeles community garden soils. Environ Pollut 197: 1-12. <http://dx.doi.org/10.1016/j.envpol.2014.11.015>.](#)
- [Coxon, TM; Odhiambo, BK; Giancarlo, LC. \(2016\). The impact of urban expansion and agricultural legacies on trace metal accumulation in fluvial and lacustrine sediments of the lower Chesapeake Bay basin, USA. Sci Total Environ 568: 402-414. <http://dx.doi.org/10.1016/j.scitotenv.2016.06.022>.](#)
- [Csavina, J; Landázuri, A; Wonaschütz, A; Rine, K; Rheinheimer, P; Barbaris, B; Conant, W; Sáez, AE; Betterton, EA. \(2011\). Metal and metalloid contaminants in atmospheric aerosols from mining operations. Water Air Soil Pollut 221: 145-157. <http://dx.doi.org/10.1007/s11270-011-0777-x>.](#)
- [Csavina, J; Taylor, MP; Félix, O; Rine, KP; Sáez, AE; Betterton, EA. \(2014\). Size-resolved dust and aerosol contaminants associated with copper and lead smelting emissions: Implications for emission management and human health. Sci Total Environ 493: 750-756. <http://dx.doi.org/10.1016/j.scitotenv.2014.06.031>.](#)
- [Cullen, JT; McAlister, J. \(2017\). Biogeochemistry of lead. Its release to the environment and chemical speciation. In A Sigel; H Sigel; RKO Sigel \(Eds.\), Lead: Its effects on environment and health \(pp. 21-48\). Berlin, Germany: Walter de Gruyter. <http://dx.doi.org/10.1515/9783110434330-002>.](#)
- [Datko-Williams, L; Wilkie, A; Richmond-Bryant, J. \(2014\). Analysis of U.S. soil lead \(Pb\) studies from 1970 to 2012 \[Review\]. Sci Total Environ 468-469: 854-863. <http://dx.doi.org/10.1016/j.scitotenv.2013.08.089>.](#)
- [Deocampo, DM; Reed, PJ; Kalenuik, AP. \(2012\). Road dust lead \(Pb\) in two neighborhoods of urban Atlanta, \(GA, USA\). Int J Environ Res Public Health 9: 2020-2030. <http://dx.doi.org/10.3390/ijerph9062020>.](#)
- [Diawara, MM; Shrestha, S; Carsella, J, im; Farmer, S. \(2018\). Smelting remains a public health risk nearly a century later: A case study in Pueblo, Colorado, USA. Int J Environ Res Public Health 15: 932. <http://dx.doi.org/10.3390/ijerph15050932>.](#)
- [Dietrich, M; O'Shea, MJ; Gieré, R; Krekeler, MPS. \(2022\). Road sediment, an underutilized material in environmental science research: A review of perspectives on United States studies with international context \[Review\]. J Hazard Mater 432: 128604. <http://dx.doi.org/10.1016/j.jhazmat.2022.128604>.](#)
- [Dong, Z; Lewis, CG; Burgess, RM; Coull, B; Shine, JP. \(2016\). Statistical evaluation of biogeochemical variables affecting spatiotemporal distributions of multiple free metal ion concentrations in an urban estuary. Chemosphere 150: 202-210. <http://dx.doi.org/10.1016/j.chemosphere.2016.02.020>.](#)
- [Drozdova, OY; Aleshina, AR; Tikhonov, VV; Lapitskiy, SA; Pokrovsky, OS. \(2020\). Coagulation of organo-mineral colloids and formation of low molecular weight organic and metal complexes in boreal humic river water under UV-irradiation. Chemosphere 250: 126216. <http://dx.doi.org/10.1016/j.chemosphere.2020.126216>.](#)

- [Drozdova, OY; Shirokova, LS; Carrein, A; Lapitskiy, SA; Pokrovsky, OS. \(2015\). Impact of heterotrophic bacterium *Pseudomonas aureofaciens* on the release of major and trace elements from podzol soil into aqueous solution. *Chem Geol* 410: 174-187. <http://dx.doi.org/10.1016/j.chemgeo.2015.06.010>.](#)
- [Du, H; Chen, W; Cai, P; Rong, X; Feng, X; Huang, Q. \(2016\). Competitive adsorption of Pb and Cd on bacteria-montmorillonite composite. *Environ Pollut* 218: 168-175. <http://dx.doi.org/10.1016/j.envpol.2016.08.022>.](#)
- [Du, L; Dyck, M; Shoty, W; He, H; Lv, J; Cuss, CW; Bie, J. \(2020\). Lead immobilization processes in soils subjected to freeze-thaw cycles. *Ecotoxicol Environ Saf* 192: 110288. <http://dx.doi.org/10.1016/j.ecoenv.2020.110288>.](#)
- [Dunnington, DW; Roberts, S; Norton, SA; Spooner, IS; Kurek, J; Kirk, JL; Muir, DCG; White, CE; Gagnon, GA. \(2020\). The distribution and transport of lead over two centuries as recorded by lake sediments from northeastern North America. *Sci Total Environ* 737: 140212. <http://dx.doi.org/10.1016/j.scitotenv.2020.140212>.](#)
- [Duren, SM; McKnight, DM. \(2013\). Wetland photochemistry as a major control on the transport of metals in an acid mine drainage impacted watershed. In A Brown; C Wolkersdorfer; L Figueroa \(Eds.\), *Reliable mine water technology*, vol II \(pp. 973-976\). Denver, CO: Publication Printers. \[https://www.imwa.info/docs/imwa_2013/IMWA2013_Duren_544.pdf\]\(https://www.imwa.info/docs/imwa_2013/IMWA2013_Duren_544.pdf\).](#)
- [Duval, BD; Cadol, D; Martin, J; Frey, B; Timmons, S. \(2020\). Effects of the Gold King Mine spill on metal cycling through river and riparian biota. *Wetlands* 40: 1033-1046. <http://dx.doi.org/10.1007/s13157-019-01258-4>.](#)
- [Ebert, M; Worrigen, A; Benker, N; Mertes, S; Weingartner, E; Weinbruch, S. \(2011\). Chemical composition and mixing-state of ice residuals sampled within mixed phase clouds. *Atmos Chem Phys* 11: 2805-2816. <http://dx.doi.org/10.5194/acp-11-2805-2011>.](#)
- [Ebling, AM; Landing, WM. \(2015\). Sampling and analysis of the sea surface microlayer for dissolved and particulate trace elements. *Mar Chem* 177: 134-142. <http://dx.doi.org/10.1016/j.marchem.2015.03.012>.](#)
- [Edmonds, M; Mason, E; Hogg, O. \(2022\). Volcanic outgassing of volatile trace metals. *Annu Rev Earth Planet Sci* 50: 79-98. <http://dx.doi.org/10.1146/annurev-earth-070921-062047>.](#)
- [Edwards, A; Johnson, E; Coor, JL; Jagoe, CH; Sachi-Kocher, A; Kenney, WF. \(2016\). Historical record of atmospheric deposition of metals and \$\delta^{15}N\$ in an ombrotrophic karst sinkhole fen, South Carolina, USA. *Journal of Cave and Karst Studies* 78: 85-93. <http://dx.doi.org/10.4311/2014ES0109>.](#)
- [Egendorf, SP; Spliethoff, HM; Shayler, HA; Russell-Anelli, J; Cheng, Z; Minsky, AH; King, T; McBride, MB. \(2021\). Soil lead \(Pb\) and urban grown lettuce: Sources, processes, and implications for gardener best management practices. *J Environ Manage* 286: 112211. <http://dx.doi.org/10.1016/j.jenvman.2021.112211>.](#)
- [Encinar, JR; Moldovan, M. \(2005\). Lead. In P Worsfold; A Townshend; C Poole \(Eds.\), *Encyclopedia of analytical science* \(2nd ed., pp. 56-63\). Amsterdam, Netherlands: Elsevier. <http://dx.doi.org/10.1016/B0-12-369397-7/00761-5>.](#)
- [Engel-Di Mauro, S. \(2021\). Atmospheric sources of trace element contamination in cultivated urban areas: A review. *J Environ Qual* 50: 38-48. <http://dx.doi.org/10.1002/jeq2.20078>.](#)
- [Ericson, B; Landrigan, P; Taylor, MP; Frostad, J; Caravanos, J; Keith, J; Fuller, R. \(2017\). The global burden of lead toxicity attributable to informal used lead-acid battery sites. *Ann Glob Health* 82: 686-699. <http://dx.doi.org/10.1016/j.aogh.2016.10.015>.](#)
- [Escobar, J; Whitmore, TJ; Kamenov, GD; Riedinger-Whitmore, MA. \(2013\). Isotope record of anthropogenic lead pollution in lake sediments of Florida, USA. *J Paleolimnol* 49: 237-252. <http://dx.doi.org/10.1007/s10933-012-9671-9>.](#)
- [Ettler, V. \(2016\). Soil contamination near non-ferrous metal smelters: A review. *Appl Geochem* 64: 56-74. <http://dx.doi.org/10.1016/j.apgeochem.2015.09.020>.](#)
- [Ettler, V; Mihaljevič, M; Sebek, O; Matys Grygar, T; Klementová, M. \(2012\). Experimental in situ transformation of Pb smelter fly ash in acidic soils. *Environ Sci Technol* 46: 10539-10548. <http://dx.doi.org/10.1021/es301474v>.](#)

- [Evangelista, H; Castagna, A; Correia, A; Potocki, M; Aquino, F; Alencar, A; Mayewski, P; Kurbatov, A; Jaña, R; Nogueira, J; Licinio, M; Alves, E; Simões, JC.](#) (2022). The 1991 explosive Hudson volcanic eruption as a geochronological marker for the Northern Antarctic Peninsula. *An Acad Bras Cienc* 94(Suppl. 1): e20210810. <http://dx.doi.org/10.1590/0001-376520220210810>.
- [FAA.](#) (2020). FAA aerospace forecast: Fiscal years 2020-2040. (TC20-0011). Washington, DC. https://www.faa.gov/data_research/aviation/aerospace_forecasts/media/FY2020-40_faa_aerospace_forecast.pdf.
- [Farahani, VJ; Soleimanian, E; Pirhadi, M; Sioutas, C.](#) (2021). Long-term trends in concentrations and sources of PM_{2.5}-bound metals and elements in central Los Angeles. *Atmos Environ* 253: 118361. <http://dx.doi.org/10.1016/j.atmosenv.2021.118361>.
- [FDA.](#) (2022). Total diet study report: Fiscal years 2018-2020 elements data. Washington, DC. <https://www.fda.gov/food/fda-total-diet-study-tds/fda-total-diet-study-tds-results>.
- [Feinberg, SN; Heiken, JG; Valdez, MP; Lyons, JM; Turner, JR.](#) (2016). Modeling of lead concentrations and hot spots at general aviation airports. *Trans Res Rec* 2569: 80-87. <http://dx.doi.org/10.3141/2569-09>.
- [Feinberg, SN; Turner, JR.](#) (2013). Dispersion modeling of lead emissions from piston engine aircraft at general aviation facilities. *Trans Res Rec* 2325: 34-42. <http://dx.doi.org/10.3141/2325-04>.
- [Félix, OI; Csavina, J; Field, J; Rine, KP; Sáez, AE; Betterton, EA.](#) (2015). Use of lead isotopes to identify sources of metal and metalloid contaminants in atmospheric aerosol from mining operations. *Chemosphere* 122: 219-226. <http://dx.doi.org/10.1016/j.chemosphere.2014.11.057>.
- [Feng, C; Guo, X; Yin, S; Tian, C; Li, Y; Shen, Z.](#) (2017). Heavy metal partitioning of suspended particulate matter-water and sediment-water in the Yangtze Estuary. *Chemosphere* 185: 717-725. <http://dx.doi.org/10.1016/j.chemosphere.2017.07.075>.
- [Fitzstevens, MG; Sharp, RM; Brabander, DJ.](#) (2017). Biogeochemical characterization of municipal compost to support urban agriculture and limit childhood lead exposure from resuspended urban soils. *Elementa: Science of the Anthropocene* 5: 51. <http://dx.doi.org/10.1525/elementa.238>.
- [Fortuna, L; Incerti, G; Da Re, D; Mazzilis, D; Tretiach, M.](#) (2020). Validation of particulate dispersion models by native lichens as point receptors: A case study from NE Italy. *Environ Sci Pollut Res Int* 27: 13384-13395. <http://dx.doi.org/10.1007/s11356-020-07859-5>.
- [Frank, JJ; Poulakos, AG; Tornero-Velez, R; Xue, J.](#) (2019). Systematic review and meta-analyses of lead (Pb) concentrations in environmental media (soil, dust, water, food, and air) reported in the United States from 1996 to 2016 [Review]. *Sci Total Environ* 694: 133489. <http://dx.doi.org/10.1016/j.scitotenv.2019.07.295>.
- [Frederick, L; Johnson, WP; Cerling, T; Fernandez, D; VanDerslice, J.](#) (2019). Source identification of particulate metals/metalloids deposited in the San Juan river delta of Lake Powell, USA. *Water Air Soil Pollut* 230: 128. <http://dx.doi.org/10.1007/s11270-019-4176-z>.
- [Furger, M; Minguillon, MC; Yadav, V; Slowik, JG; Hüglin, C; Fröhlich, R; Petterson, K; Baltensperger, U; Prévôt, ASH.](#) (2017). Elemental composition of ambient aerosols measured with high temporal resolution using an online XRF spectrometer. *Atmos Meas Tech* 10: 2061-2076. <http://dx.doi.org/10.5194/amt-10-2061-2017>.
- [Gallagher, CL; Oettgen, HL; Brabander, DJ.](#) (2020). Beyond community gardens: A participatory research study evaluating nutrient and lead profiles of urban harvested fruit. *Elementa: Science of the Anthropocene* 8: 004. <http://dx.doi.org/10.1525/elementa.2020.004>.
- [Gawel, JE; Asplund, JA; Burdick, S; Miller, M; Peterson, SM; Tollefson, A; Ziegler, K.](#) (2014). Arsenic and lead distribution and mobility in lake sediments in the south-central Puget Sound watershed: The long-term impact of a metal smelter in Ruston, Washington, USA. *Sci Total Environ* 472: 530-537. <http://dx.doi.org/10.1016/j.scitotenv.2013.11.004>.
- [Giannoukos, S; Lee, CP; Tarik, M; Ludwig, C; Biollaz, S; Lamkaddam, H; Baltensperger, U; Prevot, ASH; Slowik, J.](#) (2020). Real-time detection of aerosol metals using online extractive electrospray ionization mass spectrometry. *Anal Chem* 92: 1316-1325. <http://dx.doi.org/10.1021/acs.analchem.9b04480>.

- Gillette, DA; Blifford, IH, Jr; Fryrear, DW. (1974). The influence of wind velocity on the size distributions of aerosols generated by the wind erosion of soils. *J Geophys Res* 79: 4068-4075. <http://dx.doi.org/10.1029/JC079i027p04068>.
- Gillings, MM; Fry, KL; Morrison, AL; Taylor, MP. (2022). Spatial distribution and composition of mine dispersed trace metals in residential soil and house dust: Implications for exposure assessment and human health. *Environ Pollut* 293: 118462. <http://dx.doi.org/10.1016/j.envpol.2021.118462>.
- Gingerich, DB; Zhao, Y; Mauter, MS. (2019). Environmentally significant shifts in trace element emissions from coal plants complying with the 1990 Clean Air Act Amendments. *Energy Policy* 132: 1206-1215. <http://dx.doi.org/10.1016/j.enpol.2019.07.003>.
- Golobokova, L; Khodzher, T; Khuriganova, O; Marinayte, I; Onishchuk, N; Rusanova, P; Potemkin, V. (2020). Variability of chemical properties of the atmospheric aerosol above Lake Baikal during large wildfires in Siberia. *Atmosphere (Basel)* 11: 1230. <http://dx.doi.org/10.3390/atmos11111230>.
- Gonzalez-Maddux, C; Marcotte, A; Upadhyay, N; Herckes, P; Williams, Y; Haxel, G; Robinson, M. (2014). Elemental composition of PM_{2.5} in Shiprock, New Mexico, a rural community located near coal-burning power plants and abandoned uranium mine tailings sites. *Atmos Pollut Res* 5: 511-519. <http://dx.doi.org/10.5094/APR.2014.060>.
- Gonzalez, ME; Stahl, C; Cruz, MT; Bañaga, PA; Betito, G; Braun, RA; Aghdam, MA; Cambaliza, MO; Lorenzo, GR; MacDonald, AB; Simpas, JB; Csavina, J; Sáez, AE; Betterton, E; Sorooshian, A. (2021). Contrasting the size-resolved nature of particulate arsenic, cadmium, and lead among diverse regions. *Atmos Pollut Res* 12: 352-361. <http://dx.doi.org/10.1016/j.apr.2021.01.002>.
- Gormley-Gallagher, AM; Douglas, RW; Rippey, B. (2016). Metal to phosphorus stoichiometries for freshwater phytoplankton in three remote lakes. *PeerJ* 4: e2749. <http://dx.doi.org/10.7717/peerj.2749>.
- Gottesfeld, P; Were, FH; Adogame, L; Gharbi, S; San, D; Nota, MM; Kuepou, G. (2018). Soil contamination from lead battery manufacturing and recycling in seven African countries. *Environ Res* 161: 609-614. <http://dx.doi.org/10.1016/j.envres.2017.11.055>.
- Graney, JR; Edgerton, ES; Landis, MS. (2019). Using Pb isotope ratios of particulate matter and epiphytic lichens from the Athabasca Oil Sands Region in Alberta, Canada to quantify local, regional, and global Pb source contributions. *Sci Total Environ* 654: 1293-1304. <http://dx.doi.org/10.1016/j.scitotenv.2018.11.047>.
- Gray, JE; Pribil, MJ; Van Metre, PC; Borrok, DM; Thapalia, A. (2013). Identification of contamination in a lake sediment core using Hg and Pb isotopic compositions, Lake Ballinger, Washington, USA. *Appl Geochem* 29: 1-12. <http://dx.doi.org/10.1016/j.apgeochem.2012.12.001>.
- Griffith, JD. (2020). Electron microscopic characterization of exhaust particles containing lead dibromide beads expelled from aircraft burning leaded gasoline. *Atmos Pollut Res* 11: 1481-1486. <http://dx.doi.org/10.1016/j.apr.2020.05.026>.
- Grinshpun, SA; Yermakov, M; Reponen, T; Simmons, M; Lemasters, GK; Ryan, PH. (2014). Traffic particles in ambient air of a major US urban area: Has anything changed over a decade? *Aerosol Air Qual Res* 14: 1344-1351. <http://dx.doi.org/10.4209/aaqr.2013.11.0334>.
- Guéguen, C; Clarisse, O; Perroud, A; McDonald, A. (2011). Chemical speciation and partitioning of trace metals (Cd, Co, Cu, Ni, Pb) in the lower Athabasca river and its tributaries (Alberta, Canada). *J Environ Monit* 13: 2865-2872. <http://dx.doi.org/10.1039/c1em10563a>.
- Guney, M; Zagury, GJ. (2012). Heavy metals in toys and low-cost jewelry: critical review of u.s. And canadian legislations and recommendations for testing [Review]. *Environ Sci Technol* 46: 4265-4274. <http://dx.doi.org/10.1021/es203470x>.
- Gutiérrez, M; Qiu, X; Collette, ZJ; Lurvey, ZT. (2020). Metal content of stream sediments as a tool to assess remediation in an area recovering from historic mining contamination. *Minerals* 10: 247. <http://dx.doi.org/10.3390/min10030247>.

- [Hanna-Attisha, M; LaChance, J; Sadler, RC; Schnepf, AC.](#) (2016). Elevated blood lead levels in children associated with the flint drinking water crisis: A spatial analysis of risk and public health response. *Am J Public Health* 106: 283-290. <http://dx.doi.org/10.2105/AJPH.2015.303003>.
- [Haque, E; Thorne, PS; Nghiem, AA; Yip, CS; Bostick, BC.](#) (2021). Lead (Pb) concentrations and speciation in residential soils from an urban community impacted by multiple legacy sources. *J Hazard Mater* 416: 125886. <http://dx.doi.org/10.1016/j.jhazmat.2021.125886>.
- [Harada, Y; Whitlow, TH; Russell-Anelli, J; Walter, MT; Bassuk, NL; Rutzke, MA.](#) (2019). The heavy metal budget of an urban rooftop farm. *Sci Total Environ* 660: 115-125. <http://dx.doi.org/10.1016/j.scitotenv.2018.12.463>.
- [Harrington, JM; Nelson, CM; Weber, FX; Bradham, KD; Levine, KE; Rice, J.](#) (2014). Evaluation of methods for analysis of lead in air particulates: an intra-laboratory and inter-laboratory comparison. *Environ Sci Process Impacts* 16: 256-261. <http://dx.doi.org/10.1039/c3em00486d>.
- [Harris, AR; Davidson, CI.](#) (2005). The role of resuspended soil in lead flows in the California South Coast Air Basin. *Environ Sci Technol* 39: 7410-7415. <http://dx.doi.org/10.1021/es050642s>.
- [Harris, AR; Fifarek, BJ; Davidson, CI; Blackmon, RL.](#) (2006). Stationary sources of airborne lead: A comparison of emissions data for southern California. *J Air Waste Manag Assoc* 56: 512-517. <http://dx.doi.org/10.1080/10473289.2006.10464518>.
- [Hays, MD; Cho, SH; Baldauf, R; JJ, S; Shafer, M.](#) (2011). Particle size distributions of metal and non-metal elements in an urban near-highway environment. *Atmos Environ* 45: 925-934. <http://dx.doi.org/10.1016/j.atmosenv.2010.11.010>.
- [Hierro, A; Ollás, M; Cánovas, CR; Martín, JE; Bolivar, JP.](#) (2014). Trace metal partitioning over a tidal cycle in an estuary affected by acid mine drainage (Tinto estuary, SW Spain). *Sci Total Environ* 497-498: 18-28. <http://dx.doi.org/10.1016/j.scitotenv.2014.07.070>.
- [Hjortenkrans, DST; Bergback, BG; Haggerud, AV.](#) (2007). Metal emissions from brake linings and tires: Case studies of Stockholm, Sweden 1995/1998 and 2005. *Environ Sci Technol* 41: 5224-5230. <http://dx.doi.org/10.1021/es070198o>.
- [Holmes, LA; Turner, A; Thompson, RC.](#) (2014). Interactions between trace metals and plastic production pellets under estuarine conditions. *Mar Chem* 167: 25-32. <http://dx.doi.org/10.1016/j.marchem.2014.06.001>.
- [Hosseini, B; Stockie, JM.](#) (2016). Bayesian estimation of airborne fugitive emissions using a Gaussian plume model. *Atmos Environ* 141: 122-138. <http://dx.doi.org/10.1016/j.atmosenv.2016.06.046>.
- [Hotton, VK; Sutherland, RA.](#) (2016). The legacy of lead (Pb) in fluvial bed sediments of an urban drainage basin, Oahu, Hawaii. *Environ Sci Pollut Res Int* 23: 5495-5506. <http://dx.doi.org/10.1007/s11356-015-5777-8>.
- [HUD.](#) (2011). American Healthy Homes Survey: Lead and arsenic findings. Washington, DC: U.S. Department of Housing and Urban Development, Office of Healthy Homes and Lead Hazard Control. http://portal.hud.gov/hudportal/documents/huddoc?id=AHHS_REPORT.pdf.
- [Hudda, N; Fruin, S; Durant, JL.](#) (2022). Substantial near-field air quality improvements at a general aviation airport following a runway shortening. *Environ Sci Technol* 56: 6988-6995. <http://dx.doi.org/10.1021/acs.est.1c06765>.
- [Ikem, A; Adisa, S.](#) (2011). Runoff effect on eutrophic lake water quality and heavy metal distribution in recent littoral sediment. *Chemosphere* 82: 259-267. <http://dx.doi.org/10.1016/j.chemosphere.2010.09.048>.
- [Ilyinskaya, E; Mason, E; Wieser, PE; Holland, L; Liu, EJ; Mather, TA; Edmonds, M; Whitty, RCW; Elias, T; Nadeau, PA; Schneider, D; McQuaid, JB; Allen, SE; Harvey, J; Oppenheimer, C; Kern, C; Damby, D.](#) (2021). Rapid metal pollutant deposition from the volcanic plume of Kīlauea, Hawai'i. *Commun Earth Environ* 2: 78. <http://dx.doi.org/10.1038/s43247-021-00146-2>.
- [Isley, CF; Taylor, MP.](#) (2020). Atmospheric remobilization of natural and anthropogenic contaminants during wildfires. *Environ Pollut* 267: 115400. <http://dx.doi.org/10.1016/j.envpol.2020.115400>.

- Ito, K; Johnson, S; Kheirbek, I; Clougherty, J; Pezeshki, G; Ross, Z; Eisl, H; Matte, TD. (2016). Intraurban variation of fine particle elemental concentrations in New York City. *Environ Sci Technol* 50: 7517-7526. <http://dx.doi.org/10.1021/acs.est.6b00599>.
- Jeong, H; Choi, JY; Lim, J; Shim, WJ; Kim, YO; Ra, K. (2020). Characterization of the contribution of road deposited sediments to the contamination of the close marine environment with trace metals: Case of the port city of Busan (South Korea). *Mar Pollut Bull* 161: 111717. <http://dx.doi.org/10.1016/j.marpolbul.2020.111717>.
- Jeong, H; Ryu, JS; Ra, K. (2022). Characteristics of potentially toxic elements and multi-isotope signatures (Cu, Zn, Pb) in non-exhaust traffic emission sources. *Environ Pollut* 292: 118339. <http://dx.doi.org/10.1016/j.envpol.2021.118339>.
- Jeremiason, JD; Baumann, EI; Sebestyen, SD; Agather, AM; Seelen, EA; Carlson-Stehlin, BJ; Funke, MM; Cotner, JB. (2018). Contemporary mobilization of legacy Pb stores by DOM in a boreal peatland. *Environ Sci Technol* 52: 3375-3383. <http://dx.doi.org/10.1021/acs.est.7b06577>.
- Jovan, SE; Zuidema, C; Derrien, MM; Bidwell, AL; Brinkley, W; Smith, RJ; Blahna, D; Barnhill, R; Gould, L; Rodriguez, AJ; Amacher, MC; Abel, TD; López, P. (2022). Heavy metals in moss guide environmental justice investigation: A case study using community science in Seattle, WA, USA. *Ecosphere* 13: e4109. <http://dx.doi.org/10.1002/ecs2.4109>.
- Kaiser, ML; Williams, ML; Basta, N; Hand, M; Huber, S. (2015). When vacant lots become urban gardens: Characterizing the perceived and actual food safety concerns of urban agriculture in Ohio. *J Food Prot* 78: 2070-2080. <http://dx.doi.org/10.4315/0362-028X.JFP-15-181>.
- Kang, M; Tian, Y; Peng, S; Wang, M. (2019). Effect of dissolved oxygen and nutrient levels on heavy metal contents and fractions in river surface sediments. *Sci Total Environ* 648: 861-870. <http://dx.doi.org/10.1016/j.scitotenv.2018.08.201>.
- Karbassi, AR; Heidari, M; Vaezi, AR; Samani, ARV; Fakhraee, M; Heidari, F. (2014). Effect of pH and salinity on flocculation process of heavy metals during mixing of Aras River water with Caspian Sea water. *Environ Earth Sci* 72: 457-465. <http://dx.doi.org/10.1007/s12665-013-2965-z>.
- Kaste, JM; Bostick, BC; Heimsath, AM; Steinnes, E; Friedland, AJ. (2011). Using atmospheric fallout to date organic horizon layers and quantify metal dynamics during decomposition. *Geochim Cosmo Acta* 75: 1642-1661. <http://dx.doi.org/10.1016/j.gca.2011.01.011>.
- Katz, DR; Cantwell, MG; Sullivan, JC; Perron, MM; Burgess, RM; Ho, KT. (2017). Particle-bound metal transport after removal of a small dam in the Pawtuxet River, Rhode Island, USA. *Integr Environ Assess Manag* 13: 675-685. <http://dx.doi.org/10.1002/ieam.1844>.
- Keene, AF; Johnston, SG; Bush, RT; Burton, ED; Sullivan, LA; Dundon, M; McElnea, AE; Smith, CD; Ahern, CR; Powell, B. (2014). Enrichment and heterogeneity of trace elements at the redox-interface of Fe-rich intertidal sediments. *Chem Geol* 383: 1-12. <http://dx.doi.org/10.1016/j.chemgeo.2014.06.003>.
- Kempter, H; Krachler, M; Shotyk, W; Zacccone, C. (2017). Validating modelled data on major and trace element deposition in southern Germany using Sphagnum moss. *Atmos Environ* 167: 656-664. <http://dx.doi.org/10.1016/j.atmosenv.2017.08.037>.
- Kerr, JG; Cooke, CA. (2017). Erosion of the Alberta badlands produces highly variable and elevated heavy metal concentrations in the Red Deer River, Alberta. *Sci Total Environ* 596-597: 427-436. <http://dx.doi.org/10.1016/j.scitotenv.2017.04.037>.
- Kim, I; Kim, G; Choy, EJ. (2015). The significant inputs of trace elements and rare earth elements from melting glaciers in Antarctic coastal waters. *Polar Res* 34: 24289. <http://dx.doi.org/10.3402/polar.v34.24289>.
- Kondo, MC; Zuidema, C; Moran, HA; Jovan, S; Derrien, M; Brinkley, W; De Roos, AJ; Tabb, LP. (2022). Spatial predictors of heavy metal concentrations in epiphytic moss samples in Seattle, WA. *Sci Total Environ* 825: 153801. <http://dx.doi.org/10.1016/j.scitotenv.2022.153801>.

- [Kousehlar, M; Widom, E. \(2020\)](#). Identifying the sources of air pollution in an urban-industrial setting by lichen biomonitoring: A multi-tracer approach. *Appl Geochem* 121: 104695. <http://dx.doi.org/10.1016/j.apgeochem.2020.104695>.
- [Krahforst, C; Sherman, LA; Kehm, K. \(2022\)](#). Trace metal enrichment in a tidally influenced, rural tributary of the upper Chesapeake Bay. *Mar Pollut Bull* 175: 113377. <http://dx.doi.org/10.1016/j.marpolbul.2022.113377>.
- [Krug, JD; Dart, A; Witherspoon, CL; Gilberry, J; Malloy, Q; Kaushik, S; Vanderpool, RW. \(2017\)](#). Revisiting the size selective performance of EPA's high-volume total suspended particulate matter (Hi-Vol TSP) sampler. *Aerosol Sci Technol* 51: 868-878. <http://dx.doi.org/10.1080/02786826.2017.1316358>.
- [Kumar, T; Mohsin, R; Majid, ZA; Ghafir, MFA; Wash, AM. \(2020\)](#). Experimental optimisation comparison of detonation characteristics between leaded aviation gasoline low lead and its possible unleaded alternatives. *Fuel* 281: 118726. <http://dx.doi.org/10.1016/j.fuel.2020.118726>.
- [Kundu, S; Stone, EA. \(2014\)](#). Composition and sources of fine particulate matter across urban and rural sites in the Midwestern United States. *Environ Sci Process Impacts* 16: 1360-1370. <http://dx.doi.org/10.1039/c3em00719g>.
- [Laidlaw, MAS; Filippelli, GM. \(2008\)](#). Resuspension of urban soils as a persistent source of lead poisoning in children: A review and new directions [Review]. *Appl Geochem* 23: 2021-2039. <http://dx.doi.org/10.1016/j.apgeochem.2008.05.009>.
- [Laidlaw, MAS; Filippelli, GM; Brown, S; Paz-Ferreiro, J; Reichman, SM; Netherway, P; Truskewycz, A; Ball, AS; Mielke, HW. \(2017\)](#). Case studies and evidence-based approaches to addressing urban soil lead contamination. *Appl Geochem* 83: 14-30. <http://dx.doi.org/10.1016/j.apgeochem.2017.02.015>.
- [Laidlaw, MAS; Filippelli, GM; Sadler, RC; Gonzales, CR; Ball, AS; Mielke, HW. \(2016\)](#). Children's blood lead seasonality in Flint, Michigan (USA), and soil-sourced lead hazard risks [Review]. *Int J Environ Res Public Health* 13: 358. <http://dx.doi.org/10.3390/ijerph13040358>.
- [Laidlaw, MAS; Zahran, S; Mielke, HW; Taylor, MP; Filippelli, GM. \(2012\)](#). Re-suspension of lead contaminated urban soil as a dominant source of atmospheric lead in Birmingham, Chicago, Detroit and Pittsburgh, USA. *Atmos Environ* 49: 302-310. <http://dx.doi.org/10.1016/j.atmosenv.2011.11.030>.
- [Laidlaw, MAS; Zahran, S; Pingitore, N; Clague, J; Devlin, G; Taylor, MP. \(2014\)](#). Identification of lead sources in residential environments: Sydney Australia. *Environ Pollut* 184: 238-246. <http://dx.doi.org/10.1016/j.envpol.2013.09.003>.
- [Landis, MS; Studabaker, WB; Pancras, JP; Graney, JR; White, EM; Edgerton, ES. \(2019\)](#). Source apportionment of ambient fine and coarse particulate matter polycyclic aromatic hydrocarbons at the Bertha Ganter-Fort McKay community site in the Oil Sands Region of Alberta, Canada. *Sci Total Environ* 666: 540-558. <http://dx.doi.org/10.1016/j.scitotenv.2019.02.126>.
- [Landre, AL; Watmough, SA; Dillon, PJ. \(2010\)](#). Metal pools, fluxes, and budgets in an acidified forested catchment on the Precambrian Shield, Central Ontario, Canada. *Water Air Soil Pollut* 209: 209-228. <http://dx.doi.org/10.1007/s11270-009-0193-7>.
- [Lankey, RL; Davidson, CI; McMichael, FC. \(1998\)](#). Mass balance for lead in the California south coast air basin: An update [Review]. *Environ Res* 78: 86-93. <http://dx.doi.org/10.1006/enrs.1998.3853>.
- [Lanphear, BP; Matte, TD; Rogers, J; Clickner, RP; Dietz, B; Bornschein, RL; Succop, P; Mahaffey, KR; Dixon, S; Galke, W; Rabinowitz, M; Farfel, M; Rohde, C; Schwartz, J; Ashley, P; Jacobs, DE. \(1998\)](#). The contribution of lead-contaminated house dust and residential soil to children's blood lead levels: A pooled analysis of 12 epidemiologic studies. *Environ Res* 79: 51-68. <http://dx.doi.org/10.1006/enrs.1998.3859>.
- [Levin, R; Vieira, CLZ; Mordarski, DC; Rosenbaum, MH. \(2020\)](#). Lead seasonality in humans, animals, and the natural environment [Review]. *Environ Res* 180: 108797. <http://dx.doi.org/10.1016/j.envres.2019.108797>.
- [Li, J; McDonald-Gillespie, J. \(2020\)](#). Airborne lead (Pb) from abandoned mine waste in Northeastern Oklahoma, USA. *Geohealth* 4: e2020GH000273. <http://dx.doi.org/10.1029/2020GH000273>.

- [Li, WC; Deng, H; Wong, MH. \(2016\).](#) Metal solubility and speciation under the influence of waterlogged condition and the presence of wetland plants. *Geoderma* 270: 98-108. <http://dx.doi.org/10.1016/j.geoderma.2015.10.012>.
- [Lin, JY; Tehrani, MW; Chen, R; Heaney, CD; Rule, AM. \(2022\).](#) Characterizing spatiotemporal variability in airborne heavy metal concentration: Changes after 18 years in Baltimore, MD. *Environ Res* 209: 112878. <http://dx.doi.org/10.1016/j.envres.2022.112878>.
- [Liotta, M; Martínez Cruz, M; Ferrufino, A; Rüdiger, J; Gutmann, A; Cerda, KVR; Bobrowski, N; de Moor, JM. \(2021\).](#) Magmatic signature in acid rain at Masaya volcano, Nicaragua: Inferences on element volatility during lava lake degassing. *Chem Geol* 585: 120562. <http://dx.doi.org/10.1016/j.chemgeo.2021.120562>.
- [Liu, JJ; Diao, ZH; Xu, XR; Xie, Q. \(2019\).](#) Effects of dissolved oxygen, salinity, nitrogen and phosphorus on the release of heavy metals from coastal sediments. *Sci Total Environ* 666: 894-901. <http://dx.doi.org/10.1016/j.scitotenv.2019.02.288>.
- [Lombardi, AT; Tonietto, AE; Choueri, RB; Henriques Vieira, AA. \(2014\).](#) Chemical behavior of Cu, Zn, Cd, and Pb in a eutrophic reservoir: Speciation and complexation capacity [Abstract]. *Abstr Pap Am Chem Soc* 247: 362-COLL.
- [Louchouart, P; Kuo, LJ; Brandenberger, JM; Marcantonio, F; Garland, C; Gill, GA; Cullinan, V. \(2012\).](#) Pyrogenic inputs of anthropogenic Pb and Hg to sediments of the Hood Canal, Washington, in the 20th century: source evidence from stable Pb isotopes and PAH signatures. *Environ Sci Technol* 46: 5772-5781. <http://dx.doi.org/10.1021/es300269t>.
- [Luo, J; Tang, R; Sun, S; Yang, D; She, J; Yang, P. \(2015\).](#) Lead distribution and possible sources along vertical zone spectrum of typical ecosystems in the Gongga Mountain, eastern Tibetan Plateau. *Atmos Environ* 115: 132-140. <http://dx.doi.org/10.1016/j.atmosenv.2015.05.022>.
- [Martín-Domingo, MC; Pla, A; Hernández, AF; Olmedo, P; Navas-Acien, A; Lozano-Paniagua, D; Gil, F. \(2017\).](#) Determination of metalloid, metallic and mineral elements in herbal teas: Risk assessment for the consumers. *J Food Compos Anal* 60: 81-89. <http://dx.doi.org/10.1016/j.jfca.2017.03.009>.
- [Marx, SK; Rashid, S; Stromsoe, N. \(2016\).](#) Global-scale patterns in anthropogenic Pb contamination reconstructed from natural archives [Review]. *Environ Pollut* 213: 283-298. <http://dx.doi.org/10.1016/j.envpol.2016.02.006>.
- [Mason, E; Wieser, PE; Liu, EJ; Edmonds, M; Ilyinskaya, E; Whitty, RCW; Mather, TA; Elias, T; Nadeau, PA; Wilkes, TC; Mcgonigle, AJS; Pering, T, omD; Mims, FM; Kern, C; Schneider, DJ; Oppenheimer, C. \(2021\).](#) Volatile metal emissions from volcanic degassing and lava-seawater interactions at Kilauea Volcano, Hawai'i. *Commun Earth Environ* 2. <http://dx.doi.org/10.1038/s43247-021-00145-3>.
- [Masri, S; Kang, CM; Koutrakis, P. \(2015\).](#) Composition and sources of fine and coarse particles collected during 2002-2010 in Boston, MA. *J Air Waste Manag Assoc* 65: 287-297. <http://dx.doi.org/10.1080/10962247.2014.982307>.
- [Mazari, K; Filippelli, GM. \(2020\).](#) Using deciduous trees as bioindicators of trace element deposition in a small urban watershed, Indianapolis, IN, USA. *J Environ Qual* 49: 163-171. <http://dx.doi.org/10.1002/jeq2.20009>.
- [McCumber, A; Strevett, KA. \(2017\).](#) A geospatial analysis of soil lead concentrations around regional Oklahoma airports. *Chemosphere* 167: 62-70. <http://dx.doi.org/10.1016/j.chemosphere.2016.09.127>.
- [McKee, LJ; Gilbreath, AN. \(2015\).](#) Concentrations and loads of suspended sediment and trace element pollutants in a small semi-arid urban tributary, San Francisco Bay, California. *Environ Monit Assess* 187: 499. <http://dx.doi.org/10.1007/s10661-015-4710-4>.
- [McKenzie, ER; Young, TM. \(2013\).](#) A novel fractionation approach for water constituents: Distribution of storm event metals. *Environ Sci Process Impacts* 15: 1006-1016. <http://dx.doi.org/10.1039/c3em30612g>.

- [Meng, O; Richmond-Bryant, J; Davis, JA; Cohen, J; Svendsgaard, D; Brown, JS; Tuttle, L; Hubbard, H; Rice, J; Vinikoor-Imler, L; Sacks, JD; Kिरrane, E; Kotchmar, D; Hines, E; Ross, M. \(2014\). Contribution of particle-size-fractionated airborne lead to blood lead during the National Health and Nutrition Examination Survey, 1999–2008. *Environ Sci Technol* 48: 1263–1270. <http://dx.doi.org/10.1021/es4039825>.](#)
- [Mielke, HW; Gonzales, CR; Powell, ET; Laidlaw, MAS; Berry, KJ; Mielke, PW, Jr; Egendorf, SP. \(2019\). The concurrent decline of soil lead and children's blood lead in New Orleans. *Proc Natl Acad Sci USA* 116: 22058-22064. <http://dx.doi.org/10.1073/pnas.1906092116>.](#)
- [Mielke, HW; Gonzales, CR; Powell, ET; Mielke, PW. \(2017\). Spatiotemporal exposome dynamics of soil lead and children's blood lead pre- and ten years post-Hurricane Katrina: Lead and other metals on public and private properties in the city of New Orleans, Louisiana, U.S.A. *Environ Res* 155: 208-218. <http://dx.doi.org/10.1016/j.envres.2017.01.036>.](#)
- [Mielke, HW; Laidlaw, MA; Gonzales, C. \(2010\). Lead \(Pb\) legacy from vehicle traffic in eight California urbanized areas: Continuing influence of lead dust on children's health \[Review\]. *Sci Total Environ* 408: 3965-3975. <http://dx.doi.org/10.1016/j.scitotenv.2010.05.017>.](#)
- [Mielke, HW; Laidlaw, MA; Gonzales, CR. \(2011\). Estimation of leaded \(Pb\) gasoline's continuing material and health impacts on 90 US urbanized areas \[Review\]. *Environ Int* 37: 248-257. <http://dx.doi.org/10.1016/j.envint.2010.08.006>.](#)
- [Milačić, R; Zuliani, T; Vidmar, J; Oprčkal, P; Ščančar, J. \(2017\). Potentially toxic elements in water and sediments of the Sava River under extreme flow events. *Sci Total Environ* 605-606: 894-905. <http://dx.doi.org/10.1016/j.scitotenv.2017.06.260>.](#)
- [Morgan, B; Rate, AW; Burton, ED. \(2012\). Trace element reactivity in FeS-rich estuarine sediments: Influence of formation environment and acid sulfate soil drainage. *Sci Total Environ* 438: 463-476. <http://dx.doi.org/10.1016/j.scitotenv.2012.08.088>.](#)
- [Murphy, DM; Hudson, PK; Cziczo, DJ; Gallavardin, S; Froyd, KD; Johnston, MV; Middlebrook, AM; Reinard, MS; Thomson, DS; Thornberry, T; Wexler, AS. \(2007\). Distribution of lead in single atmospheric particles. *Atmos Chem Phys* 7: 3195-3210. <http://dx.doi.org/10.5194/acp-7-3195-2007>.](#)
- [NASEM. \(2021\). Options for reducing lead emissions from piston-engine aircraft. Washington, DC: National Academies Press. <http://dx.doi.org/10.17226/26050>.](#)
- [NCBI. \(2022\). PubChem substance record for SID 176263083, chrysotile asbestos. Available online at <https://pubchem.ncbi.nlm.nih.gov/substance/176263083> \(accessed August 26, 2022\).](#)
- [Ni, L; Gu, G; Rong, S; Hu, L; Wang, P; Li, S; Li, D; Liu, X; Wang, Y; Acharya, K. \(2019\). Effects of cyanobacteria decomposition on the remobilization and ecological risk of heavy metals in Taihu Lake. *Environ Sci Pollut Res Int* 26: 35860-35870. <http://dx.doi.org/10.1007/s11356-019-06649-y>.](#)
- [Nicholson, KW. \(1988\). A review of particle resuspension \[Review\]. *Atmos Environ* 22: 2639-2651. \[http://dx.doi.org/10.1016/0004-6981\\(88\\)90433-7\]\(http://dx.doi.org/10.1016/0004-6981\(88\)90433-7\).](#)
- [Nicholson, KW; Branson, JR. \(1990\). Factors affecting resuspension by road traffic. *Sci Total Environ* 93: 349-358. \[http://dx.doi.org/10.1016/0048-9697\\(90\\)90126-F\]\(http://dx.doi.org/10.1016/0048-9697\(90\)90126-F\).](#)
- [Niemitz, J; Haynes, C; Lasher, G. \(2013\). Legacy sediments and historic land use: Chemostratigraphic evidence for excess nutrient and heavy metal sources and remobilization. *Geology* 41: 47-50. <http://dx.doi.org/10.1130/G33547.1>.](#)
- [Nowell, LH; Moran, PW; Gilliom, RJ; Calhoun, DL; Ingersoll, CG; Kemble, NE; Kuivila, KM; Phillips, PJ. \(2013\). Contaminants in stream sediments from seven United States metropolitan areas: Part I: Distribution in relation to urbanization. *Arch Environ Contam Toxicol* 64: 32-51. <http://dx.doi.org/10.1007/s00244-012-9813-0>.](#)
- [Nowinski, P; Hodge, VF; Gerstenberger, S. \(2012\). Application of field portable X-ray fluorescence to the analysis of desert varnish samples in areas affected by coal-fired power plants. *Environ Chem* 9: 379-388. <http://dx.doi.org/10.1071/EN11139>.](#)
- [NRC. \(1980\). Lead in the human environment. Washington, DC: National Academy Press.](#)

- [Nriagu, JO; Pacyna, JM. \(1988\)](#). Quantitative assessment of worldwide contamination of air, water and soils by trace metals. *Nature* 333: 134-139. <http://dx.doi.org/10.1038/333134a0>.
- [O'Shea, MJ; Vann, DR; Hwang, WT; Gieré, R. \(2020\)](#). A mineralogical and chemical investigation of road dust in Philadelphia, PA, USA. *Environ Sci Pollut Res Int* 27: 14883-14902. <http://dx.doi.org/10.1007/s11356-019-06746-y>.
- [O'Shea, MJ; Krekeler, MPS; Vann, DR; Gieré, R. \(2021\)](#). Investigation of Pb-contaminated soil and road dust in a polluted area of Philadelphia. *Environ Monit Assess* 193: 440. <http://dx.doi.org/10.1007/s10661-021-09213-9>.
- [Oakes, MM; Burke, JM; Norris, GA; Kovalcik, KD; Pancras, JP; Landis, MS. \(2016\)](#). Near-road enhancement and solubility of fine and coarse particulate matter trace elements near a major interstate in Detroit, Michigan. *Atmos Environ* 145: 213-224. <http://dx.doi.org/10.1016/j.atmosenv.2016.09.034>.
- [Obeng-Gyasi, E; Roostaei, J; Gibson, JM. \(2021\)](#). Lead distribution in urban soil in a medium-sized city: Household-scale analysis. *Environ Sci Technol* 55: 3696-3705. <http://dx.doi.org/10.1021/acs.est.0c07317>.
- [Odhiambo, B; Brown, V; Armentrout, G; Giancarlo, LC; Wegner, C. \(2013\)](#). Sediment trace metals and PCB input history in Lake Anna, Virginia, USA. *Environ Earth Sci* 69: 2103-2117. <http://dx.doi.org/10.1007/s12665-013-2500-2>.
- [Odigie, KO; Flegal, AR. \(2011\)](#). Pyrogenic remobilization of historic industrial lead depositions. *Environ Sci Technol* 45: 6290-6295. <http://dx.doi.org/10.1021/es200944w>.
- [Odigie, KO; Flegal, AR. \(2014\)](#). Trace metal inventories and lead isotopic composition chronicle a forest fire's remobilization of industrial contaminants deposited in the Angeles National Forest. *PLoS ONE* 9: e107835. <http://dx.doi.org/10.1371/journal.pone.0107835>.
- [Ostrofsky, ML; Schworm, AE. \(2011\)](#). A history of acid mine contamination, recovery, and eutrophication in Sandy Lake, Pennsylvania. *J Paleolimnol* 46: 229-242. <http://dx.doi.org/10.1007/s10933-011-9535-8>.
- [Pakbin, P; Ning, Z; Shafer, MM; Schauer, JJ; Sioutas, C. \(2011\)](#). Seasonal and spatial coarse particle elemental concentrations in the Los Angeles area. *Aerosol Sci Technol* 45: 949-963. <http://dx.doi.org/10.1080/02786826.2011.571309>.
- [Pancras, JP; Landis, MS. \(2011\)](#). Performance evaluation of modified Semi-continuous Elements in Aerosol Sampler-III. *Atmos Environ* 45: 6751-6759. <http://dx.doi.org/10.1016/j.atmosenv.2011.08.029>.
- [Pavilonis, B; Cheng, Z; Johnson, G; Maroko, A. \(2022\)](#). Lead, soils, and children: An ecological analysis of lead contamination in parks and elevated blood lead levels in Brooklyn, New York. *Arch Environ Contam Toxicol* 82: 1-10. <http://dx.doi.org/10.1007/s00244-021-00902-7>.
- [Pawlowsky, RT; Lecce, SA; Owen, MR; Martin, DJ. \(2017\)](#). Legacy sediment, lead, and zinc storage in channel and floodplain deposits of the Big River, Old Lead Belt Mining District, Missouri, USA. *Geomorphology* 299: 54-75. <http://dx.doi.org/10.1016/j.geomorph.2017.08.042>.
- [Pearson, MA; Biagioni, RN; Gutiérrez, M. \(2019\)](#). Geochemical fractionation of stream sediments impacted by Pb-Zn mining wastes: Missouri, USA. *Mine Water Environ* 38: 378-384. <http://dx.doi.org/10.1007/s10230-018-0568-3>.
- [Peltier, RE; Lippmann, M. \(2011\)](#). Spatial and seasonal distribution of aerosol chemical components in New York City: (1) Incineration, coal combustion, and biomass burning. *J Expo Sci Environ Epidemiol* 21: 473-483. <http://dx.doi.org/10.1038/jes.2011.16>.
- [Peng, L; Li, L; Lin, Q; Li, M; Zhang, G; Bi, X; Wang, X; Sheng, G. \(2020\)](#). Does atmospheric processing produce toxic Pb-containing compounds? A case study in suburban Beijing by single particle mass spectrometry. *J Hazard Mater* 382: 121014. <http://dx.doi.org/10.1016/j.jhazmat.2019.121014>.
- [Perdrial, N; Liewig, N; Delphin, JE; Elsass, F. \(2008\)](#). TEM evidence for intracellular accumulation of lead by bacteria in subsurface environments. *Chem Geol* 253: 196-204. <http://dx.doi.org/10.1016/j.chemgeo.2008.05.008>.

- [Pérez-Rodríguez, M; Silva-Sánchez, N; Kylander, ME; Bindler, R; Mighall, TM; Schofield, JE; Edwards, KJ; Martínez Cortizas, A. \(2018\). Industrial-era lead and mercury contamination in southern Greenland implicates North American sources. *Sci Total Environ* 613-614: 919-930. <http://dx.doi.org/10.1016/j.scitotenv.2017.09.041>.](#)
- [Pieper, KJ; Krometis, LA; Gallagher, DL; Benham, BL; Edwards, M. \(2015\). Incidence of waterborne lead in private drinking water systems in Virginia. *J Water Health* 13: 897-908. <http://dx.doi.org/10.2166/wh.2015.275>.](#)
- [Pingitore, NE, Jr.; Clague, JW; Amaya, MA; Maciejewska, B; Reynoso, JJ. \(2009\). Urban airborne lead: X-ray absorption spectroscopy establishes soil as dominant source. *PLoS ONE* 4: e5019. <http://dx.doi.org/10.1371/journal.pone.0005019>.](#)
- [Prabhakar, G; Sorooshian, A; Toffol, E; Arellano, AF; Betterton, EA. \(2014\). Spatiotemporal distribution of airborne particulate metals and metalloids in a populated arid region. *Atmos Environ* 92: 339-347. <http://dx.doi.org/10.1016/j.atmosenv.2014.04.044>.](#)
- [Pratte, S; Mucci, A; Garneau, M. \(2013\). Historical records of atmospheric metal deposition along the St. Lawrence Valley \(eastern Canada\) based on peat bog cores. *Atmos Environ* 79: 831-840. <http://dx.doi.org/10.1016/j.atmosenv.2013.07.063>.](#)
- [Qureshi, S; Dutkiewicz, VA; Khan, AR; Swami, K; Yang, KX; Husain, L; Schwab, JJ; Demerjian, KL. \(2006\). Elemental composition of PM_{2.5} aerosols in Queens, New York: Solubility and temporal trends. *Atmos Environ* 40: S238-S251. <http://dx.doi.org/10.1016/j.atmosenv.2005.12.070>.](#)
- [Rahim, MF; Pal, D; Ariya, PA. \(2019\). Physicochemical studies of aerosols at Montreal Trudeau Airport: The importance of airborne nanoparticles containing metal contaminants. *Environ Pollut* 246: 734-744. <http://dx.doi.org/10.1016/j.envpol.2018.12.050>.](#)
- [Requia, WJ; Coull, BA; Koutrakis, P. \(2019\). The influence of spatial patterning on modeling PM_{2.5} constituents in Eastern Massachusetts. *Sci Total Environ* 682: 247-258. <http://dx.doi.org/10.1016/j.scitotenv.2019.05.012>.](#)
- [Resongles, E; Dietze, V; Green, DC; Harrison, RM; Ochoa-Gonzalez, R; Tremper, AH; Weiss, DJ. \(2021\). Strong evidence for the continued contribution of lead deposited during the 20th century to the atmospheric environment in London of today. *Proc Natl Acad Sci USA* 118: e2102791118. <http://dx.doi.org/10.1073/pnas.2102791118>.](#)
- [Richardson, JB. \(2021\). Comparing trace elements \(As, Cu, Ni, Pb, and Zn\) in soils and surface waters among montane, upland watersheds and lowland, urban watersheds in New England, USA. *Water* 13: 59. <http://dx.doi.org/10.3390/w13010059>.](#)
- [Richardson, JB; Friedland, AJ; Kaste, JM; Jackson, BP. \(2014\). Forest floor lead changes from 1980 to 2011 and subsequent accumulation in the mineral soil across the Northeastern United States. *J Environ Qual* 43: 926-935. <http://dx.doi.org/10.2134/jeq2013.10.0435>.](#)
- [Ritchie, JAB; Gerstenberger, SL. \(2013\). An evaluation of lead concentrations in imported hot sauces. *J Environ Sci Health B* 48: 530-538. <http://dx.doi.org/10.1080/03601234.2013.774226>.](#)
- [Rodes, CE; Evans, EG. \(1985\). Preliminary assessment of 10 µm particulate sampling at eight locations in the United States. *Atmos Environ* 19: 293-303. \[http://dx.doi.org/10.1016/0004-6981\\(85\\)90097-6\]\(http://dx.doi.org/10.1016/0004-6981\(85\)90097-6\).](#)
- [Romanok, KM; Szabo, Z; Reilly, TJ; Defne, Z; Ganju, NK. \(2016\). Sediment chemistry and toxicity in Barnegat Bay, New Jersey: Pre- and post-Hurricane Sandy, 2012-13. *Mar Pollut Bull* 107: 472-488. <http://dx.doi.org/10.1016/j.marpolbul.2016.04.018>.](#)
- [Rosales-Hoz, L; Carranza-Edwards, A; Martinez-Serrano, RG; Alatorre, MA; Armstrong-Altrin, JS. \(2015\). Textural and geochemical characteristics of marine sediments in the SW Gulf of Mexico: Implications for source and seasonal change. *Environ Monit Assess* 187: 205. <http://dx.doi.org/10.1007/s10661-015-4423-8>.](#)
- [Rosen, MB; Pokhrel, LR; Weir, MH. \(2017\). A discussion about public health, lead and Legionella pneumophila in drinking water supplies in the United States \[Review\]. *Sci Total Environ* 590-591: 843-852. <http://dx.doi.org/10.1016/j.scitotenv.2017.02.164>.](#)

- [Rossi, RJ; Bain, DJ; Hillman, AL; Pompeani, DP; Finkenbinder, MS; Abbott, MB.](#) (2017). Reconstructing early industrial contributions to legacy trace metal contamination in Southwestern Pennsylvania. *Environ Sci Technol* 51: 4173-4181. <http://dx.doi.org/10.1021/acs.est.6b03372>.
- [Rothwell, JJ; Taylor, KG; Evans, MG; Allott, TEH.](#) (2011). Contrasting controls on arsenic and lead budgets for a degraded peatland catchment in Northern England. *Environ Pollut* 159: 3129-3133. <http://dx.doi.org/10.1016/j.envpol.2011.05.026>.
- [Sabin, LD; Lim, JH; Stolzenbach, KD; Schiff, KC.](#) (2006). Atmospheric dry deposition of trace metals in the coastal region of Los Angeles, California, USA. *Environ Toxicol Chem* 25: 2334-2341. <http://dx.doi.org/10.1897/05-300R.1>.
- [Sanderson, P; Naidu, R; Bolan, N; Bowman, M; McLure, S.](#) (2012). Effect of soil type on distribution and bioaccessibility of metal contaminants in shooting range soils. *Sci Total Environ* 438: 452-462. <http://dx.doi.org/10.1016/j.scitotenv.2012.08.014>.
- [Santucci, RJ, Jr; Scully, JR.](#) (2020). The pervasive threat of lead (Pb) in drinking water: Unmasking and pursuing scientific factors that govern lead release. *PNAS* 117: 23211-23218. <http://dx.doi.org/10.1073/pnas.1913749117>.
- [Sarkar, S; Ahmed, T; Swami, K; Judd, CD; Bari, A; Dutkiewicz, VA; Husain, L.](#) (2015). History of atmospheric deposition of trace elements in lake sediments, similar to 1880 to 2007. *J Geophys Res Atmos* 120: 5658-5669. <http://dx.doi.org/10.1002/2015JD023202>.
- [Scheid, S; Gunthardt-Goerg, MS; Schulin, R; Nowack, B.](#) (2009). Accumulation and solubility of metals during leaf litter decomposition in non-polluted and polluted soil. *Eur J Soil Sci* 60: 613-621. <http://dx.doi.org/10.1111/j.1365-2389.2009.01153.x>.
- [Schindler, M; Kamber, BS.](#) (2013). High-resolution lake sediment reconstruction of industrial impact in a world-class mining and smelting center, Sudbury, Ontario, Canada. *Appl Geochem* 37: 102-116. <http://dx.doi.org/10.1016/j.apgeochem.2013.07.014>.
- [Schindler, M; Weatherhead, K; Mantha, H.](#) (2021). The release of incidental nanoparticles during the weathering of gunshot residue in soils of a shooting range in Ontario, Canada. *Can Mineral* 59: 69-89. <http://dx.doi.org/10.3749/canmin.1900092>.
- [Schuler, MS; Relyea, RA.](#) (2018). A review of the combined threats of road salts and heavy metals to freshwater systems. *Bioscience* 68: 327-335. <http://dx.doi.org/10.1093/biosci/biy018>.
- [Schwarz, K; Cutts, BB; London, JK; Cadenasso, ML.](#) (2016). Growing gardens in shrinking cities: A solution to the soil lead problem? *Sustainability* 8: 141. <http://dx.doi.org/10.3390/su8020141>.
- [Sebastiao, AG; Wagner, EJ; Goldsmith, ST.](#) (2017). Trace metal sediment loading in the Mill Creek: A spatial and temporal analysis of vehicular pollutants in suburban waterways. *Appl Geochem* 83: 50-61. <http://dx.doi.org/10.1016/j.apgeochem.2017.04.001>.
- [Shang, SB; Li, XQ.](#) (2011). Study on the co-migration of Pb with soil colloids under rainfall. In Y Shi; J Zuo (Eds.), *Environmental biotechnology and materials engineering* (pp. 437-441). Zurich, Switzerland: Trans Tech Publications. <http://dx.doi.org/10.4028/www.scientific.net/AMR.183-185.437>.
- [Shelley, RU; Landing, WM; Ussher, SJ; Planquette, H; Sarthou, G.](#) (2018). Regional trends in the fractional solubility of Fe and other metals from North Atlantic aerosols (GEOTRACES cruises GA01 and GA03) following a two-stage leach. *Biogeosciences* 15: 2271-2288. <http://dx.doi.org/10.5194/bg-15-2271-2018>.
- [Shepherd, NL; Nairn, RW.](#) (2020). Metals retention in a net alkaline mine drainage impacted stream due to the colonization of the North American Beaver (*Castor canadensis*). *Sci Total Environ* 731: 139203. <http://dx.doi.org/10.1016/j.scitotenv.2020.139203>.
- [Sher, F; Raore, D; Klemeš, JJ; Rafi-Ul-Shan, PM; Khzouz, M; Marintseva, K; Razmkhah, O.](#) (2021). Unprecedented impacts of aviation emissions on global environmental and climate change scenario [Review]. *Curr Pollut Rep* 7: 549-564. <http://dx.doi.org/10.1007/s40726-021-00206-3>.

- [Shotyk, W; Appleby, PG; Bicalho, B; Davies, L; Froese, D; Grant-Weaver, I; Krachler, M; Magnan, G; Mullan-Boudreau, G; Noernberg, T; Pelletier, R; Shannon, B. ob; van Bellen, S; Zaccone, C.](#) (2016). Peat bogs in northern Alberta, Canada reveal decades of declining atmospheric Pb contamination. *Geophys Res Lett* 43: 9964-9974. <http://dx.doi.org/10.1002/2016GL070952>.
- [Silva, E; Huang, S; Lawrence, J; Martins, MAG; Li, J; Koutrakis, P.](#) (2021). Trace element concentrations in ambient air as a function of distance from road. *J Air Waste Manag Assoc* 71: 129-136. <http://dx.doi.org/10.1080/10962247.2020.1866711>.
- [Skeaff, JM; Thibault, Y; Hardy, DJ.](#) (2011). A new method for the characterisation and quantitative speciation of base metal smelter stack particulates. *Environ Monit Assess* 177: 165-192. <http://dx.doi.org/10.1007/s10661-010-1627-9>.
- [Smith, DB; Cannon, WF; Woodruff, LG; Solano, F; Kilburn, JE; Fey, DL.](#) (2013). Geochemical and mineralogical data for soils of the conterminous United States. (Data Series 801). Reston, VA: U.S. Department of the Interior, U.S. Geological Survey. <http://pubs.usgs.gov/ds/801/>.
- [Smith, HG; Sheridan, GJ; Lane, PNJ; Nyman, P; Haydon, S.](#) (2011). Wildfire effects on water quality in forest catchments: A review with implications for water supply [Review]. *J Hydrol* 396: 170-192. <http://dx.doi.org/10.1016/j.jhydrol.2010.10.043>.
- [Sofowote, UM; Di Federico, LM; Healy, RM; Debosz, J; Su, U; Wang, J; Munoz, A.](#) (2019). Heavy metals in the near-road environment: Results of semi-continuous monitoring of ambient particulate matter in the greater Toronto and Hamilton area. *Atmospheric Environment: X* 1: 100005. <http://dx.doi.org/10.1016/j.aeaoa.2019.100005>.
- [Song, F; Gao, Y.](#) (2011). Size distributions of trace elements associated with ambient particular matter in the affinity of a major highway in the New Jersey-New York metropolitan area. *Atmos Environ* 45: 6714-6723. <http://dx.doi.org/10.1016/j.atmosenv.2011.08.031>.
- [Sorooshian, A; Csavina, J; Shingler, T; Dey, S; Brechtel, FJ; Sáez, AE; Betterton, EA.](#) (2012). Hygroscopic and chemical properties of aerosols collected near a copper smelter: Implications for public and environmental health. *Environ Sci Technol* 46: 9473-9480. <http://dx.doi.org/10.1021/es302275k>.
- [Sparks, TL; Wagner, J.](#) (2021). Composition of particulate matter during a wildfire smoke episode in an urban area. *Aerosol Sci Technol* 55: 734-747. <http://dx.doi.org/10.1080/02786826.2021.1895429>.
- [Spliethoff, HM; Mitchell, RG; Shayler, H; Marquez-Bravo, LG; Russell-Anelli, J; Ferenz, G; McBride, M.](#) (2016). Estimated lead (Pb) exposures for a population of urban community gardeners. *Environ Geochem Health* 38: 955-971. <http://dx.doi.org/10.1007/s10653-016-9790-8>.
- [Stankwitz, C; Kaste, JM; Friedland, AJ.](#) (2012). Threshold increases in soil lead and mercury from tropospheric deposition across an elevational gradient. *Environ Sci Technol* 46: 8061-8068. <http://dx.doi.org/10.1021/es204208w>.
- [Stevens, C; Williams, R; Jones, P.](#) (2014). Progress on understanding spatial and temporal variability of PM(2.5) and its components in the Detroit Exposure and Aerosol Research Study (DEARS). *Environ Sci Process Impacts* 16: 94-105. <http://dx.doi.org/10.1039/c3em00364g>.
- [Stillo, F; Macdonald Gibson, J.](#) (2017). Exposure to Contaminated Drinking Water and Health Disparities in North Carolina. *Am J Public Health* 107: 180-185. <http://dx.doi.org/10.2105/AJPH.2016.303482>.
- [Stockdale, A; Tipping, E; Lofts, S; Mortimer, RJG.](#) (2016). Effect of ocean acidification on organic and inorganic speciation of trace metals. *Environ Sci Technol* 50: 1906-1913. <http://dx.doi.org/10.1021/acs.est.5b05624>.
- [Stolpe, B; Guo, L; Shiller, AM; Aiken, GR.](#) (2013). Abundance, size distributions and trace-element binding of organic and iron-rich nanocolloids in Alaskan rivers, as revealed by field-flow fractionation and ICP-MS. *Geochim Cosmo Acta* 105: 221-239. <http://dx.doi.org/10.1016/j.gca.2012.11.018>.
- [Stromsoe, N; Marx, SK; McGowan, HA; Callow, N; Heijnis, H; Zawadzki, A.](#) (2015). A landscape-scale approach to examining the fate of atmospherically derived industrial metals in the surficial environment. *Sci Total Environ* 505: 962-980. <http://dx.doi.org/10.1016/j.scitotenv.2014.10.072>.

- Sullivan, M; Green, D. (2020). Toward eliminating children's lead exposure: A comparison of policies and their outcomes in three lead producing and using countries [Review]. *Environ Res Lett* 15: 103008. <http://dx.doi.org/10.1088/1748-9326/abb55e>.
- Sun, C, hi; Li, C; Liu, J; Shi, X; Zhao, S; Wu, Y; Tian, W. (2018). First-principles study on the migration of heavy metal ions in ice-water medium from Ulansuhai Lake. *Water* 10: 1149. <http://dx.doi.org/10.3390/w10091149>.
- Swanson, SM; Engle, MA; Ruppert, LF; Affolter, RH; Jones, KB. (2013). Partitioning of selected trace elements in coal combustion products from two coal-burning power plants in the United States. *Int J Coal Geol* 113: 116-126. <http://dx.doi.org/10.1016/j.coal.2012.08.010>.
- Swift Fuels. (2023). Frequently asked questions. Available online at <https://www.swiftfuelsavgas.com/faq> (accessed August 22, 2023).
- Tan, B; Liu, S; Dai, C; Zhou, H; Hui, Z; Zhong, G; Zhang, H. (2017). Modelling of colloidal particle and heavy metal transfer behaviours during seawater intrusion and refreshing processes. *Hydrolog Process* 31: 3920-3931. <http://dx.doi.org/10.1002/hyp.11309>.
- Tansel, B; Rafiuddin, S. (2016). Heavy metal content in relation to particle size and organic content of surficial sediments in Miami River and transport potential. *International Journal of Sediment Research* 31: 324-329. <http://dx.doi.org/10.1016/j.ijsrc.2016.05.004>.
- Taylor, HE; Antweiler, RC; Roth, DA; Alpers, CN; Dileanis, P. (2012). Selected trace elements in the Sacramento River, California: Occurrence and distribution. *Arch Environ Contam Toxicol* 62: 557-569. <http://dx.doi.org/10.1007/s00244-011-9738-z>.
- Taylor, MP; Isley, CF; Fry, KL; Liu, X; Gillings, MM; Rouillon, M; Soltani, NS; Gore, DB; Filippelli, GM. (2021). A citizen science approach to identifying trace metal contamination risks in urban gardens. *Environ Int* 155: 106582. <http://dx.doi.org/10.1016/j.envint.2021.106582>.
- Tovar-Sánchez, A; González-Ortegón, E; Duarte, CM. (2019). Trace metal partitioning in the top meter of the ocean. *Sci Total Environ* 652: 907-914. <http://dx.doi.org/10.1016/j.scitotenv.2018.10.315>.
- Tremper, AH; Font, A; Priestman, M; Hamad, SH; Chung, TC; Pribadi, A; Brown, RJC; Goddard, SL; Grassineau, N; Petterson, K; Kelly, FJ; Green, DC. (2018). Field and laboratory evaluation of a high time resolution x-ray fluorescence instrument for determining the elemental composition of ambient aerosols. *Atmos Meas Tech* 11: 3541-3557. <http://dx.doi.org/10.5194/amt-11-3541-2018>.
- Turgut, ET; Açıkel, G; Gaga, EO; Çalişir, D; Odabasi, M; Ari, A; Artun, G; İlhan, SÖ; Savaci, U; Can, E; Turan, S. (2020). A comprehensive characterization of particulate matter, trace elements, and gaseous emissions of piston-engine aircraft. *Environ Sci Technol* 54: 7818-7835. <http://dx.doi.org/10.1021/acs.est.0c00815>.
- Turgut, ET; Gaga, EO; Jovanović, G; Odabasi, M; Artun, G; Ari, A; Urošević, MA. (2019). Elemental characterization of general aviation aircraft emissions using moss bags. *Environ Sci Pollut Res Int* 26: 26925-26938. <http://dx.doi.org/10.1007/s11356-019-05910-8>.
- U.S. EPA. (1977). Air quality criteria for lead [EPA Report]. (EPA-600/8-77-017). Washington, DC. <http://nepis.epa.gov/Exec/ZyPURL.cgi?Dockey=20013GWR.txt>.
- U.S. EPA. (1986). Air quality criteria for lead [EPA Report]. (EPA/600/8-83/028aF-dF). Research Triangle Park, NC. <http://cfpub.epa.gov/ncea/cfm/recorddisplay.cfm?deid=32647>.
- U.S. EPA. (2006). Air quality criteria for lead [EPA Report]. (EPA/600/R-05/144aF-bF). Research Triangle Park, NC. <https://cfpub.epa.gov/ncea/risk/recorddisplay.cfm?deid=158823>.
- U.S. EPA. (2009). Integrated science assessment for particulate matter. (EPA/600/R-08/139F). Washington, DC. <http://cfpub.epa.gov/ncea/cfm/recorddisplay.cfm?deid=216546>.
- U.S. EPA. (2013). Integrated science assessment for lead (contains errata sheet created 5/12/2014) [EPA Report]. (EPA/600/R-10/075F). Washington, DC. <https://nepis.epa.gov/Exec/ZyPURL.cgi?Dockey=P100K82L.txt>.

- [U.S. EPA. \(2015\)](#). Program overview: Airport lead monitoring [EPA Report]. (EPA-420-F-15-003). Washington, DC: U.S. Environmental Protection Agency, Office of Transportation and Air Quality. <https://nepis.epa.gov/Exe/ZyPURL.cgi?Dockey=P100LJDW.txt>.
- [U.S. EPA. \(2019\)](#). Integrated Science Assessment (ISA) for particulate matter (final report, Dec 2019). (EPA/600/R-19/188). Washington, DC. <https://cfpub.epa.gov/ncea/isa/recordisplay.cfm?deid=347534>.
- [U.S. EPA. \(2020a\)](#). Integrated science assessment for oxides of nitrogen, oxides of sulfur, and particulate matter—Ecological criteria (final report) [EPA Report]. (EPA/600/R-20/278). Research Triangle Park, NC: U.S. Environmental Protection Agency, Office of Research and Development. <https://cfpub.epa.gov/ncea/isa/recordisplay.cfm?deid=349473>.
- [U.S. EPA \(U.S. Environmental Protection Agency\)](#). (2020b). Model-extrapolated estimates of airborne lead concentrations at U.S. airports [EPA Report]. (EPA-420-R-20-003). Washington, DC: U.S. Environmental Protection Agency, Office of Transportation and Air Quality, Assessment and Standards Division. <https://nepis.epa.gov/Exe/ZyPURL.cgi?Dockey=P100YG52.txt>.
- [U.S. EPA. \(2021a\)](#). 2017 National Emissions Inventory (NEI) data. Available online at <https://www.epa.gov/air-emissions-inventories/2017-national-emissions-inventory-nei-data> (accessed August 31, 2022).
- [U.S. EPA. \(2021b\)](#). 2017 National Emissions Inventory: January 2021 updated release, technical support document [EPA Report]. (EPA-454/R-21-001). Research Triangle Park, NC. https://www.epa.gov/sites/default/files/2021-02/documents/nei2017_tsd_full_jan2021.pdf.
- [U.S. EPA. \(2022a\)](#). Overview of lead (Pb) air quality in the United States, 2021. Washington, DC.
- [U.S. EPA. \(2022b\)](#). Proposed finding that lead emissions from aircraft engines that operate on leaded fuel cause or contribute to air pollution that may reasonably be anticipated to endanger public health and welfare; proposed rule. Fed Reg 87: 62753-62781.
- [U.S. EPA. \(2023a\)](#). 2020 National Emissions Inventory (NEI) Data (August 2023 version) (Version August 2023). Washington, DC: US Environmental Protection Agency. Retrieved from <https://www.epa.gov/air-emissions-inventories/2020-national-emissions-inventory-nei-data>
- [U.S. EPA. \(2023b\)](#). Air Quality Design Values (Version 8/7/2023). Washington, DC. Retrieved from <https://www.epa.gov/air-trends/air-quality-design-values>
- [U.S. EPA. \(2023c\)](#). NAAQS Review Analysis. Available online at <https://www.epa.gov/air-quality-analysis/naaqs-review-analysis> (accessed
- [U.S. EPA. \(2023d\)](#). TRI National Analysis: Lead. Available online at <https://www.epa.gov/trinationalanalysis/lead> (accessed
- [Upadhyay, N; Clements, A; Fraser, M; Herckes, P.](#) (2011). Chemical speciation of PM2.5 and PM10 in South Phoenix, AZ, USA. *J Air Waste Manag Assoc* 61: 302-310. <http://dx.doi.org/10.3155/1047-3289.61.3.302>.
- [USGS. \(2018\)](#). Lead end-use statistics [through 2003; last modified September 1, 2005]. In *Historical statistics for mineral and material commodities in the United States*. (USGS Data Series 140). Reston, VA. <https://www.usgs.gov/centers/nmic/historical-statistics-mineral-and-material-commodities-united-states>.
- [USGS. \(2022\)](#). Lead. In *Mineral commodity summaries 2022* (pp. 96-97). Reston, VA. <https://pubs.er.usgs.gov/publication/mcs2022>.
- [Valencia-Avellan, M; Slack, R; Stockdale, A; Mortimer, RJG.](#) (2017). Effect of episodic rainfall on aqueous metal mobility from historical mine sites. *Environ Chem* 14: 469-475. <http://dx.doi.org/10.1071/EN17133>.
- [van Geen, A; Yao, Y; Ellis, T; Gelman, A.](#) (2020). Fallout of lead over Paris from the 2019 Notre-Dame cathedral fire. *Geohealth* 4: e2020GH000279. <http://dx.doi.org/10.1029/2020GH000279>.
- [Van Metre, PC; Horowitz, AJ.](#) (2013). An 80-year record of sediment quality in the lower Mississippi River. *Hydrolog Process* 27: 2438-2448. <http://dx.doi.org/10.1002/hyp.9336>.

- [Van Pelt, RS; Shekhter, EG; Barnes, MAW; Duke, SE; Gill, TE; Pannell, KH. \(2020\). Spatial and temporal patterns of heavy metal deposition resulting from a smelter in El Paso, Texas. J Geochem Explor 210: 106414. <http://dx.doi.org/10.1016/j.gexplo.2019.106414>.](#)
- [Vanderpool, RW; Krug, JD; Kaushik, S; Gilberry, J; Dart, A; Witherspoon, CL. \(2018\). Size-selective sampling performance of six low-volume "total" suspended particulate \(TSP\) inlets. Aerosol Sci Technol 52: 98-113. <http://dx.doi.org/10.1080/02786826.2017.1386766>.](#)
- [Vasyukova, E; Pokrovsky, OS; Viers, J; Dupré, B. \(2012\). New operational method of testing colloid complexation with metals in natural waters. Appl Geochem 27: 1226-1237. <http://dx.doi.org/10.1016/j.apgeochem.2012.02.026>.](#)
- [Velinsky, DJ; Riedel, GF; Ashley, JTF; Cornwell, JC. \(2011\). Historical contamination of the Anacostia River, Washington, D.C. Environ Monit Assess 183: 307. <http://dx.doi.org/10.1007/s10661-011-1923-z>.](#)
- [Wade, AM; Richter, DD; Craft, CB; Bao, NY; Heine, PR; Osteen, MC; Tan, KG. \(2021\). Urban-soil pedogenesis drives contrasting legacies of lead from paint and gasoline in city soil. Environ Sci Technol 55: 7981-7989. <http://dx.doi.org/10.1021/acs.est.1c00546>.](#)
- [Wang, G; Hopke, PK; Turner, J. \(2011\). Using highly time resolved fine particulate compositions to find particle sources in St. Louis, MO. Atmos Pollut Res 2: 219-230. <http://dx.doi.org/10.5094/APR.2011.028>.](#)
- [Wang, Y; Jiao, JJ; Zhang, K; Zhou, Y. \(2016\). Enrichment and mechanisms of heavy metal mobility in a coastal quaternary groundwater system of the Pearl River Delta, China. Sci Total Environ 545-546: 493-502. <http://dx.doi.org/10.1016/j.scitotenv.2015.12.019>.](#)
- [Wang, Y; Kanter, RK. \(2014\). Disaster-related environmental health hazards: Former lead smelting plants in the United States. Disaster Med Public Health Prep 8: 44-50. <http://dx.doi.org/10.1017/dmp.2014.3>.](#)
- [Wang, Y; Zhou, L; Zheng, X; Qian, P; Wu, Y. \(2013\). Influence of *Spartina alterniflora* on the mobility of heavy metals in salt marsh sediments of the Yangtze River Estuary, China. Environ Sci Pollut Res Int 20: 1675-1685. <http://dx.doi.org/10.1007/s11356-012-1082-y>.](#)
- [Wang, Z; Dwyer, GS; Coleman, DS; Vengosh, A. \(2019\). Lead isotopes as a new tracer for detecting coal fly ash in the environment. Environ Sci Technol Lett 6: 714-719. <http://dx.doi.org/10.1021/acs.estlett.9b00512>.](#)
- [Wang, Z; Wade, AM; Richter, DD; Stapleton, HM; Kaste, JM; Vengosh, A. \(2022\). Legacy of anthropogenic lead in urban soils: Co-occurrence with metal\(loids\) and fallout radionuclides, isotopic fingerprinting, and in vitro bioaccessibility. Sci Total Environ 806: 151276. <http://dx.doi.org/10.1016/j.scitotenv.2021.151276>.](#)
- [Ward, D, Jr; Gentile, T; Felton, H. \(2019\). Comparison of current Federal Reference Methods for ambient lead measurements adjacent to a secondary lead smelter. J Air Waste Manag Assoc 69: 956-966. <http://dx.doi.org/10.1080/10962247.2019.1587554>.](#)
- [Webster-Brown, JG; Dee, TJ; Hegan, AF. \(2012\). Metal removal via particulate material in a lowland river system. Water Sci Technol 66: 1439-1445. <http://dx.doi.org/10.2166/wst.2012.313>.](#)
- [Wedding, JB; McFarland, AR; Cermak, JE. \(1977\). Large particle collection characteristics of ambient aerosol samplers. Environ Sci Technol 11: 387-390. <http://dx.doi.org/10.1021/es60127a005>.](#)
- [Whitehead, TP; Ward, MH; Colt, JS; Dahl, G; Ducore, J; Reinier, K; Gunier, RB; Katharine Hammond, S; Rappaport, SM; Metayer, C. \(2015\). Dust metal loadings and the risk of childhood acute lymphoblastic leukemia. J Expo Sci Environ Epidemiol 25: 593-598. <http://dx.doi.org/10.1038/jes.2015.9>.](#)
- [Widory, D; Vautour, G; Poirier, A. \(2018\). Atmospheric dispersion of trace metals between two smelters: An approach coupling lead, strontium and osmium isotopes from bioindicators. Ecol Indic 84: 497-506. <http://dx.doi.org/10.1016/j.ecolind.2017.09.003>.](#)
- [Wiklund, JA; Hall, RI; Wolfe, BB; Edwards, TWD; Farwell, AJ; Dixon, DG. \(2012\). Has Alberta oil sands development increased far-field delivery of airborne contaminants to the Peace-Athabasca Delta? Sci Total Environ 433: 379-382. <http://dx.doi.org/10.1016/j.scitotenv.2012.06.074>.](#)

- [Wiseman, CL; Zereini, F; Püttmann, W. \(2015\).](#) Metal and metalloid accumulation in cultivated urban soils: A medium-term study of trends in Toronto, Canada. *Sci Total Environ* 538: 564-572. <http://dx.doi.org/10.1016/j.scitotenv.2015.08.085>.
- [Wiseman, CLS; Levesque, C; Rasmussen, PE. \(2021\).](#) Characterizing the sources, concentrations and resuspension potential of metals and metalloids in the thoracic fraction of urban road dust. *Sci Total Environ* 786: 147467. <http://dx.doi.org/10.1016/j.scitotenv.2021.147467>.
- [Wu, L; Fu, S; Wang, X; Chang, X. \(2020\).](#) Mapping of atmospheric heavy metal deposition in Guangzhou city, southern China using archived bryophytes. *Environ Pollut* 265: 114998. <http://dx.doi.org/10.1016/j.envpol.2020.114998>.
- [Wu, L; Taylor, MP; Handley, HK; Wu, M. \(2016\).](#) Australian atmospheric lead deposition reconstructed using lead concentrations and isotopic compositions of archival lichen and fungi. *Environ Pollut* 208: 678-687. <http://dx.doi.org/10.1016/j.envpol.2015.10.046>.
- [Wu, SC; Luo, YM; Cheung, KC; Wong, MH. \(2006\).](#) Influence of bacteria on Pb and Zn speciation, mobility and bioavailability in soil: A laboratory study. *Environ Pollut* 144: 765-773. <http://dx.doi.org/10.1016/j.envpol.2006.02.022>.
- [Xie, BY; Jiang, YJ; Zhang, Z; Cao, G; Sun, HM; Wang, N; Wang, SS. \(2018\).](#) Co-transport of Pb (II) and Cd (II) in saturated porous media: Effects of colloids, flow rate and grain size. *Chem Speciation Bioavailability* 30: 55-63. <http://dx.doi.org/10.1080/09542299.2018.1531727>.
- [Xing, J; Song, J; Yuan, H; Wang, Q; Li, X; Li, N; Duan, L; Qu, B. \(2017\).](#) Atmospheric wet deposition of dissolved trace elements to Jiaozhou Bay, North China: Fluxes, sources and potential effects on aquatic environments. *Chemosphere* 174: 428-436. <http://dx.doi.org/10.1016/j.chemosphere.2017.02.004>.
- [Xu, J; Martin, RV; Henderson, BH; Meng, J; Öztaner, YB; Hand, JL; Hakami, A; Strum, M; Phillips, SB. \(2019\).](#) Simulation of airborne trace metals in fine particulate matter over North America. *Atmos Environ* 214: 116883. <http://dx.doi.org/10.1016/j.atmosenv.2019.116883>.
- [Yadav, V; Turner, J. \(2014\).](#) Gauging intraurban variability of ambient particulate matter arsenic and other air toxic metals from a network of monitoring sites. *Atmos Environ* 89: 318-328. <http://dx.doi.org/10.1016/j.atmosenv.2014.02.030>.
- [Yao, Q; Wang, X; Jian, H; Chen, H; Yu, Z. \(2016\).](#) Behavior of suspended particles in the Changjiang Estuary: Size distribution and trace metal contamination. *Mar Pollut Bull* 103: 159-167. <http://dx.doi.org/10.1016/j.marpolbul.2015.12.026>.
- [Yatkin, S; Amin, HS; Trzepla, K; Dillner, AM. \(2016\).](#) Preparation of lead (Pb) X-ray fluorescence reference materials for the EPA Pb monitoring program and the IMPROVE network using an aerosol deposition method. *Aerosol Sci Technol* 50: 309-320. <http://dx.doi.org/10.1080/02786826.2016.1150956>.
- [Youn, JS; Csavina, J; Rine, KP; Shingler, T; Taylor, MP; Sáez, AE; Betterton, EA; Sorooshian, A. \(2016\).](#) Hygroscopic properties and respiratory system deposition behavior of particulate matter emitted by mining and smelting operations. *Environ Sci Technol* 50: 11706-11713. <http://dx.doi.org/10.1021/acs.est.6b03621>.
- [Yu, CH; Fan, ZH; Meng, Q; Zhu, X; Korn, L; Bonanno, LJ. \(2011\).](#) Spatial/temporal variations of elemental carbon, organic carbon, and trace elements in PM10 and the impact of land-use patterns on community air pollution in Paterson, NJ. *J Air Waste Manag Assoc* 61: 673-688. <http://dx.doi.org/10.3155/1047-3289.61.6.673>.
- [Zahrán, S; Iverson, T; McElmurry, SP; Weiler, S. \(2017\).](#) The effect of leaded aviation gasoline on blood lead in children. *J Assoc Environ Resour Econ* 4: 575-610. <http://dx.doi.org/10.1086/691686>.
- [Zahrán, S; Keyes, C; Lanphear, B. \(2023\).](#) Leaded aviation gasoline exposure risk and child blood lead levels. *PNAS Nexus* 2: pgac285. <http://dx.doi.org/10.1093/pnasnexus/pgac285>.
- [Zahrán, S; Laidlaw, MAS; McElmurry, SP; Filippelli, GM; Taylor, M. \(2013\).](#) Linking source and effect: Resuspended soil lead, air lead, and children's blood lead levels in Detroit, Michigan. *Environ Sci Technol* 47: 2839-2845. <http://dx.doi.org/10.1021/es303854c>.

- [Zhang, Z; Wang, JJ; Ali, A; DeLaune, RD. \(2016a\).](#) Heavy metal distribution and water quality characterization of water bodies in Louisiana's Lake Pontchartrain Basin, USA. *Environ Monit Assess* 188: 628. <http://dx.doi.org/10.1007/s10661-016-5639-y>.
- [Zhang, Z; Wang, JJ; Ali, A; DeLaune, RD. \(2016b\).](#) Heavy metals and metalloid contamination in Louisiana Lake Pontchartrain estuary along I-10 Bridge. *Transport Res Transport Environ* 44: 66-77. <http://dx.doi.org/10.1016/j.trd.2016.02.014>.
- [Zhao, S; Feng, C; Wang, D; Liu, Y; Shen, Z. \(2013\).](#) Salinity increases the mobility of Cd, Cu, Mn, and Pb in the sediments of Yangtze Estuary: Relative role of sediments' properties and metal speciation. *Chemosphere* 91: 977-984. <http://dx.doi.org/10.1016/j.chemosphere.2013.02.001>.
- [Zhou, J; Du, B; Wang, Z; Zhang, W; Xu, L; Fan, X; Liu, X; Zhou, J. \(2019\).](#) Distributions and pools of lead (Pb) in a terrestrial forest ecosystem with highly elevated atmospheric Pb deposition and ecological risks to insects. *Sci Total Environ* 647: 932-941. <http://dx.doi.org/10.1016/j.scitotenv.2018.08.091>.
- [Zhou, Q; Yang, N; Li, Y; Ren, B; Ding, X; Bian, H; Yao, X. \(2020a\).](#) Total concentrations and sources of heavy metal pollution in global river and lake water bodies from 1972 to 2017. *Glob Ecol Conserv* 22: e00925. <http://dx.doi.org/10.1016/j.gecco.2020.e00925>.
- [Zhou, Y; Sherpa, S; McBride, MB. \(2020b\).](#) Pb and Cd chemisorption by acid mineral soils with variable Mn and organic matter contents. *Geoderma* 368: 114274. <http://dx.doi.org/10.1016/j.geoderma.2020.114274>.
- [Zierold, KM; Odoh, C. \(2020\).](#) A review on fly ash from coal-fired power plants: chemical composition, regulations, and health evidence [Review]. *Rev Environ Health* 35: 401-418. <http://dx.doi.org/10.1515/reveh-2019-0039>.
- [Zota, AR; Schaidler, LA; Ettinger, AS; Wright, RO; Shine, JP; Spengler, JD. \(2011\).](#) Metal sources and exposures in the homes of young children living near a mining-impacted Superfund site. *J Expo Sci Environ Epidemiol* 21: 495-505. <http://dx.doi.org/10.1038/jes.2011.21>.